UNIVERSIDADE FEDERAL DE SANTA CATARINA
CENTRO DE CIÊNCIAS DA SAÚDE
PROGRAMA DE PÓS-GRADUAÇÃO EM ODONTOLOGIA

Luiz Carlos de Lima Dias Junior

Fatores associados à acurácia diagnóstica de fraturas radiculares verticais completas e incompletas

Florianópolis
2022

Luiz Carlos De Lima Dias Junior

Fatores associados à acurácia diagnóstica de fraturas radiculares verticais completas e incompletas

Tese submetida ao Programa de Pós-Graduação em Odontologia da Universidade Federal de Santa Catarina como requisito parcial para a obtenção do título de Doutor em Odontologia, Área de concentração: Endodontia.

Orientador: Prof. Lucas da Fonseca Roberti Garcia, Dr.
Coorientador: Prof. Dr. Eduardo Antunes Bortoluzzi, Dr.

Florianópolis
2022

Ficha de identificação da obra elaborada pelo autor,
através do Programa de Geração Automática da Biblioteca Universitária da UFSC.

Dias Junior, Luiz Carlos de Lima
Fatores associados à acurácia diagnóstica de fraturas radiculares verticais completas e incompletas / Luiz Carlos de Lima Dias Junior ; orientador, Lucas da Fonseca Roberti Garcia, coorientador, Eduardo Antunes Bortoluzzi, 2022.
153 p.

Tese (doutorado) - Universidade Federal de Santa Catarina, Centro de Ciências da Saúde, Programa de Pós Graduação em Odontologia, Florianópolis, 2022.

Inclui referências.

1. Odontologia. 2. Endodontia. 3. Diagnóstico. 4. Fratura radicular vertical. 5. Tomografia Computadorizada de Feixe Cônico. I. Garcia, Lucas da Fonseca Roberti. II. Bortoluzzi, Eduardo Antunes. III. Universidade Federal de Santa Catarina. Programa de Pós-Graduação em Odontologia. IV. Título.

Luiz Carlos De Lima Dias Junior

Fatores associados à acurácia diagnóstica de fraturas radiculares verticais completas e incompletas

O presente trabalho em nível de Doutorado foi avaliado e aprovado, em 14 de dezembro de 2022, pela banca examinadora composta pelos seguintes membros:

Prof. Lucas da Fonseca Roberti Garcia, Dr.
Universidade Federal de Santa Catarina

Profª. Cleonice da Silveira Teixeira, Drª.
Universidade Federal de Santa Catarina

Prof. Márcio Correa, Dr.
Universidade Federal de Santa Catarina

Profª. Josiane de Almeida Cava da Silveira, Drª.
Universidade do Sul de Santa Catarina – UNISUL

Certificamos que esta é a versão original e final do trabalho de conclusão que foi julgado adequado para obtenção do título de Doutor em Odontologia, Área de Concentração: Endodontia.

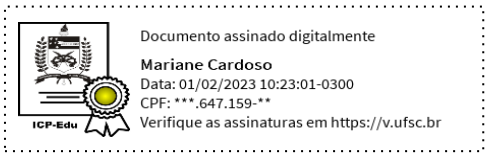

Coordenação do Programa de Pós-Graduação

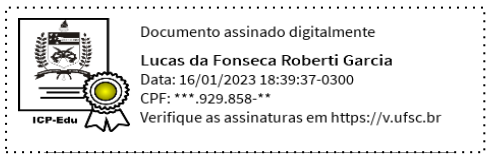

Prof. Lucas da Fonseca Roberti Garcia, Dr.
Orientador

Florianópolis, 2022

Dedico este trabalho aos meus pais, Luiz Carlos e Lianne, e minha esposa, Adriana. Os meus maiores incentivadores.

AGRADECIMENTOS

Aos meus pais, Luiz Carlos e Lianne, por todo o amor, e compreensão. Agradeço principalmente pelo apoio absoluto em todos os momentos da minha vida. Vocês sempre serão meus maiores exemplos. Obrigado por não medirem esforços para que eu pudesse realizar os meus sonhos. Minha maior recompensa é ter o orgulho de vocês.

À Adriana, minha esposa, companheira, melhor amiga, e maior incentivadora. Quando enfrentei os maiores desafios, foram as suas palavras e o seu abraço que me deram forças para seguir em frente. Agradeço imensamente por todo o apoio, paciência, carinho e amor. A vida é muito mais fácil, e infinitamente mais alegre porque posso dividi-la com você.

Aos meus sogros, Maria Dilma, e Pedro Edson, por terem me acolhido com muito amor. Obrigado por todo o incentivo, suporte e carinho, sempre.

A todos os meus amigos e familiares que me apoiaram e incentivaram durante essa caminhada. Agradeço especialmente aos amigos Danilo Pinheiro, Gabriela Sabatini, e João Eccel, que tornam a vida mais leve e prazerosa.

Ao Prof. Dr. Eduardo Antunes Bortoluzzi, que acreditou no meu potencial desde o início, e me permitiu realizar muito mais do que eu imaginava ser capaz durante o doutorado. Obrigado pela orientação, e por todos os ensinamentos, sempre com paciência, dedicação e carinho. E obrigado, principalmente, por ter sido um grande exemplo de professor. A sua paixão por ensinar foi contagiante para mim.

Ao Prof. Dr. Lucas da Fonseca Roberti Garcia, pela orientação, e por todo o conhecimento compartilhado. Agradeço por compartilhar tanto conhecimento, com tanta humildade. Tenho a certeza de que me tornei um melhor aluno, professor, pesquisador, e profissional, porque tive a oportunidade da sua orientação. Obrigado por me inspirar tanto.

Ao Prof. Dr. Marcio Correa, pela colaboração desde a elaboração à conclusão desta tese de doutorado. Sua contribuição e parceria foram fundamentais para o desenvolvimento desta tese. Obrigado por todo o auxílio, disponibilidade e suporte.

Agradeço à Prof. Cleonice da Silveira Teixeira, por ter sido um exemplo de professora, que sabe ensinar, e estimular o melhor em cada aluno. Agradeço a sua motivação em me fazer buscar excelência em tudo. Obrigado também por toda a colaboração, preocupação e carinho durante todo esse período.

Aos professores de endodontia da UFSC, por compartilharem conhecimento com tanta simplicidade e disponibilidade. Obrigado Prof.ª Dr.ª Thais Mageste Duque, e Prof.ª Dr.ª Ana Maria Hecke Alves. Foi um grande privilégio poder aprender um pouco com vocês durante a

minha formação. Obrigado pelo acolhimento, carinho, disponibilidade e sensibilidade em ensinar. Foi uma honra fazer parte da equipe EndoUFSC.

À amiga Roberta Castro, pela amizade, apoio, e incentivo constante. Obrigado por ser uma grande amiga de vida, e pela consideração, conselhos e parceria. Essa caminhada se tornou mais leve porque pude contar com você. Conte sempre comigo.

À amiga Daniela Peressoni, pela amizade, e parceria de pesquisa. Obrigado por todo apoio ao longo desta caminhada. Me sinto muito feliz por ter convivido e aprendido tanto com você. Pode contar comigo, sempre.

Aos colegas professores Tamer Schimdt, Jardel Dorigon, e Lincon Nomura, pela colaboração nas salas de aula, laboratórios e clínicas. Vocês me inspiram e me fazem amar a pesquisa, e a docência.

Aos amigos Amanda Rosa, Bruna Fischer, Dayana Chaves, Diego Souza, Dilma Henriques, Filipe Vitali, Gabriel Hernandez, Gabriela Rover, Ihan Cardoso, Júlia Savaris, Maria Eduarda Dotto, Mariana Pandolfo, Matheus Pompeo, Patrícia Cancelier, Taynara Goulart, e Wesley Gonçalves, e todos os colegas de pós-graduação, pela amizade, e troca de experiências. Obrigado pela parceria, risadas e por compartilhar momentos que sempre ficarão guardados em minha memória.

Agradeço a todos os meus alunos por confiarem no meu trabalho, e manterem viva em mim a vontade de ensinar e aprender.

Ao Programa de Pós-Graduação em Odontologia da Universidade Federal de Santa Catarina, pela oportunidade de me formar como professor e pesquisador. Obrigado a todos os professores, que trabalham com muito esmero para produzir ciência de qualidade, e formar profissionais qualificados.

A todos os servidores e funcionários da Universidade Federal de Santa Catarina, por todo auxílio, disponibilidade e suporte.

À Coordenação de Aperfeiçoamento de Pessoal de Nível Superior (CAPES) pela concessão de bolsa de estudos durante todo o período do doutorado.

“Daria tudo que sei, pela metade do que ignoro”

René Descartes

RESUMO

As fraturas radiculares verticais (FRVs) são fraturas completas ou incompletas que ocorrem no sentido longitudinal, e afetam principalmente dentes com tratamento endodôntico, e pinos intrarradiculares. O diagnóstico dessas condições é especialmente desafiador quando os fragmentos apresentam mínima separação, como nas FRVs incompletas. Esta tese é constituída por três estudos. O primeiro deles teve como objetivo desenvolver um método para indução de FRVs incompletas em dentes humanos extraídos, para futuras pesquisas laboratoriais. O segundo estudo objetivou analisar a acurácia diagnóstica da tomografia computadorizada de feixe cônico (TCFC) na detecção de FRVs completas e incompletas em dentes com diferentes materiais intracanais, e avaliar a influência da utilização do filtro *Blooming Artifact Reduction* (BAR) do software e-Vol DX (CDT Software) sobre a acurácia diagnóstica. O terceiro estudo consistiu em uma revisão sistemática e meta-análises, para identificar os fatores associados à acurácia diagnóstica de FRV, em estudos *in vitro*. No primeiro estudo, dentes humanos extraídos foram inspecionados com magnificação e transiluminação para excluir dentes previamente fraturados. Após a seleção, 35 dentes tiveram suas coroas removidas e os canais preparados. FRVs incompletas foram induzidas nos espécimes pela introdução de uma cunha metálica personalizada no interior do canal radicular, sob velocidade de 5mm/min e força de 2kN, em máquina de ensaios universal. Os espécimes foram inspecionados sob magnificação de 20× e transiluminação para determinação da presença e características das fraturas. A taxa de sucesso na obtenção de FRV incompletas foi avaliada. No segundo estudo, 20 dentes foram selecionados. As coroas foram removidas, e os canais radiculares preparados. TCFCs foram realizadas no aparelho Prexion 3D, com os seguintes parâmetros: 90 kVp e 4 mA, voxel de 0.09 mm^3 e FOV (Field-of-view) de 5×5 cm. Para avaliar a influência dos materiais intracanais, as imagens foram obtidas com os canais vazios, e na presença de cone de guta-percha, pino de fibra de vidro, e pino metálico. As imagens foram obtidas com os raízes íntegras, e com FRV incompleta e completa. As imagens foram analisadas no software e-Vol DX inicialmente sem a utilização do filtro BAR, e depois da aplicação do filtro. Foram calculadas a área sob a curva (AUC) ROC, acurácia, sensibilidade e especificidade. Na revisão sistemática, as bases de dados PubMed, Embase, Scopus, Web of Science, e Lilacs, foram consultadas. A análise qualitativa foi realizada com a ferramenta QUADAS-2. As meta-análises foram realizadas utilizando-se o modelo bivariado de efeitos randômicos para determinar a sensibilidade e especificidade sumárias. A influência dos fatores de confusão sobre a acurácia diagnóstica foi investigada por modelos de meta-regressão. Os resultados do primeiro estudo mostraram que o método apresentou alta eficiência, induzindo com sucesso FRV incompletas em todos os espécimes analisados. No segundo estudo, a utilização do filtro BAR não alterou a acurácia diagnóstica de FRVs completas ou incompletas. Os materiais intracanais também não apresentaram influência sobre os valores diagnósticos. As FRV incompletas apresentaram diminuição da AUC, acurácia e sensibilidade, em comparação as FRV completas. A revisão sistemática identificou 85 estudos, dos quais 18 apresentaram baixo risco de viés, 22 risco moderado, e 45 alto risco de viés. Foi identificado que a TCFC apresenta maior sensibilidade para a identificação de FRVs completas. A presença de pinos metálicos afeta significativamente o diagnóstico de FRV. Tamanhos de voxels menores aumentaram a acurácia diagnóstica em dentes com pinos metálicos. Em conclusão, o método desenvolvido apresentou-se altamente eficaz para indução de FRV incompletas. Novas estratégias de diagnóstico devem ser desenvolvidas para favorecer o diagnóstico de FRV incompletas, especialmente em dentes com pinos metálicos.

Palavras-chave: Artefatos; Diagnóstico por Imagem; Fraturas dos Dentes; Meta-Análise; Revisão Sistemática; Tomografia Computadorizada de Feixe Cônico.

ABSTRACT

Vertical root fractures (VRFs) are complete or incomplete fractures that occur longitudinally and affect mainly teeth with endodontic treatment and intracanal posts. The diagnosis of VRFs is especially challenging when the fragments present minimal separation, as in incomplete fractures. This Ph.D. thesis is composed of three studies. The first study aimed to develop a method to induct incomplete VRFs in human-extracted teeth, for future laboratory investigations. The objective of the second study was to analyze the diagnostic accuracy of cone-beam computed tomography (CBCT) in the detection of complete and incomplete VRFs, in teeth with different intracanal materials. Also, analyze the influence of the Blooming Artifact Reduction (BAR) filter from the software e-Vol DX (CDT Software). The third study was a systematic review and meta-analysis, to identify the factors that might be associated with the diagnostic accuracy of VRFs, using *in vitro* studies. In the first study, human-extracted teeth were inspected under magnification and transillumination to exclude previous fractures. After selection, 35 teeth had their crowns removed, and the root canals were prepared. Incomplete VRFs were induced in the specimens using a customized conical wedge inside the root canals, under 5 mm per minute, and 2 kN, in a universal testing machine. The specimens were inspected under ×20 magnification and transillumination to identify the presence of fractures, and their characteristics. The success rate of achieving incomplete VRFs was assessed. In the second study, 20 teeth were selected. The crowns were removed, and the root canals were prepared. CBCT scans were taken with the Prexion 3D device, with the following parameters: 90 kVp and 4 mA, 0.09 mm^3 voxel, and 5×5 cm field-of-view. To evaluate the influence of the intracanal materials, the CBCT scans were acquired with empty root canals, and with gutta-percha cones, fiberglass posts, and metallic posts. The images were obtained with sound roots, and roots with incomplete and complete VRFs. The images were analyzed in the e-Vol DX software, without the BAR filter initially. Then, the images were reanalyzed with the BAR filter. The area under the curve (AUC) ROC, accuracy, sensitivity, and specificity were calculated. In the systematic review, the scientific databases PubMed, Embase, Scopus, Web of Science, and Lilacs were accessed. The qualitative analysis was accomplished with the QUADAS-2 tool. The meta-analyses were performed using the bivariate model, with random effects, to verify the summary sensitivity and specificity. The influence of confounding factors was investigated with meta-regression models. The results of the first study showed high effectiveness, successfully inducing incomplete VRFs in all analyzed specimens. The second study demonstrated that the BAR filter application did not alter the diagnostic accuracy of VRF complete or incomplete. The intracanal materials also did not impact the diagnostic values. The incomplete VRFs presented lower AUC, accuracy, and sensitivity, in comparison with the complete VRFs. The systematic review detected 85 studies. Among the included studies, 18 presented a low risk of bias, 22 a moderate risk, and 45 presented a high risk of bias. It was identified that CBCT presented high sensitivity for the detection of complete VRFs. The presence of metallic posts significantly affected the diagnosis of VRFs. Smaller voxel sizes improved diagnostic accuracy for teeth with metallic posts. In conclusion, the reported method presented high effectiveness for the induction of incomplete VRFs. New diagnostic strategies must be developed to improve the diagnosis of incomplete VRFs, especially in teeth with metal posts.

Keywords: Artifacts; Cone-Beam Computed Tomography; Diagnosis; Meta-Analysis; Systematic Review; Tooth Fractures.

LISTA DE FIGURAS

ARTIGO 1

ARTIGO 2

ARTIGO 3

LISTA DE QUADROS

ARTIGO 1

ARTIGO 2

ARTIGO 3

LISTA DE TABELAS

ARTIGO 1

ARTIGO 2

ARTIGO 3

LISTA DE ABREVIAÇÕES E SIGLAS

AINO	*Adaptive Image Noise Optimiser*
ALARA	*As low as reasonably achievable*
ARA	Algoritmos redutores de artefatos
AUC	*Area under the curve*
B	*Buccal*
BAR	*Blooming artifact reduction*
CAPES	Coordenação de Aperfeiçoamento de Pessoal de Nível Superior
CBCT	*Cone-beam computed tomography*
CEJ	*Cementoenamel junction*
cm	*Centimeter*
D	*Distal*
DICOM	*Digital Imaging and Communications in Medicine*
DL	*Distolingual*
FGP	*Fiberglass post*
FN	*False negative*
FOV	*Field-of-view*
FP	*False positive*
FRV	Fratura radicular vertical
GP	*Gutta-percha*
GRADE	*Grading of Recommendations, Assessment, Development, and Evaluation*
kN	*Kilonewton*
kVp	*Kilovoltage peak*
L	*Lingual*
LED	*Light-emitting diode*
M	*Mesial*
mA	*Milliampere*
MAR	*Metal artifact reduction*
MB	*Mesiobuccal*
ML	*Mesiolingual*
mL	*Milliliter*

mm	*Millimeter*
MP	*Metal post*
N	*Newton*
NF	*No filling*
NPV	*Negative predictive value*
PPV	*Positive predictive value*
PRILE	*Preferred Reporting Items for Laboratory studies in Endodontology*
PRISMA	*Preferred Reporting Items for Systematic Reviews and Meta-Analyses*
PRISMA-DTA	*Preferred Reporting Items for Systematic Reviews and Meta-Analyses of Diagnostic Test Accuracy*
PROSPERO	*International Prospective Register of Systematic Reviews*
QUADAS-2	*Quality Assessment of Diagnostic Accuracy Studies 2*
ROC	*Receiver operating characteristic*
rpm	*Rotations per minute*
SSe	*Summary sensitivity*
SSp	*Summary specificity*
STARD	*Standards for Reporting of Diagnostic Accuracy Studies*
TCFC	Tomografia computadorizada de feixe cônico
TN	*True negative*
TP	*True positive*
UTM	*Universal testing machine*
VRF	*Vertical root fracture*
µm	*Micrometer*

SUMÁRIO

1 INTRODUÇÃO

As condições denominadas fraturas radiculares longitudinais consistem em fraturas completas ou incompletas que se estendem no longo eixo do dente, de cervical para apical, e da parede do canal radicular para a superfície externa da raiz (RIVERA; WALTON, 2015). Estas linhas de fratura lineares costumam crescer ao longo do tempo, iniciam-se como uma trinca e progridem até a fratura completa (RIVERA; WALTON, 2015). Dessa forma, dois padrões distintos de fraturas radiculares verticais (FRV) podem ser observados: incompleta e completa (RIVERA; WALTON, 2015). Além disso, ambas podem envolver apenas um ou os dois lados da raiz (VARSHOSAZ *et al.*, 2010). As fraturas radiculares longitudinais podem ocorrer em dentes sem tratamento endodôntico, onde as principais causas são os traumas, forças oclusais excessivas, a má oclusão, entre outros (BRADY *et al.*, 2014). Contudo, a sua etiologia é comumente iatrogênica, principalmente devido ao desgaste excessivo das paredes do canal radicular, causado pela instrumentação, e/ou a pressão excessiva realizada durante a obturação e cimentação de retentores intrarradiculares (COHEN *et al.*, 2006).

O diagnóstico de FRVs costuma ser um desafio, devido à variedade da orientação e localização das linhas de fratura, aliada a ausência de sinal ou sintoma patognomônico (FERREIRA *et al.*, 2015). A presença das FRVs leva à inflamação do periodonto adjacente, havendo consequente reabsorção óssea com a formação de tecido de granulação, resultando muitas vezes na necessidade da extração dentária (HEKMATIAN *et al.*, 2018). Os sinais e sintomas comumente encontrados incluem a dor de intensidade variável, mobilidade dentária, edema, bolsa periodontal localizada e fístula (CHAN *et al.*, 1999). Estes apresentam-se inconsistentes na maioria das vezes, e somado a isto, a realização de uma radiografia periapical fornece informações limitadas (WENZEL *et al.*, 2009). Usualmente os únicos sinais radiográficos visíveis são causados pela reabsorção óssea na região afetada, representados por áreas radiolúcidas perirradiculares com descontinuidade do espaço do ligamento periodontal (WENZEL *et al.*, 2009). No entanto, esses sinais podem ser provenientes de uma variedade de situações clínicas como alterações periodontais e falha do tratamento endodôntico (KHASNIS *et al.*, 2014). Dessa forma, o diagnóstico de FRV precisa envolver uma avaliação criteriosa dos sinais e sintomas clínicos, dos exames de imagem, e as vezes lançar mão de cirurgias exploratórias.

O prognóstico de FRV incompleta é questionável, enquanto as fraturas completas tem prognóstico sombrio, muitas vezes sendo indicada a exodontia do elemento acometido (COHEN *et al.*, 2006). A comunicação entre o canal radicular e o periodonto, criada por estas condições,

permite a penetração bacteriana e induz processo inflamatório na região, levando à reabsorção óssea local, e podendo mimetizar condições adversas como doença periodontal ou falha no tratamento endodôntico (MOULE; KAHLER, 1999; COHEN *et al.*, 2006). Dessa forma, faz-se necessário um diagnóstico preciso para determinação e diferenciação da presença de FRV completa ou incompleta. Além disso, o diagnóstico precoce favorece o planejamento e tratamento, evitando tratamentos desnecessários, e danos adicionais aos tecidos periodontais (RIVERA; WALTON, 2015).

Atualmente, os exames de imagem são grandes aliados no diagnóstico de alterações endodônticas (NASCIMENTO *et al.*, 2015). Todavia, o diagnóstico dessas condições ainda não é uma tarefa simples (NASCIMENTO *et al.*, 2015). As radiografias periapicais causam uma sobreposição das estruturas, devido a sua natureza bidimensional, que limitam a visualização da linha de fratura, de forma que o próprio dente e tecido ósseo adjacente mascaram a sua presença (NASCIMENTO *et al.*, 2015). Isto torna-se ainda mais evidente em FRVs incompletas, ou fraturas que ocorrem no sentido mésio-distal, e quando os fragmentos não se apresentam separados por edema ou tecido de granulação (HASSAN *et al.*, 2009; DE MARTIN *et al.*, 2018). A observação de uma linha radiolúcida, que representa a separação dos fragmentos da FRV só é possível em radiografias periapicais quando estas são feitas de forma que o feixe de raios-x esteja paralelo à linha de fratura, ou em estágios mais avançados onde há maior separação dos fragmentos (CHANG *et al.*, 2016; DE MARTIN *et al.*, 2018). Nascimento *et al.* (2015) avaliaram o diagnóstico de FRVs por meio de diferentes sistemas de radiografia digital intraoral, e foram observados valores de sensibilidade notavelmente baixos, variando de 0,38 a 0,53. Os autores ressaltaram que a presença de guta-percha e pinos metálicos, dificultou ainda mais o diagnóstico dessa entidade.

Por outro lado, a tomografia computadorizada de feixe cônico (TCFC) pode gerar melhor visualização das fraturas, por permitir a análise em múltiplos planos (coronal, axial e sagital), evitando que a sobreposição anatômica das estruturas prejudique o diagnóstico de trincas e fraturas radiculares (HASSAN *et al.*, 2009; DE MARTIN *et al.*, 2018). Além disso, a TCFC permite o diagnóstico precoce, evitando danos ao tecido periodontal, e a necessidade de exposição cirúrgica para o diagnóstico, podendo antecipar o tratamento (BRADY *et al.*, 2014). Dessa forma, estudos tem demonstrado que a TCFC representa uma excelente ferramenta para a visualização de fraturas radiculares, apresentando boa eficácia diagnóstica em dentes sem material intracanal (FERREIRA *et al.*, 2015; CHANG *et al.*, 2016; GAETA-ARAUJO *et al.*, 2017; DE MARTIN *et al.*, 2018).

Entretanto, em dentes preenchidos por material intracanal com alta radiodensidade, como guta-percha, pinos radiculares e núcleos metálicos, ocorre a formação de artefatos de imagem devido a diferenças desses materiais na atenuação e absorção do feixe de raios-x, causando o fenômeno *beam-hardening* (SCHULZE *et al.*, 2011). O resultado é a formação de uma imagem com qualidade diminuída pela presença de artefatos em forma de faixas hipodensas, listras hiperdensas e distorções de objetos metálicos (SCHULZE *et al.*, 2011). Estes elementos dificultam a visualização da estrutura dentária, e, portanto, a interpretação diagnóstica, podendo levar a resultados falso-positivos. Assim, o diagnóstico de FRV é substancialmente prejudicado pela formação de artefatos. Pinto *et al.* (2017) avaliaram a acurácia diagnóstica em dentes com FRV e restaurados com pinos metálicos. Os autores observaram intensa formação de artefatos associados aos pinos metálicos, que contribuíram significativamente para a menor acurácia diagnóstica. De forma semelhante, Hekmatian *et al.* (2018) demonstraram a maior dificuldade de diagnóstico de FRV em dentes obturados com guta-percha.

Deste modo, objetivando a redução de artefatos nas imagens de TCFC para facilitar a visualização de linhas de fraturas, diversos estudos têm sido realizados avaliando a mudança nos parâmetros de aquisição das imagens, a aplicação de algoritmos de redução de artefatos (ARA), e utilização de *softwares* com filtros de aprimoramento das imagens (BEZERRA *et al.*, 2015; FERREIRA *et al.*, 2015; DE REZENDE BARBOSA *et al.*, 2016; DE MARTIN *et al.*, 2018).

Os algoritmos redutores de artefato (ARA) foram desenvolvidos para melhorar a relação contraste-ruído durante a aquisição das imagens (BECHARA *et al.*, 2012). No entanto, a utilização de ARA não tem demonstrado resultados satisfatórios para a redução adequada de artefatos. Bezerra *et al.* (2015) avaliaram o diagnóstico de FRV em dentes com pinos metálicos, e concluíram que apesar de diminuir a formação de artefatos, contrariamente, o ARA teve impacto negativo sobre o diagnóstico. Em estudo semelhante, De Rezende Barbosa *et al.* (2016) observaram redução na capacidade diagnóstica de FRV na presença de pinos metálicos no interior dos canais, independentemente da utilização do ARA.

Os *softwares* de filtros de aprimoramento objetivam a redução de ruídos e aumento da qualidade das imagens com artefatos, através de algoritmos matemáticos aplicados em *softwares* específicos (WENZEL *et al.*, 2009; FERREIRA *et al.*, 2015; DE MARTIN *et al.*, 2018). Estes filtros vêm sendo analisados para o diagnóstico das fraturas radiculares (WENZEL *et al.*, 2009; FERREIRA *et al.*, 2015; DE MARTIN *et al.*, 2018), além da determinação precisa da posição do forame apical (ESTRELA *et al.*, 2018). Wenzel *et al.* (2009) observaram aumento da sensibilidade no diagnóstico de fraturas radiculares transversais após a aplicação de filtro de

aprimoramento de nitidez (*High-pass angio-sharpen filter*), em relação as imagens de TCFC originais geradas pelo equipamento i-CAT (Dental Imaging System, Salt Lake City, UT, EUA). Em contrapartida, outros estudos recentes não observaram diferenças na acurácia diagnóstica de FRV em dentes com pinos metálicos no interior dos canais em imagens obtidas em i-CAT com os filtros "Hard" e "Sharpen" (DE MARTIN *et al.*, 2018), além de "S9", "Smooth", "Smooth 3x3", "Sharpen-mild", e "Sharpen 3x3" (FERREIRA *et al.*, 2015). Dessa forma, o diagnóstico de FRV ainda representa um desafio clínico, especialmente na presença material intracanal, e os softwares com filtros de aprimoramento de imagens de TCFC analisados até o momento não demonstraram resultados consistentes.

Recentemente, um novo *software* de visualização de imagens de TCFC (e-Vol DX, CDT Software, Bauru, SP, Brasil) foi desenvolvido (BUENO *et al.*, 2018; ESTRELA *et al.*, 2018) para facilitar o diagnóstico em endodontia, por meio de diferentes ferramentas, como o filtro "*Blooming Artifact Reduction*" (BAR), que reduz a formação de artefatos brancos associados a materiais radiodensos. No entanto, poucos estudos foram encontrados sobre o diagnóstico de fraturas radiculares verticais por meio da utilização do *software* e-Vol DX, com o filtro BAR.

2 JUSTIFICATIVA

Diversos fatores estão associados a qualidade da imagem de TCFC, afetando diretamente a resolução espacial e de contraste. A identificação dos principais fatores que afetam a acurácia diagnóstica de FRV é importante para o desenvolvimento de ferramentas e estratégias diagnósticas mais precisas. A formação de artefatos causados por materiais de alta densidade, como pinos metálicos e guta-percha, dificultam a análise e interpretação de imagens tomográficas. A utilização de um novo *software* para aplicação de filtro de aprimoramento de imagens de TCFC, pode representar um grande avanço para o diagnóstico preciso de fraturas radiculares verticais completas e incompletas.

3 OBJETIVOS

3.1 OBJETIVO GERAL

Avaliar a acurácia diagnóstica de FRV completas e incompletas, por meio de imagens de TCFC, em diferentes situações clínicas.

3.2 OBJETIVOS ESPECÍFICOS

1. Desenvolver e reportar um método eficaz para a indução de FRV incompleta;
2. Comparar a acurácia diagnóstica após utilização das imagens originais de TCFC, e após a aplicação do filtro BAR do *software* e-Vol DX;
3. Avaliar a influência do material intracanal sobre a acurácia diagnóstica de FRV;
4. Comparar a acurácia diagnóstica de FRVs completas e incompletas.
5. Revisar sistematicamente a literatura para responder à seguinte questão: quais são os fatores associados com a acurácia diagnóstica de FRV por imagens de TCFC?

4 ARTIGO 1

Development and validation of a method for creating incomplete vertical root fracture in extracted teeth

Luiz Carlos de Lima Dias-Junior[1], Lucas da Fonseca Roberti Garcia[1], Eduardo Antunes Bortoluzzi[2].

[1] Department of Dentistry, Federal University of Santa Catarina (UFSC), Florianópolis, SC, Brazil.

[2] Department of Diagnosis & Oral Health, Division of Endodontics, School of Dentistry, University of Louisville, Louisville, KY, USA.

Artigo formatado conforme normas do periódico **Odontology**.

Abstract

The present study reported a method for inducing incomplete root fracture in human extracted teeth for the purpose of evaluating the merits of different diagnostic imaging techniques. Thirty-five single-rooted teeth were inspected under magnification and transillumination to exclude previously fractured teeth. Tooth crowns were removed, and the root canals were prepared until the ProTaper Next® X4 file. Each root was lined with wax and embedded in a polystyrene resin block. The setup was attached to a universal testing machine for pressing a customized conical wedge (diameter at tip: 0.6 mm; taper: 0.2 mm/mm) into the instrumented canal with a 2 kN load at 5 mm/min. The machine was programmed to stop after a sudden 10% drop in loading force. Each specimen was removed from the resin block and inspected under 20× magnification and transillumination to identify the fracture characteristics (pattern, surfaces and root-third affected). The gap width of each specimen was measured at different locations along the fracture line. The protocol induced incomplete vertical root fractures in all specimens. Fracture widths were <100 μm in all specimens (mean gap width: 34.9 μm). The proposed methodology was successful in inducing incomplete vertical root fractures with characteristics that resemble the clinical presentation of these conditions. The method is easy to execute, highly reproducible and helps to minimize bias in laboratory studies that aims to mimic vertical root fractures.

Keywords: Cone-Beam Computed Tomography, diagnosis, endodontics, fracture width, vertical root fracture.

Introduction

Cracks and fractures are often found in teeth with extensive restorations [1]. They may occur immediately upon completion of the restoration or after a long period or intraoral function [1]. Horizontal root fracture is highly associated with dental trauma [1]. An impact with substantial kinetic energy causes immediate horizontal fracture of the root structure [1]. Conversely, vertical root fracture (VRF) may be caused by trauma or fatigue, with persistent occlusal forces slowly causing rupture of the tooth substrate [1].

The etiology of VRF is multifactorial [2]. These fractures are often associated with excessive occlusal forces, parafunctional habits, dental trauma or after root canal treatment [3]. Iatrogenic factors during root canal treatment include excessive root canal enlargement, exaggerated forces during lateral or vertical compaction of root canal filling or insertion of intraradicular screw posts [4].

VRFs are longitudinally-oriented fractures of the root [1]. They represent approximately 2-5% of all dental fractures [3] and are present in 3.7-13.4% of root-treated teeth [5]. VRFs occur more frequently in older patients and represent 7.7-32.1% of all causes of tooth extraction [6]. In root-treated teeth, VRFs are the third most common reason for extraction [5]. The communication between the root canal and the periodontium created by a VRF creates a pathway for bacterial contamination, which results in rapid alveolar bone loss. Prompt and accurate diagnosis of VRF is required to prevent additional damage to the alveolar bone by removing the cause of inflammation and the source of contamination [3].

The diagnosis of VRF is a colossal challenge to dental clinicians [2]. Clinical signs and symptoms are often non-specific, such as the presence of deep osseous defects or sinus tracts. There is also a lack of pathognomonic signs and symptoms [3]. A robust diagnostic strategy needs to involve a patient's dental history, clinical signs and symptoms, as well as radiographic imaging [1]. During the initial stage of VRFs, the clinical signs are similar to those of failed root canal therapy, periodontal disease or even endodontic-periodontal complications [7]. Hence, it is essential to differentiate VRF from other clinical problems. Imaging plays an important role in the differential diagnosis of the clinical problem.

Cone-beam computed tomography (CBCT) has been used for attempted detection of VRFs in unfilled roots [7-10]. However, VRF diagnosis using CBCT is severely hindered in the presence of root canal fillings or metal posts [7-10]. These high-density materials create

beam-hardening artifacts which resemble fracture lines [7-10]. Diagnostic accuracy is compromised in incomplete VRFs even with the use of high-resolution CBCT [7-10]. This is attributed to minimal separation of the fractured root fragments that is typically found in these cases [11]. Because the prognosis of VRF is poor, the only possible approach in most cases is tooth extraction [10].

Countless efforts have been made to develop tools that improve the diagnostic accuracy of CBCT imaging in detecting VRFs, particularly in the presence of root canal fillings or metallic posts. Artifact reduction algorithms [12-14] and filters [7, 15, 16] have been evaluated, associated with acquisition parameters such as resolution [7, 15, 17] and field of view [14, 17]. Nevertheless, definitive diagnosis of VRFs, especially incomplete VRFs, often requires invasive exploratory surgery [18, 6]. Studies that evaluate the diagnosis of incomplete VRFs are urgently needed to improve diagnostic accuracy and reduce the need of invasive procedures.

Diagnostic research on VRF is challenging because its identification depends on different aspects, such as fracture width [11, 19-21], direction (buccolingual or mesiodistal) [7] and the tooth position in the field of view (central or peripheral) [14]. Previous studies artificially induced complete VRFs and bonded the fragments back to simulate incomplete root fractures [9, 15]. This technical procedure does not simulate the clinical features of VRF in terms of fracture width and fragment position [11]. Moreover, fractured teeth with more than two fragments or fracture patterns that do not permit repositioning are usually discarded, causing unnecessary loss of specimens [12, 8, 10, 22].

There is limited reproducibility of the methodologies used to induce artificial incomplete VRF in extracted human teeth. Towards this objective, the development of a highly reproducible and evidence-based laboratory model able to identify the presence of incomplete VRFs is crucial. Accordingly, the purpose of the present in vitro study was to develop and to validate a deep learning method for creating incomplete VRF in single-rooted human teeth.

Material and methods

Sample selection

The present in vitro study was conducted in accordance with the Preferred Reporting Items for Laboratory studies in Endodontology (PRILE) 2021 guidelines [23]. The study proposal was approved by the institutional Ethics Committee (Protocol n. 4.444.914/2020).

Freshly extracted human permanent teeth were selected with consent received by the donors for the use of the unidentified teeth for benchtop research. Single-rooted teeth were used to avoid anatomic differences that might complicate the analysis and create bias. The teeth were inspected under stereomicroscope (Stereo Discovery V12; Carl Zeiss, Oberkochen, Germany) at ×20 magnification and transillumination. Teeth with open apices, root curvatures, supernumerary roots, obliterated canals, pulp calcifications, internal/external resorption, root canal fillings, cavities or pre-existing cracks/fractures were excluded. from the final sample. Periapical radiographs were taken and examined by a previously trained radiologist to validate the specimen selection.

Specimen preparation

The selected teeth were hand-scaled to remove soft tissue and calculus. The cleaned teeth were disinfected with 2% glutaraldehyde for two hours and kept hydrated until fractures were induced. The tooth crowns were sectioned at the cementoenamel junction (CEJ) with a double-sided diamond saw (Buehler Ltd., Lake Bluff, IL, USA) coupled to a metallographic-cutter (Isomet 1000; Buehler Ltd.) under copious water cooling. A size 10 K-file (Dentsply Maillefer, Ballaigues, Switzerland) was placed in the canal until it was visible at the apical foramen. The working length was determined by subtracting 1 mm from this measurement.

The root canals were prepared with nickel-titanium rotary instruments (ProTaper Next; Dentsply Sirona, Bensheim, Germany). In order to standardize the apical portion up to a size 40/.06 instrument, the instruments X1 (17/.04), X2 (25/.06), X3 (30/.07) and X4 (40/.06) were sequentially used. Each instrument was coupled to a 6:1 contra-angle device powered by an electric motor (X-Smart Plus; Dentsply Sirona), driven in rotary motion (400 rpm; 2 Ncm) with light apical pressure. Gentle back-and-forth motions were used until the working length reaching and each instrument was capable of rotating freely within the root canal. Foraminal patency was maintained with a size 10 K-file (Dentsply Maillefer). The root canals were irrigated with 2 mL of 2.5% sodium hypochlorite solution (Rio Química, São José do Rio Preto, SP, Brazil) at each instrument change. The irrigating solution was delivered within the root canals with a 5-mL syringe (Ultradent, Salt Lake City, UT, USA) and a 30-gauge needle (Endo-Eze; Ultradent) with back-and-forth movements. After completion of the chemical-mechanical preparation, the root canals were irrigated with 5 mL of 2.5% sodium hypochlorite solution and dried with absorbent paper cones (Dentsply Maillefer).

Incomplete VRF induction

Each tooth root was lined with a 1 mm-thick layer of wax and temporarily fixed in polystyrene resin (ComFibras, Florianopolis, SC, Brazil) to 3 mm from the CEJ, using a cylindrical mold (19 mm in diameter x 24 mm in height). Fractures were induced with a universal testing machine (Instron Corp., Canton, MA, USA). The fractures were mechanically created by applying a customized metallic wedge apically at the root canal. The tapered metal wedge was placed inside the root canal. The testing machine was set to apply a maximum load of 2 kN. The universal testing machine was programed to stop automatically when 10% force reduction was recorded. This force was strong enough to create root dentin fracture without fragment separation, producing an incomplete VRF [24] (Fig. 1).

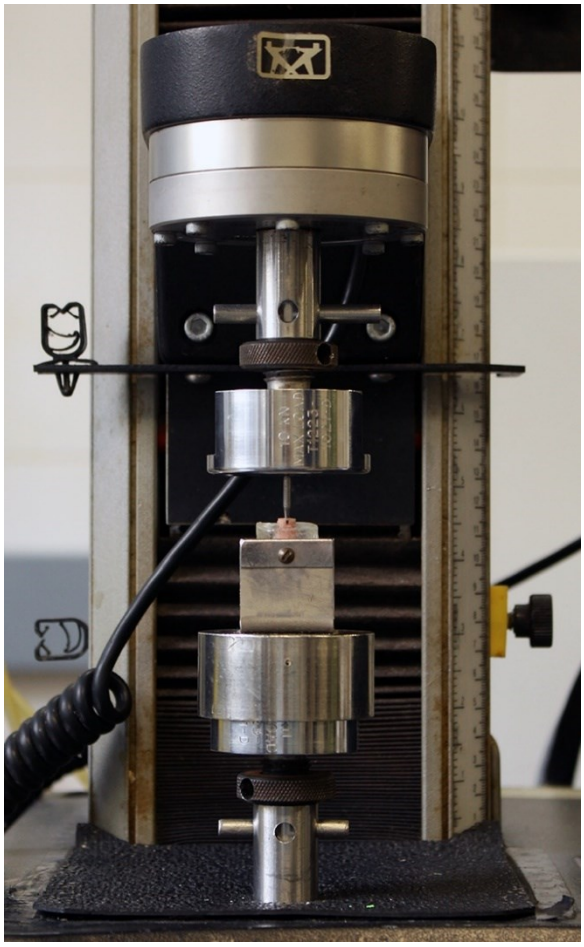

Fig. 1 Experimental setup for inducing incomplete VRF: a universal test machine with the specimen temporarily fixed in an acrylic resin block. Each specimen was positioned in a fixed platform with the metal conical wedge inside the root canal. A flat base was adapted to the top of the testing machine to gradually force the wedge into the root canal.

Pilot study

A pilot study was conducted to identify the most appropriate characteristics for creating incomplete VRFs. The following wedges were tested in the pilot study: 40.3 (diameter at tip = 0.4 mm; taper = 0.3 mm/mm); 60.2 (diameter at tip = 0.6 mm; taper = 0.2 mm/mm) and 60.05 (diameter at tip= 0.6 mm; taper = 0.05 mm/mm). In addition, two crosshead speeds were tested: 1 mm/min and 5 mm/min. Thirty specimens were used in the pilot study, with six groups of five teeth each for testing the customized wedges and crosshead speeds.

Each specimen was removed from the resin block immediately after fracture to verify the presence of incomplete VRF. Examination was performed under stereomicroscope (Stereo Discovery V12; Carl Zeiss) at ×20 magnification and transillumination. The success rate of the experimental groups from the pilot study were compared using the Fisher Exact test (SPSS Statistics, Version 25.0; IBM Corp., IBM Armonk, NY, USA). Statistical significance was set at alpha = 0.05.

Success rate

The most appropriate protocol was further analyzed for its success rate in creating incomplete VRNs to ensure the reproducibility of the protocol. Sample size was calculated using data from the pilot study. A priori power analysis indicated that a total of 35 teeth would be required for 5% error margin and 95% confidence level. Using the protocol selected from the pilot study, 35 additional teeth were subjected to the VRF induction.

After fracture, the 35 specimens were re-inspected under stereomicroscope (Stereo Discovery V12; Carl Zeiss) at ×20 magnification and transillumination. Additional verification was performed using 1% methylene blue dye to highlight the pathway of each fracture (Fig. 2). The fracture pattern (complete or incomplete fracture) affected root surface (buccal, lingual, mesial, distal or combination), extension (root-thirds involved: cervical, middle or apical) and the fracture origin (cervical or apical) were recorded.

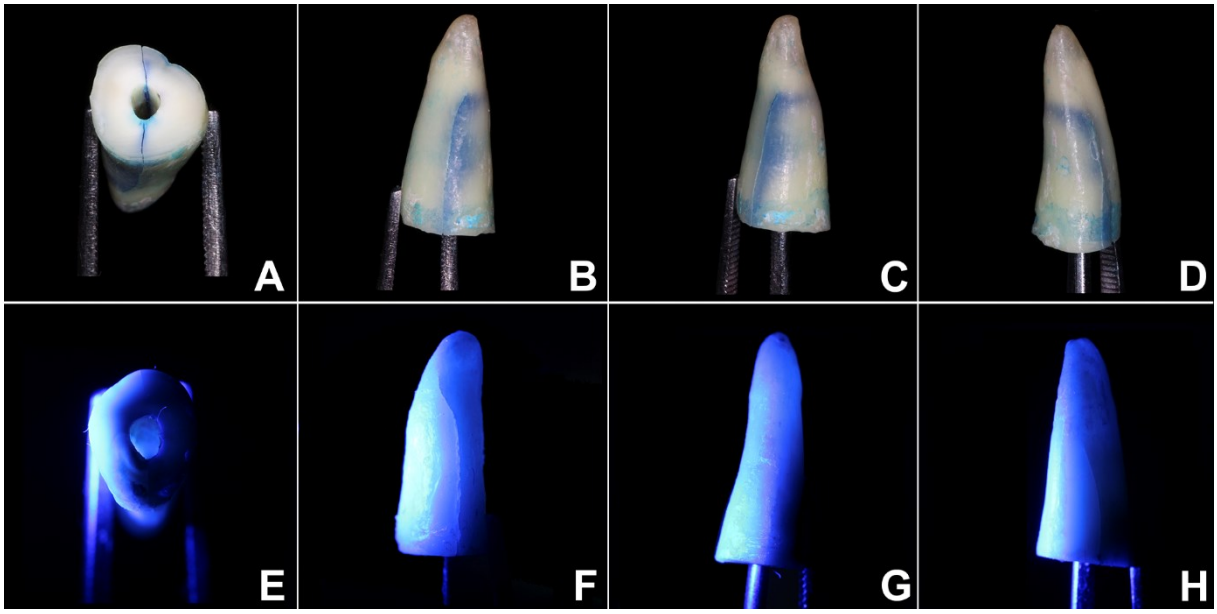

Fig. 2 Inspection via application of 1% methylene blue (A, B, C and D), and light-emitting diode transillumination (E, F, G and H) for identification and characterization of incomplete VRFs.

Fracture width

Fracture width was determined by a previously calibrated and trained examiner, using a stereomicroscope video-based system (Stereo Discovery V12; Carl Zeiss, Oberkochen, Germany) installed with the AxioVision v. 4.8.3 software (Carl Zeiss). A plastic transparent ruler was positioned on top of the cervical aspect of each specimen as a measuring scale. The distance between fragments was measured at three points: P1 - as close as possible to the root canal; P2 - as close as possible to the external root surface; and P3 - intermediate point between P1 and P2 (Figure 3). This was repeated for both fracture lines of each specimen. The values from P1, P2, and P3 of both fracture lines were used to calculate the mean fracture width for each specimen.

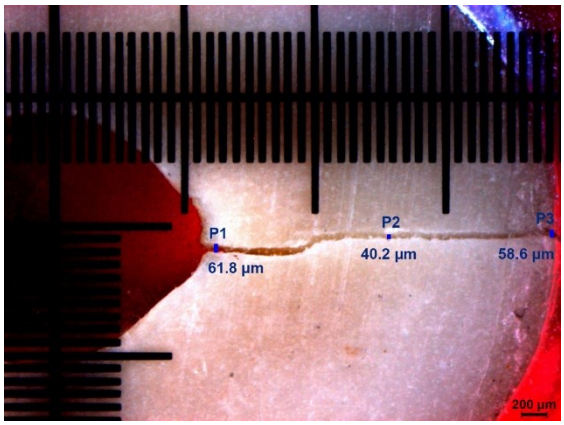

Fig. 3 Representative stereomicroscopic image of a narrow incomplete VRF with gap width measurements at locations P1, P2 and P3 (see text for detailed descriptions of these locations).

Results

Pilot study

There was a statistically significant difference among the tested protocols of the pilot study ($P < 0.05$). The success rate of the protocol that used a 60.2 wedge at 5 mm/min was significantly higher than the other protocols ($P < 0.05$). This protocol successfully induced incomplete VRFs in all 5 specimens. When the 60.2 wedge was used at 1 mm/min, two specimens were lost because it chipped the coronal third, creating an unrealistic fracture that was not vertically oriented. The protocols using the 40.3 wedge also chipped the coronal third in three of the specimens, regardless of the crosshead speed.

The 60.05 wedge created catastrophic failure with multiple fragments at the apical third of three specimens when the crosshead speed of 1 mm/min was employed. Likewise, the 60.05 wedge created similar catastrophic failure in two specimens when the crosshead speed of 5 mm/min was employed. In addition, one specimen from each group was lost because of the generation of a complete VRF.

Final success rate

The overall success rate of the protocol using 60.2 wedge at 5 mm/min was 100%. Incomplete root fracture was obtained for all 35 specimens. There was no loss of specimens that was attributed to complex root fractures or complete separation of fragments. Regarding the root thirds that were affected by the fracture line, in 8 specimens the fracture was limited to the cervical root third, 20 specimens presented fractures at the cervical and middle root thirds, and in 7 specimens the fracture extended to the apical root third (Fig. 4A). The mean fracture width was 34.9 μm (20.4-86.3 μm) (Fig. 4B). Table 1 summarizes the fracture characteristics of each specimen and the respective mean fracture width.

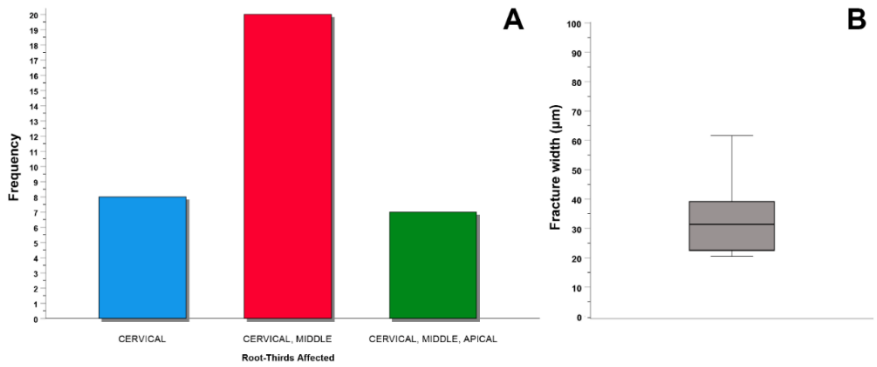

Fig. 4 Frequency of root thirds affected by the fracture lines (A). Box-plot of the mean fracture width (μm) (B).

Table 1. Vertical root fracture characteristics, including tooth type, fracture pattern and origin, surfaces and root-thirds affected by the fractures, and mean fracture width of the experimental protocol (60.2 wedge at 5 mm/min)

Sample	Tooth	Pattern	Surfaces affected	Root-thirds affected	Fracture origin	Mean fracture width (μm)
1	11	Incomplete	B, L	cervical, middle	cervical	50.7
2	22	Incomplete	M, D	cervical, middle	cervical	38.1
3	12	Incomplete	B, L	cervical	cervical	22.2
4	35	Incomplete	B, L	cervical, middle, apical	cervical	20.4
5	11	Incomplete	MB, DL	cervical, middle, apical	cervical	86.3
6	12	Incomplete	B, L	cervical, middle, apical	cervical	38.4
7	44	Incomplete	B, DL	cervical, middle	cervical	57.2
8	35	Incomplete	M, D	cervical, middle	cervical	39.8
9	22	Incomplete	B, L	cervical	cervical	31.5
10	15	Incomplete	MB, ML	cervical, middle	cervical	32.5
11	21	Incomplete	B, L	cervical, middle, apical	cervical	37.2
12	45	Incomplete	DB, L	cervical	cervical	32.1
13	12	Incomplete	B, L	cervical, middle	cervical	51.9
14	21	Incomplete	B, L	cervical, middle	cervical	61.6
15	25	Incomplete	B, L	cervical, middle, apical	cervical	65.9
16	21	Incomplete	MB, DL	cervical, middle	cervical	28.5
17	45	Incomplete	M, D	cervical, middle	cervical	22.4
18	11	Incomplete	M, D	cervical	cervical	21.9
19	21	Incomplete	MB, ML	cervical	cervical	46.2
20	12	Incomplete	DB, L	cervical, middle	cervical	28.2
21	12	Incomplete	MB, DL	cervical, middle	cervical	24.5
22	35	Incomplete	B, L	cervical, middle, apical	cervical	49.3
23	21	Incomplete	MB, DL	cervical, middle	cervical	31.4
24	44	Incomplete	ML, D	cervical, middle	cervical	20.8
25	12	Incomplete	M, D	cervical, middle, apical	cervical	34.8
26	21	Incomplete	DB, ML	cervical, middle	cervical	21.3
27	15	Incomplete	M, D	cervical	cervical	25.1
28	21	Incomplete	B, D	cervical, middle	cervical	23.2
29	34	Incomplete	MB, ML	cervical, middle	cervical	22.4
30	35	Incomplete	M, DB	cervical, middle	cervical	21.4
31	11	Incomplete	M, D	cervical, middle	cervical	30.2
32	12	Incomplete	M, MB	cervical, middle	cervical	22.6
33	15	Incomplete	DB, ML	cervical	cervical	21.5
34	34	Incomplete	B, D	cervical	cervical	34.4
35	11	Incomplete	MB, DL	cervical, middle	cervical	25.3

Abbreviations. B: buccal; L: lingual; M: mesial; D: distal; MB: mesiobuccal; ML: mesiolingual; DB: distobuccal; DL: distolingual

Discussion

Incomplete VRFs, also known as hairline fractures, are manifested by minimal fragment separation. These fractures are not easily detected by periapical radiographs [11, 22] and are less likely to be associated with abrupt increases in periodontal pocket depth and the presence of sinus tracts [22]. CBCT is insensitive and has low specificity in diagnosing hairline fracture [19, 22], even for teeth with unfilled root canals [11, 20].

Although the diagnosis of VRF has been extensively investigated using *in vitro* studies, the methods used so far to induce root fractures are heterogeneous and often poorly described. In a method reported for inducing complete VRFs in canine teeth, a conical wedge was placed inside the root canal and tapped with a hammer in the apical direction [25]. This method had been utilized by several studies for artificially producing incomplete VRF [19, 13, 8, 20]. Other studies created artificial incomplete VRFs by splitting teeth directly with a chisel and hammer [7, 9]. Some studies induced fractures by placing a pin inside the root canal and turning with a screwdriver [14] or wrench [12]. Another study applied mechanical force directly to the roots with a hammer placed on a soft rubber foundation [15]. These methods suffer from serious reproducibility problems. Information is lacking on the characteristics of the wedges [19, 13, 8, 20, 10, 21], pins [14, 15] or chisels [7, 9, 21], as well as the magnitude and direction of load applied to the teeth [19, 7, 13, 8, 9, 20, 10, 21, 15]. Because these variables are difficult to control, it is unlikely that these methods can be accurately replicated.

Although some studies employed universal testing machines to create incomplete VRFs [11, 22, 17, 16], the settings varied in terms of forces and crosshead speeds. The crosshead speed that was most commonly used was 1 mm/min [11, 22, 16]. Regarding the characteristics of the wedges or conical tips applied to the root canals, there is a general lack of information on their diameters and tapers [17, 16]. However, the characteristics of the wedges or pins also affected the technique. A thin sewing needle was used to induce incomplete VRF, and a large needle was used to induce complete VRF with a universal testing machine [22]. In the present work, a pilot study was performed using different types of wedges and pins with different diameters and tapers. A common observation in the pilot study was that the teeth usually chipped at the cervical region with the use of low crosshead speeds. The most consistent setting to induce incomplete VRF was identified to be 5 mm/min. The use of a highly-tapered pin (40.3) also caused chipping of the cervical region. In contrast, wedges with lower tapers

usually created catastrophic root dentin failure at the apical region (60.05). A conical wedge with 0.6 mm diameter at the tip and 0.2 mm/mm taper was ultimately chosen. This instrument enabled the authors to create incomplete VRF reliably.

Previous studies [26, 11, 22] programmed the universal testing machine to automatically stop applying loading force upon a sudden drop in force of 20% or more. This method was modified in the present work by setting the threshold to 10%. In this manner, it is possible to check the propagation of the fracture line after the machine stopped; further loading force may be applied if required. For creating incomplete VRF, it was necessary to create a customized support base to fix the specimen at the platform of the universal testing machine. This support base prevented further spontaneous propagation of the fracture and prevented the tooth from splitting into two fragments (i.e., complete VRF).

The diagnostic accuracy of CBCT depends on the width of the VRF [11, 19-21]. It has been reported [22] that an incomplete VRF this is less than 150 μm wide is impossible to create using a chisel and hammer or tapping a conical wedge into the root canal. According to those authors, the widths of the fractures obtained using these methods were over 200 μm, which approximate complete VRF more than incomplete VRF [11, 22]. The present study attempted to establish a highly-reproducible method to induce incomplete VRFs that simulate clinical scenarios. Therefore, it was imperative to control the fracture width. Clinically, incomplete VRFs usually have minimal fragment separation, with an average gap size of 53.5 μm [11]. The method reported in the present study successfully reproduced the width range of *in vivo* incomplete VRFs [22], with a mean gap width of 34.9 μm.

Clinically, the width of VRFs ranges from 60 to 770 μm [27]. Incomplete VRFs have gap widths between 30 and 110 μm [11, 22], while the gap widths of complete VRFs are usually over 200 μm [22]. After induction of complete VRFs, some studies bonded the fragments together to simulate incomplete VRFs [8, 10, 17, 15]. Although most of the published studies did not report the fracture width, it is unlikely that investigations with bonded fragments generated fractures with gap widths that are smaller than 200 μm [21]. Thus, previous studies might have created artificial VRFs that are unrealistic in simulating clinical incomplete VRFs [13, 8, 10, 21, 17, 15].

The present study induced root fractures using a quasi-static model. In this model, the wedge was progressively introduced into the root canal, with increased applied force, until the fracture occurs. Conversely, a dynamic model based on fatigue loading has been used to

evaluate the fracture resistance of endodontically treated teeth [28]. It is likely that most VRFs occur after repetitive occlusal loading due to fatigue, rather than a single episode of high occlusal stress. However, it is impossible to clinically differentiate these two conditions in the diagnosis of VRFs. The use of fatigue loading to induce VRFs might impair the method's reproducibility in consistently producing incomplete VRFs.

With respect to reproducibility, one may argue that differences in the root surface morphology, the root-third in which VRF occurs, as well as the fracture width, may invalidate the proposed method. However, the progress of fracture through dentin is dependent upon tooth structure factors such as dentin volume, root canal shape and the presence of sclerotic dentin [29]. These features are impossible to be standardized. The fracture width varied from 20.4 to 86.3 μm. Considering the microscopical scale of incomplete VRFs, this difference is clinically insignificant. Moreover, the clinical aspect of VRFs is highly variable, producing identical VRFs would have no practical value for *in vitro* diagnostic studies. The present manuscript does not deliver direct new evidence. However, it offers support for further diagnostic investigations by providing a reliable method to artificially create incomplete VRFs. The current method has been demonstrated in different single-rooted teeth (i.e., maxillary incisors and maxillary/mandibular premolars). Specimen selection criteria did not include the anatomical diameter of the root canals nor the root shape (i.e., round, oval, long oval). This is because over-restricting the criteria for standardization of tooth specimens will hinder the reproducibility of the method employed. The objective here was to develop a method that can be replicated using single-rooted teeth.

Notwithstanding the numerous efforts to calibrate operators and standardize fracture methods, problems of specimen wastage have been reported [12, 13, 8, 22, 15]. Specimen loss due to fracture with more than two fragments occurs in 13.3-25% of the specimens [8, 22]. Because of the lower reproducibility of the fracture methods, it has been reported that 6-10 specimens must be used in pilot experiments to determine the load required to induce root fracture [13, 15]. In comparison, there was no specimen loss in the present study, with a 100% success rate in creating incomplete VRF. Although most fractures occurred at the buccal and lingual surfaces and propagated across the cervical and middle root-thirds, the methodology presented created different types of incomplete VRF similar to the clinical manifestations of this condition. Because fracture induction was performed in a controlled manner, it is possible to apply additional loading forces to the specimens, after examination of the incomplete VRFs,

to obtain complete VRFs.

Conclusions

The protocol reported in the present study bridged a gap in the current literature, on the availability of a reliable method to create laboratory-induced incomplete VRFs that simulate the clinical characteristics of these conditions. Further investigations are required to improve the diagnostic accuracy of CBCT imaging of incomplete VRF. The proposed method provides the basis for future analysis using CBCT softwares for the diagnosis of incomplete VRFs.

Declarations

Conflict of interest

The authors declare that they have no known competing financial interests or personal relationships that could have appeared to influence the work reported in this paper.

Ethical approval

All procedures performed in studies involving human participants were in accordance with the ethical standards of the institutional and/or national research committee and with the 1964 Helsinki Declaration and its later amendments or comparable ethical standards. The study was approved by the Ethics Committee of the Federal University of Santa Catarina - UFSC (No. 4.444.914/2020).

References

1. Rivera EM, Walton RE. Longitudinal tooth cracks and fractures: an update and review. Endodontic Topics. 2015;33(1):14-42. doi:10.1111/etp.12085.
2. Garcia-Guerrero C, Parra-Junco C, Quijano-Guauque S, Molano N, Pineda GA, Marin-Zuluaga DJ. Vertical root fractures in endodontically-treated teeth: A retrospective analysis of possible risk factors. J Investig Clin Dent. 2018;9(1). doi:10.1111/jicd.12273.
3. Cohen S, Blanco L, Berman L. Vertical root fractures: clinical and radiographic diagnosis. J Am Dent Assoc. 2003;134(4):434-41. doi:10.14219/jada.archive.2003.0192.
4. Fuss Z, Lustig J, Katz A, Tamse A. An evaluation of endodontically treated vertical root fractured teeth: impact of operative procedures. J Endod. 2001;27(1):46-8. doi:10.1097/00004770-200101000-00017.
5. Toure B, Faye B, Kane AW, Lo CM, Niang B, Boucher Y. Analysis of reasons for extraction of endodontically treated teeth: a prospective study. J Endod. 2011;37(11):1512-5. doi:10.1016/j.joen.2011.07.002.
6. Chen SC, Chueh LH, Hsiao CK, Wu HP, Chiang CP. First untoward events and reasons for tooth extraction after nonsurgical endodontic treatment in Taiwan. J Endod. 2008;34(6):671-4. doi:10.1016/j.joen.2008.03.016.
7. De Martin ESD, Campos CN, Pires Carvalho AC, Devito KL. Diagnosis of Mesiodistal Vertical Root Fractures in Teeth with Metal Posts: Influence of Applying Filters in Cone-beam Computed Tomography Images at Different Resolutions. J Endod. 2018;44(3):470-4. doi:10.1016/j.joen.2017.08.030.
8. Dutra KL, Pacheco-Pereira C, Bortoluzzi EA, Flores-Mir C, Lagravere MO, Correa M. Influence of Intracanal Materials in Vertical Root Fracture Pathway Detection with Cone-beam Computed Tomography. J Endod. 2017;43(7):1170-5. doi:10.1016/j.joen.2017.02.006.
9. Hassan B, Metska ME, Ozok AR, van der Stelt P, Wesselink PR. Detection of vertical root fractures in endodontically treated teeth by a cone beam computed tomography scan. J Endod. 2009;35(5):719-22. doi:10.1016/j.joen.2009.01.022.
10. Melo SL, Bortoluzzi EA, Abreu-Junior M, Correa LR, Correa M. Diagnostic ability of a cone-beam computed tomography scan to assess longitudinal root fractures in prosthetically treated teeth. J Endod. 2010;36(11):1879-82. doi:10.1016/j.joen.2010.08.025.
11. Brady E, Mannocci F, Brown J, Wilson R, Patel S. A comparison of cone beam computed tomography and periapical radiography for the detection of vertical root fractures in nonendodontically treated teeth. Int Endod J. 2014;47(8):735-46. doi:10.1111/iej.12209.
12. Dalili Kajan Z, Taramsari M, Khosravi Fard N, Khaksari F, Moghasem Hamidi F. The Efficacy of Metal Artifact Reduction Mode in Cone-Beam Computed Tomography Images on Diagnostic Accuracy of Root Fractures in Teeth with Intracanal Posts. Iranian endodontic journal. 2018;13(1):47-53. doi:10.22037/iej.v13i1.17352.
13. de Rezende Barbosa GL, Sousa Melo SL, Alencar PN, Nascimento MC, Almeida SM. Performance of an artefact reduction algorithm in the diagnosis of in vitro vertical root fracture in four different root filling conditions on CBCT images. Int Endod J. 2016;49(5):500-8. doi:10.1111/iej.12477.
14. Nikbin A, Dalili Kajan Z, Taramsari M, Khosravifard N. Effect of object position in the field of view and application of a metal artifact reduction algorithm on the detection of vertical root fractures on cone-beam computed tomography scans: An in vitro study. Imaging Sci Dent. 2018;48(4):245-54. doi:10.5624/isd.2018.48.4.245.
15. Wenzel A, Haiter-Neto F, Frydenberg M, Kirkevang LL. Variable-resolution cone-beam computerized tomography with enhancement filtration compared with intraoral photostimulable phosphor radiography in detection of transverse root fractures in an in vitro

model. Oral Surg Oral Med Oral Pathol Oral Radiol Endod. 2009;108(6):939-45. doi:10.1016/j.tripleo.2009.07.041.
16. Gaeta-Araujo H, Nascimento EHL, Oliveira-Santos N, Queiroz PM, Oliveira ML, Freitas DQ et al. Effect of digital enhancement on the radiographic assessment of vertical root fractures in the presence of different intracanal materials: an in vitro study. Clin Oral Investig. 2021;25(1):195-202. doi:10.1007/s00784-020-03353-x.
17. Queiroz PM, Santaella GM, Capelozza ALA, Rosalen PL, Freitas DQ, Haiter-Neto F. Zoom Reconstruction Tool: Evaluation of Image Quality and Influence on the Diagnosis of Root Fracture. J Endod. 2018;44(4):621-5. doi:10.1016/j.joen.2017.10.011.
18. Quintero-Alvarez M, Bolanos-Alzate LM, Villa-Machado PA, Restrepo-Restrepo FA, Tobon-Arroyave SI. In vivo detection of vertical root fractures in endodontically treated teeth: Accuracy of cone-beam computed tomography and assessment of potential predictor variables. J Clin Exp Dent. 2021;13(2):e119-e31. doi:10.4317/jced.57471.
19. Byakova SF, Novozhilova NE, Makeeva IM, Grachev VI, Kasatkina IV. The detection of vertical root fractures in post-core restored teeth with cone-beam CT: in vivo and ex vivo. Dentomaxillofac Radiol. 2019;48(6):20180327. doi:10.1259/dmfr.20180327.
20. Makeeva IM, Byakova SF, Novozhilova NE, Adzhieva EK, Golubeva GI, Grachev VI et al. Detection of artificially induced vertical root fractures of different widths by cone beam computed tomography in vitro and in vivo. Int Endod J. 2016;49(10):980-9. doi:10.1111/iej.12549.
21. Ozer SY. Detection of vertical root fractures of different thicknesses in endodontically enlarged teeth by cone beam computed tomography versus digital radiography. J Endod. 2010;36(7):1245-9. doi:10.1016/j.joen.2010.03.021.
22. Patel S, Brady E, Wilson R, Brown J, Mannocci F. The detection of vertical root fractures in root filled teeth with periapical radiographs and CBCT scans. Int Endod J. 2013;46(12):1140-52. doi:10.1111/iej.12109.
23. Nagendrababu V, Murray PE, Ordinola-Zapata R, Peters OA, Rocas IN, Siqueira JF, Jr. et al. PRILE 2021 guidelines for reporting laboratory studies in Endodontology: A consensus-based development. Int Endod J. 2021;54(9):1482-90. doi:10.1111/iej.13542.
24. Fayad MI, Ashkenaz PJ, Johnson BR. Different representations of vertical root fractures detected by cone-beam volumetric tomography: a case series report. J Endod. 2012;38(10):1435-42. doi:10.1016/j.joen.2012.05.015.
25. Monaghan P, Bajalcaliev JG, Kaminski EJ, Lautenschlager EP. A method for producing experimental simple vertical root fractures in dog teeth. J Endod. 1993;19(10):512-5. doi:10.1016/S0099-2399(06)81493-7.
26. Fox A, Basrani B, Lam EWN. The Performance of a Zirconium-based Root Filling Material with Artifact Reduction Properties in the Detection of Artificially Induced Root Fractures Using Cone-beam Computed Tomographic Imaging. J Endod. 2018;44(5):828-33. doi:10.1016/j.joen.2018.02.007.
27. Chavda R, Mannocci F, Andiappan M, Patel S. Comparing the In Vivo Diagnostic Accuracy of Digital Periapical Radiography with Cone-beam Computed Tomography for the Detection of Vertical Root Fracture. Journal of Endodontics. 2014;40(10):1524-9. doi:10.1016/j.joen.2014.05.011.
28. Ambica K, Mahendran K, Talwar S, Verma M, Padmini G, Periasamy R. Comparative evaluation of fracture resistance under static and fatigue loading of endodontically treated teeth restored with carbon fiber posts, glass fiber posts, and an experimental dentin post system: an in vitro study. J Endod. 2013;39(1):96-100. doi:10.1016/j.joen.2012.07.003.

29. Sodvadiya UB, Bhat GS, Shetty A, Hegde MN, Shetty P. The "Butterfly Effect" and Its Correlation to the Direction of the Fracture Line in Root Dentin. J Endod. 2021;47(5):787-92. doi:10.1016/j.joen.2021.01.011.

Figure Legends

Fig. 1 Experimental setup for inducing incomplete VRF: a universal test machine with the specimen temporarily fixed in an acrylic resin block. Each specimen was positioned in a fixed platform with the metal conical wedge inside the root canal. A flat base was adapted to the top of the testing machine to gradually force the wedge into the root canal

Fig. 2 Inspection via application of 1% methylene blue (A, B, C and D), and light-emitting diode transillumination (E, F, G and H) for identification and characterization of incomplete VRFs

Fig. 3 Representative stereomicroscopic image of a narrow incomplete VRF with gap width measurements at locations P1, P2 and P3 (see text for detailed descriptions of these locations)

Fig. 4 Frequency of root thirds affected by the fracture lines (A). Box-plot of the mean fracture width (μm) (B)

Supplemental material 1. PRILE 2021 checklist.

Section/Topic	Item Number	Checklist Items	Reported on page number
Title	1a	The Title must identify the study as being laboratory-based, e.g. "laboratory investigation" or "*in vitro*," or "*ex vivo*" or another appropriate term	23
	1b	The area/field of interest must be provided (briefly) in the Title	23
Keywords	2a	At least two keywords related to the subject and content of the investigation must be provided	24
Abstract	3a	The rationale/justification of what the investigation contributes to the literature and/or addresses a gap in knowledge must be provided	24
	3b	The aim/objectives of the investigation must be provided	24
	3c	The body of the Abstract must describe the materials and methods used in the investigation and include information on data management and statistical analysis	24
	3d	The body of the Abstract must describe the most significant scientific results for all experimental and control groups	24
	3e	The main conclusion(s) of the study must be provided	24
Introduction	4a	A background summary of the scientific investigation with relevant information must be provided	25-27
	4b	The aim(s), purpose(s) or hypothesis(es) of an investigation must be provided ensuring they align with the methods and results	27
Materials and methods	5a	A clear ethics statement and the ethical approval granted by an ethics board, such as an Institutional Review Board or Institutional Animal Care and Use Committee, must be described	27
	5b	When harvesting cells and tissues for research, all the legal, ethical, and welfare rights of human subjects and animal donors must be respected, and applicable procedures described	27
	5c	The use of reference samples must be included, as well as negative and positive control samples, and the adequacy of the sample size justified	27
	5d	Sufficient information about the methods/materials/supplies/samples/specimens/instruments used in the study must be provided to enable it to be replicated	27-32
	5e	The use of categories must be defined, reliable and be described in detail	Not applicable
	5f	The numbers of replicated identical samples must be described within each test group. The number of times each test was repeated must be described	Not applicable
	5g	The details of all the sterilization, disinfection, and handling conditions must be provided, if relevant	28-29
	5h	The process of randomization and allocation concealment, including who generated the random allocation sequence, who decided on which specimens to be included and who assigned specimens to the intervention must be provided(if applicable)	Not applicable
	5i	The process of blinding the operator who is conducting the experiment (if applicable) and the examiners when assessing the results must be provided	Not applicable
	5j	Information on data management and analysis including the statistical tests and software used must be provided	29
Results	6a	The estimated effect size and its precision for all the objective (primary and secondary) for each group including controls must be provided	32-33
	6b	Information on the loss of samples during experimentation and the reasons must be provided, if relevant	32-33
	6c	All the statistical results, including all comparisons between groups must be provided	32
Discussion	7a	The relevant literature and status of the hypothesis must be described	35-38

	7b	The true significance of the investigation must be described	35
	7c	The strength(s) of the study must be described	35
	7d	The limitations of the study must be described	37-38
	7e	The implications for future research must be described	38
Conclusions	8a	The rationale for the conclusion(s) must be provided	38-39
	8b	Explicit conclusion(s) must be provided, i.e. the main "take-away" lessons	38-39
Funding and support	9a	Sources of funding and other support (such as supply of drugs, equipment) as well as the role of funders must be acknowledged and described	39
Conflicts of interest	10a	An explicit statement on conflicts of interest must be provided	39
Quality of images	11a	Details of the relevant equipment, software and settings used to acquire the image(s) must be described in the text or legend	29-33
	11b	If an image(s) is included in the manuscript, the reason why the image(s) was acquired and why it is included must be provided in the text	29-33
	11c	The circumstances (conditions) under which the image(s) were viewed and evaluated must be provided in the text	29-33
	11d	The resolution and any magnification of the image(s) or any modifications/ enhancements (e.g. brightness, image smoothing, staining etc.) that were carried out must be described in the text or legend	29-33
	11e	An interpretation of the findings (meaning and implications) from the image (s) must be provided in the text	29-33
	11f	The legend associated with each image must describe clearly what the subject is and what specific feature(s) it illustrates	42
	11g	Markers/labels must be used to identify the key information in the image(s) and defined in the legend	42
	11h	If relevant, the legend of each image must include an explanation whether it is pre-experiment, intra-experiment or post-experiment and, if relevant, how images over time were standardized	Not applicable

5 ARTIGO 2

Influence of a metal artifact reduction filter on the diagnostic accuracy of complete and incomplete vertical root fractures

Luiz Carlos de Lima Dias-Junior[1], Lucas da Fonseca Roberti Garcia[1], Eduardo Antunes Bortoluzzi[2].

[1] Department of Dentistry, Federal University of Santa Catarina (UFSC), Florianópolis, SC, Brazil.

[2] Department of Diagnosis & Oral Health, Division of Endodontics, School of Dentistry, University of Louisville, Louisville, KY, USA.

Artigo formatado conforme normas do periódico **Journal of Endodontics**.

Abstract

Introduction: This study aimed to assess the influence of the e-vol DX BAR filter on the diagnostic accuracy of complete and incomplete vertical root fractures (VRFs).

Methods: Twenty single-rooted teeth were selected. The tooth crowns were removed, and the root canals were prepared up to a 40.06 file. Each specimen was scanned in a Prexion 3D CBCT device, in a dry human skull, in four different situations: no root canal fillings, gutta-percha, fiberglass post, and metal post. The specimens were fractured in a universal testing machine (UTM) by pressing a customized conical wedge inside the root canal. The machine was programmed to stop after a sudden 10% drop in loading force. Each specimen was reinspected to confirm the presence of an incomplete VRF. Another set of CBCT scans was performed. Then, the fractures were completed in the UTM, the teeth were reinspected, and the CBCT images were acquired again. Images were assessed with the BAR filter, and with the original images, for the diagnosis of VRFs.

Results: The use of the BAR filter did not improve the diagnostic values of AUC, accuracy, sensitivity, and specificity, in both fracture patterns ($p>0.05$). The intracanal materials also did not influence on the diagnostic values of VRF ($p>0.05$). Incomplete VRFs presented significantly lower AUC, accuracy, and sensitivity, compared to complete VRFs ($p<0.0001$).

Conclusions: The BAR filter did not improve the diagnostic accuracy of VRFs. The intracanal materials also did not influence the diagnosis. Incomplete VRFs were highly associated with a decrease in sensitivity.

Keywords: Cone-Beam Computed Tomography, Diagnosis, Tooth Fractures, Root Canal Filling Materials, Artifacts

Introduction

Longitudinal tooth fractures are non-traumatic injuries that occur in the coronal-apical direction due to fatigue after masticatory forces (1) and represent 10.9 – 31.7% of causes for tooth extraction (2, 3). Vertical root fractures (VRF) are complete or incomplete longitudinal fractures that usually develops in teeth with root canal treatment (1). This type of fracture can initiate at any level of the root, but commonly present buccolingual direction (4). The diagnosis of VRF is clinically challenging as it presents a varied range of signs and symptoms such as swelling, sinus tract, pain on chewing, sensitivity to cold, or spontaneous pain, which might be indistinguishable from failed root canal treatment or periodontal disease (1, 4, 5).

In addition, because of its two-dimensional nature, periapical radiographs only detect fracture lines when the x-ray beam is perfectly parallel to the fracture plane, or when the root fragments are highly separated (6). Also, the fracture lines are often hidden by the presence of root canal fillings and intracanal posts (7). Thus, only one-third to half of VRFs are visible in periapical radiographs (7). Most of the teeth affected by VRF are extracted, as it frequently present poor prognosis (1, 4). Delaying the identification of VRFs might lead to an increased perirradicular bone loss, which impairs future implant replacements (4). Hence, a conclusive diagnosis is crucial for clinicians to develop appropriate treatment strategies.

On the other hand, cone-beam computed tomography (CBCT) provide a three-dimensional evaluation of the root structure through multiplanar reconstructed images (axial, coronal, and sagittal planes), which improves the detection of VRFs (8, 9). However, several factors might influence on the detection of VRFs by CBCT scans. Some fracture lines, especially at incomplete VRFs, are too narrow to be detected by CBCT (9, 10), as the fracture width might be smaller than the images' spatial resolution. Also, in the presence of high-density materials, such as gutta-percha and metal posts, image artifacts are formed during the CBCT scans acquisitions. Image artifacts are distortions discrepancies between the reconstructed image and the scanned structure, which reduces the image contrast and spatial resolution. As consequence, the adjacent structures might be obscured, and the visualization of fracture lines is hindered (10-13).

However, removing root canal fillings and intracanal posts before CBCT scans in the suspicion of root fractures might fragilize tooth structure, impairing the treatment prognosis in the absence of fracture. Moreover, early diagnosis of VRF prevent further perirradicular bone loss, and also avoid inappropriate treatments in non-fractured teeth (4, 5). Thus, several image

enhancement filters have been assessed to reduce artifacts caused by high-density materials (11, 12, 14). The diagnostic accuracy of CBCT scans was recently assessed using the e-vol DX BAR filter (CDT Software, Bauru, SP, Brazil), for the detection of complete VRFs (11). However, to the best of our knowledge, this is the first study to evaluate both complete and incomplete VRFs with different intracanal materials, using the e-vol DX BAR filter. Hence, the aim of this study was to determine whether the use of BAR filter can improve the diagnostic accuracy for complete and incomplete VRFs, specially in teeth with root canal filling, metal posts and fiberglass posts. The null hypothesis was that there is no difference regarding the accuracy values for the detection of VRFs using CBCT scans with or without the BAR filter.

Materials and Methods

This study was conducted in accordance with the STARD 2015 guidelines (Standards for Reporting of Diagnostic Accuracy Studies) (15). Ethical approval was obtained from the local University Research Ethics Committee (Protocol n. 4.444.910/2020). The sample size was determined using the data from a pilot study. The calculation was performed with a test power of 0.8 and an alpha-type error of 0.05, using G∗Power 3.1.9.4 software (Heinrich-Heine-Universität Düsseldorf, Düsseldorf, Germany). The minimum sample size was established at 20 specimens per group.

Sample selection

After clinical and radiographic evaluation, twenty single-rooted teeth were selected. Exclusion criteria included: presence of endodontic treatment; pulp calcification; incomplete root formation; internal or external root resorptions; root curvatures; and dental anomalies. Also, each tooth was inspected with a stereomicroscope (Carl Zeiss, Oberkochen, Germany) at ×20 magnification and transillumination, to exclude previously fractured teeth. The visual inspection with magnification and transillumination was used as reference standard for the diagnosis of VRFs.

All teeth were disinfected in 2.5% sodium hypochlorite solution, had dental calculus and soft tissue remnants removed, and were kept hydrated in distilled water. Then the teeth were decoronated, at the level of the cementoenamel junction (CEJ) using a rotating diamond blade (Isomet 1000; Buehler Ltd, Lake Bluff, IL, USA) with water cooling. This procedure intended to reduce the bias arising from the identification and memorization of the tooth structures during the evaluations.

Sample preparation

The root canals were prepared with nickel-titanium rotary instruments (ProTaper Next; Dentsply Sirona, Ballaigues, Switzerland) and standardized to a size 40, 0.06 taper. The instruments X1 (17/.04), X2 (25/.06), X3 (30/.07) and X4 (40/.06) were used sequentially with light apical pressure (300 rpm; 2 N.cm). Gentle in-and-out motions were used until the working length was reached and each instrument was capable of rotating freely. Patency was maintained with a size 10 K-file. The root canals were irrigated with 2 mL of 2.5% sodium hypochlorite using a 30-gauge irrigation needle. The irrigant was used after each instrument and at the end of the biomechanical preparation.

Then, a randomly selected specimen was used to produce a custom-made metal post, using a gold alloy. The metal post adaptation to each specimen was assessed later, using periapical radiographs. Similarly, a fiberglass post (Exacto, number 1, Angelus, Londrina, PR, Brazil) was selected and tested on each specimen to assure its adaptation. The posts were adapted at 4 millimeters from the working length.

CBCT scan

CBCT scans were acquired at three different points: before VRF induction, using sound roots; after incomplete VRF induction; and after complete VRF induction. Also, at each moment, the CBCT scans were obtained with different intracanal materials: no filling (NF); guta-percha (40.06 cone, Dentsply Sirona) (GP); fiberglass post (FGP); and metal post (MP). For the image acquisition of teeth with fiberglass and metal posts, a 4-mm gutta-percha cone was placed at the apical root third before the insertion of the posts. Hence, a total of 240 images were obtained, according to the type of fracture and intracanal material, as follows: no fracture/NF; no fracture/GP; no fracture/FGP; no fracture/MP; incomplete VRF/NF; incomplete VRF/GP; incomplete VRF/FGP; incomplete VRF MP; complete VRF/NF; complete VRF/GP; complete VRF/FGP; complete VRF/MP. A flow diagram was created to summarize the processes used during this laboratory study (**Figure 1**).

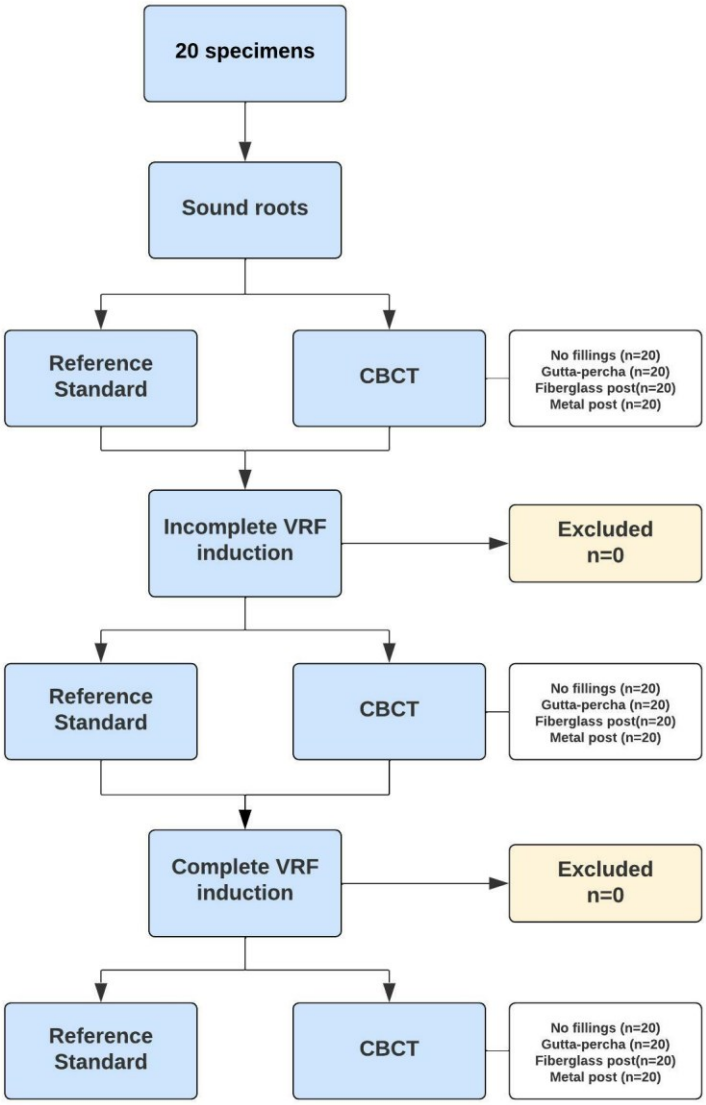

Figure 1. Flow diagram showing the acquisition of the reference standard (i.e., direct visualization of the fracture line) and index test (CBCT scans), before and after incomplete and complete VRFs. Adapted from STARD 2015 flow diagram (Cohen et al. 2016).

For the CBCT image acquisition, each tooth was lined with a fine layer of utility wax to simulate the presence of the periodontal ligament at the radiographical images. The socket of the right maxillary central incisor of a dry human skull was used for each CBCT scan. The skull was coated with a 5 mm layer of utility wax to simulate the attenuation of soft tissues, mimicking the clinical situation. The socket was slightly larger than the specimens, thus, the alveolus was prepared using a mix of particulate bone and silicone impression material (Redelease, Barueri, SP, Brazil), to improve the roots adaptation. Then, each tooth was placed in the socket, with their buccal aspect facing forward.

CBCT images were obtained with Prexion 3D (San Mateo, CA, USA) device using the high-resolution mode, set at 90 kVp and 4 mA, with an acquisition time of 19 seconds. A limited field of view of 5x5 cm was used, with a voxel size of 0.09 mm^3. The CBCT volumes were coded using a three-digit number (http://www.random.org), to avoid the identification of the specimens at the imaging software.

Fracture induction

Each tooth root was lined with a 1 mm-thick layer of wax and embedded in polystyrene resin (ComFibras, Florianopolis, SC, Brazil) using a cylindrical mold (19 mm in diameter, 24 mm in height) at 3 mm from the CEJ. The specimens were placed on a fixed platform of an Instron 444 machine (Instron Corp., Canton, MA, USA).

Initially, incomplete VRFs were induced in all 20 specimens at the universal testing machine, set at 2 kN and 5 mm per minute cross-speed. The fractures were mechanically created by applying a customized metallic wedge (diameter at tip = 0.6 mm; taper = 0.2 mm/mm) apically at the root canal. The universal testing machine was programed to stop automatically when 10% force reduction was recorded.

Then, each tooth was immediately removed from the resin blocks and inspected using a stereomicroscope at ×20 magnification and transillumination, to verify the presence of incomplete VRF (i.e., non-separable fragments).

Later, the specimens were fixed at the universal testing machine again, and submitted to the fracture induction method previously described, to complete the fracture lines, and create the complete VRF pattern. The visual inspection was performed as described before, to confirm the complete separation of the fragments. Then, the root fragments were placed together in their original position.

Image assessments

The acquired CBCT images were exported in the Digital Imaging and Communications in Medicine (DICOM) format and were analyzed by a blinded dental radiologist who already had experience in dentomaxillofacial tomography. The images were analyzed using the e-vol DX software (CDT software, Bauru, SP, Brazil), displayed on a 24-inch color LED (light-emitting diode) monitor with a resolution of 1920x1080 pixels, placed in a quiet room with dimmed light.

Prior to all examinations, the evaluator was instructed and calibrated, regarding the software features, such as adjustments on zoom, brightness, and contrast settings, which were left to the observer discretion. The evaluator was allowed to navigate dynamically throughout the CBCT volume using the axial, coronal, sagittal planes, as well as the 3D reconstruction. A maximum of 10 volumes were evaluated per day, with an interval of at least 24 hours between sessions.

The CBCT scans were analyzed at two different moments: initially all images were assessed without the aid of the BAR filter. One month after the first assessment, the images were reassessed with the aid of the BAR filter. The observer was allowed to switch between four levels of filter intensity. The diagnosis of VRF was scored using a 5-point confidence scale: 1 - VRF definitely present; 2 - VRF probably present; 3 - uncertain; 4 - VRF probably not present; 5 - VRF definitely not present. The evaluator was unaware of the prevalence of VRF on the sample.

Statistical analysis

Statistical analysis was performed using the MedCalc software 19.0.7 (MedCalc Software, Mariakerke, Belgium). The visual inspection of the sample was used as reference standard. Receiver operating characteristic (ROC) curves were generated, and the accuracy, sensitivity, specificity, positive predictive and negative predictive values were obtained after dichotomization of the evaluator's data considering the score of 3 as a positive cutoff point.

The area under the ROC curves (AUC) was compared using the DeLong method (16). The influence of the intracanal materials on the values of accuracy, sensitivity, and specificity was assessed with Cochran's Q test. The influence or the method of CBCT assessment (with or without BAR filter) on the values of accuracy, sensitivity, and specificity was evaluated through McNemar test. The statistical significance level was set at 5% (alpha= 0.05).

Results

Regarding the use of the BAR filter, there was no statistical difference in the AUC, accuracy, sensitivity, and specificity values, compared to the assessment without the filter, regardless of the intracanal material, or the fracture pattern ($p>0.05$). **Figure 2** presents the ROC curves for the assessment of teeth with complete VRFs, **Figure 3** presents teeth with incomplete VRFs, and **Figure 4** presents an overall assessment of both complete and

incomplete fracture patterns. The evaluation of the intracanal material showed no statistically significant differences among teeth with no fillings, gutta-percha, fiberglass posts, or metal posts, in either of the fracture patterns ($p>0.05$). Representative images of each group of CBCT scans are presented in **Figure 5**.

There were statistical differences between complete and incomplete fracture patterns, regardless of the intracanal materials, or the application of the BAR filter. The diagnostic of incomplete VRFs presented lower AUC, accuracy, and sensitivity, compared to the complete pattern ($p<0.0001$). There was no difference regarding the specificity of either complete or incomplete VRFs ($p>0.05$). The values of AUC, accuracy, sensitivity, specificity, positive predictive value (PPV) and negative predictive value (NPV) for complete and incomplete VRFs are shown in **Table 1** and **Table 2**, respectively. The overall values, for both fracture patterns together, are shown in **Table 3**.

Table 1. Values of accuracy, sensitivity, specificity, AUC, PPV and NPV, and 95% confidence interval, for the assessment with no filter, or with BAR filter, under different intracanal conditions, in teeth with complete VRFs.

Diagnostic values	CBCT assessment	Intracanal materials			
		No filling	Gutta-percha	Fiberglass post	Metal post
Accuracy	No filter	0.90 (0.76–0.97)Aa	0.93 (0.80–0.98)Aa	0.98 (0.87–1.0)Aa	0.88 (0.73– 0.96)Aa
	BAR 2	0.95 (0.83–0.99)Aa	1.0 (0.91–1.0)Aa	1.0 (0.91–1.0)Aa	0.90 (0.76– 0.97)Aa
Sensitivity	No filter	0.95 (0.75–1.0)Aa	0.95 (0.75–1.0)Aa	1.0 (0.82–1.0)Aa	0.90 (0.68– 0.99)Aa
	BAR 2	1.0 (0.83–1.0)Aa	1.0 (0.83–1.0)Aa	1.0 (0.82–1.0)A	0.90 (0.68– 0.99)Aa
Specificity	No filter	0.85 (0.62–0.97)Aa	0.9 (0.68–0.99)Aa	0.95 (0.75–1.0)Aa	0.85 (0.62– 0.97)Aa
	BAR 2	0.90 (0.68–0.99)Aa	1.0 (0.83–1.0)Aa	1.0 (0.83–1.0)Aa	0.90 (0.68– 0.99)Aa
AUC	No filter	0.90 (0.76–0.97)Aa	0.93 (0.80–0.98)Aa	0.98 (0.87–1.0)Aa	0.88 (0.73– 0.96)Aa
	BAR 2	0.95 (0.83–0.99)Aa	1.0 (0.91–1.0)Aa	1.0 (0.91–1.0)Aa	0.90 (0.76–0.97)Aa
PPV	No filter	0.86 (0.69–0.95)	0.90 (0.72–0.97)	0.95 (0.75–0.99)	0.86 (0.68– 0.95)
	BAR 2	0.91 (0.73–0.97)	1.0	1.0	0.90 (0.71– 0.97)
NPV	No filter	0.94 (0.71–0.99)	0.95 (0.73–0.99)	1.0	0.89 (0.69– 0.97)
	BAR 2	1.0	1.0	1.0	0.90 (0.71– 0.97)

AUC, area under the curve; PPV, positive predictive value; NPV, negative predictive value.
Different capital letters in a column indicate significant differences regarding the CBCT assessment (AUC - DeLong test; Accuracy, sensitivity and specificity – McNemar test; $p<0.05$).
Different lowercase letters in a row indicate significant differences regarding the intracanal materials (AUC - DeLong test; Accuracy, sensitivity and specificity – Cochran's Q test; $p<0.05$).

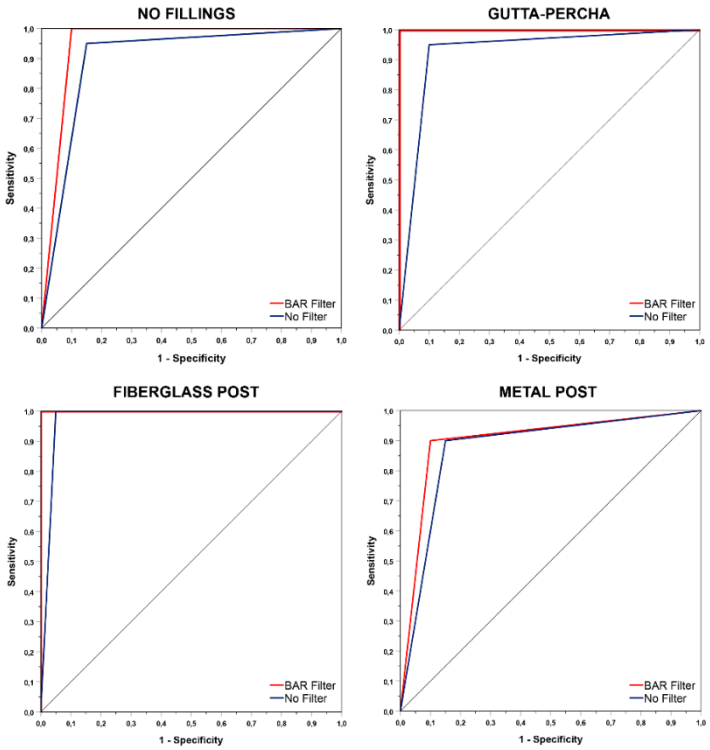

Figure 2. ROC curves for the comparison between the CBCT assessment method, with or without BAR filter, for each intracanal material, in teeth with complete VRFs.

Table 2. Values of accuracy, sensitivity, specificity, AUC, PPV and NPV, and 95% confidence interval, for the assessment with no filter, or with BAR filter, under different intracanal conditions, in teeth with incomplete VRFs.

Diagnostic values	CBCT assessment	Intracanal materials			
		No filling	Gutta-percha	Fiberglass post	Metal post
Accuracy	No filter	0.63 (0.46–0.77)^{Aa}	0.65 (0.48–0.79)^{Aa}	0.68 (0.51–0.81)^{Aa}	0.50 (0.34– 0.66)^{Aa}
	BAR 2	0.65 (0.48–0.79)^{Aa}	0.68 (0.51–0.81)^{Aa}	0.63 (0.46–0.77)^{Aa}	0.58 (0.41– 0.73)^{Aa}
Sensitivity	No filter	0.40 (0.19–0.64)^{Aa}	0.40 (0.19–0.64)^{Aa}	0.40 (0.19–0.64)^{Aa}	0.15 (0.03– 0.38)^{Aa}
	BAR 2	0.40 (0.19–0.64)^{Aa}	0.35 (0.15–0.59)^{Aa}	0.25 (0.09–0.49)^{Aa}	0.25 (0.09– 0.49)^{Aa}
Specificity	No filter	0.85 (0.62–0.97)^{Aa}	0.90 (0.68–0.99)^{Aa}	0.95 (0.75–1.0)^{Aa}	0.85 (0.62– 0.97)^{Aa}
	BAR 2	0.90 (0.683–0.988)^{Aa}	1.0 (0.83–1.0)^{Aa}	1.0 (0.83–1.0)^{Aa}	0.90 (0.64– 0.99)^{Aa}
AUC	No filter	0.63 (0.46–0.77)^{Aa}	0.65 (0.48–0.79)^{Aa}	0.68 (0.51–0.81)^{Aa}	0.50 (0.34– 0.66)^{Aa}
	BAR 2	0.65 (0.48–0.79)^{Aa}	0.68 (0.51–0.81)^{Aa}	0.63 (0.46–0.77)^{Aa}	0.58 (0.41– 0.73)^{Aa}
PPV	No filter	0.73 (0.45–0.90)	0.80 (0.49–0.94)	0.89 (0.52–0.98)	0.50 (0.19– 0.81)
	BAR 2	0.80 (0.49–0.94)	1.0	1.0	0.71 (0.35– 0.92)
NPV	No filter	0.59 (0.49–0.68)	0.60 (0.50–0.69)	0.61 (0.52–0.70)	0.50 (0.44 – 0.56)
	BAR 2	0.60 (0.50–0.69)	0.61 (0.53–0.68)	0.57 (0.51–0.63)	0.55 (0.47– 0.62)

AUC, area under the curve; PPV, positive predictive value; NPV, negative predictive value.
Different capital letters in a column indicate significant differences regarding the CBCT assessment (AUC - DeLong test; Accuracy, sensitivity and specificity – McNemar test; $p<0.05$).
Different lowercase letters in a row indicate significant differences regarding the intracanal materials (AUC - DeLong test; Accuracy, sensitivity and specificity – Cochran's Q test; $p<0.05$).

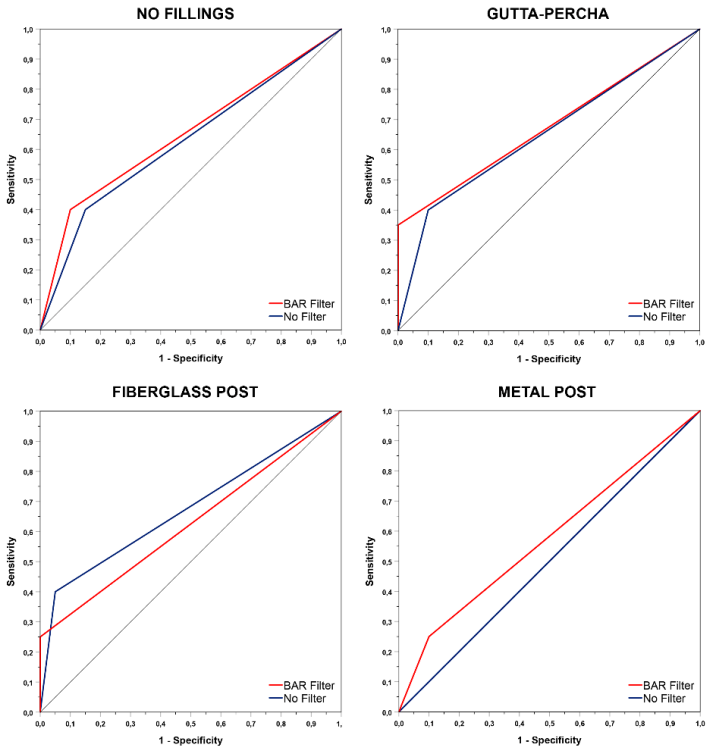

Figure 3. ROC curves for the comparison between the CBCT assessment method, with or without BAR filter, for each intracanal material, in teeth with incomplete VRFs.

Table 3. Overall values of accuracy, sensitivity, specificity, AUC, PPV and NPV, and 95% confidence interval, for the assessment with no filter, or with BAR filter, under different intracanal conditions.

Diagnostic values	CBCT assessment	Intracanal materials			
		No filling	Gutta-percha	Fiberglass post	Metal post
Accuracy	No filter	0.73 (0.60–0.84)Aa	0.75 (0.62–0.85)Aa	0.78 (0.65–0.88)Aa	0.63 (0.50 –0.75)Aa
	BAR	0.77 (0.64–0.87)Aa	0.78 (0.66–0.88)Aa	0.75 (0.62–0.85)Aa	0.68 (0.55– 0.80)Aa
Sensitivity	No filter	0.68 (0.51–0.81)Aa	0.68 (0.51–0.81)Aa	0.69 (0.52–0.83)Aa	0.53 (0.36–0.69)Aa
	BAR	0.70 (0.54–0.83)Aa	0.68 (0.51–0.81)Aa	0.62 (0.45–0.77)Aa	0.58 (0.41–0.73)Aa
Specificity	No filter	0.85 (0.62–0.97)Aa	0.9 (0.68–0.99)Aa	0.95 (0.75–1.0)Aa	0.85 (0.62 –0.97)Aa
	BAR	0.90 (0.68–0.99)Aa	1.0 (0.83–1.0)Aa	1.0 (0.83–1.0)Aa	0.90 (0.68 –0.99)Aa
AUC	No filter	0.76 (0.64–0.86)Aa	0.79 (0.66–0.88)Aa	0.82 (0.70–0.91)Aa	0.69 (0.56 –0.80)Aa
	BAR	0.80 (0.68–0.89)Aa	0.84 (0.72–0.92)Aa	0.81 (0.68–0.90)Aa	0.74 (0.61–0.84)Aa
PPV	No filter	0.90 (0.76–0.96)	0.93 (0.78–0.98)	0.96 (0.80–0.99)	0.88 (0.70 – 0.95)
	BAR	0.93 (0.79–0.98)	1.0	1.0	0.92 (0.75– 0.98)
NPV	No filter	0.57 (0.45–0.68)	0.58 (0.46–0.69)	0.61 (0.49–0.72)	0.47 (0.38– 0.57)
	BAR	0.60 (0.48–0.71)	0.61 (0.50–0.71)	0.57 (0.47–0.66)	0.51 (0.42– 0.61)

AUC, area under the curve; PPV, positive predictive value; NPV, negative predictive value.
Different capital letters in a column indicate significant differences regarding the CBCT assessment (AUC - DeLong test; Accuracy, sensitivity and specificity – McNemar test; $p<0.05$).
Different lowercase letters in a row indicate significant differences regarding the intracanal materials (AUC - DeLong test; Accuracy, sensitivity and specificity – Cochran's Q test; $p<0.05$).

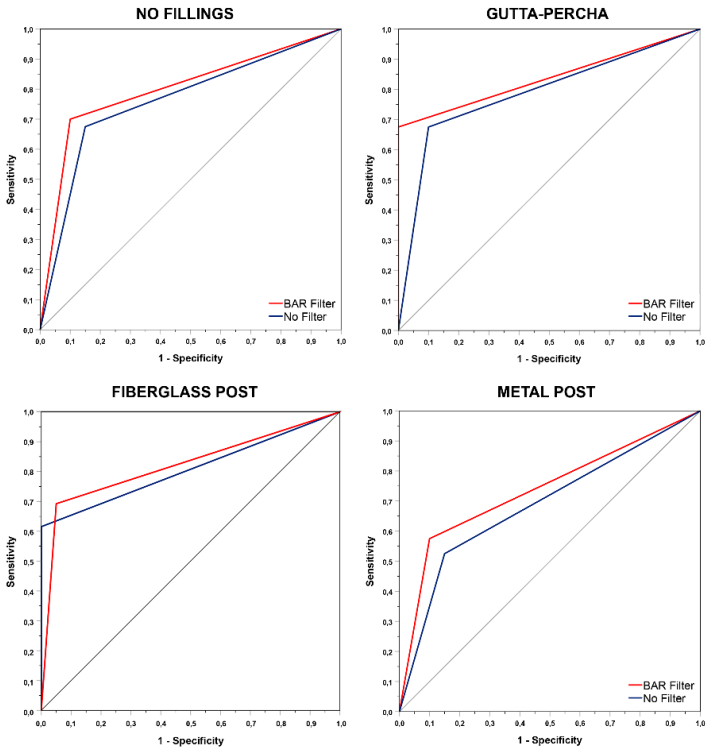

Figure 4. ROC curves for the overall comparison between the CBCT assessment method, with or without BAR filter, for each intracanal material, in teeth with both complete and incomplete fracture patterns.

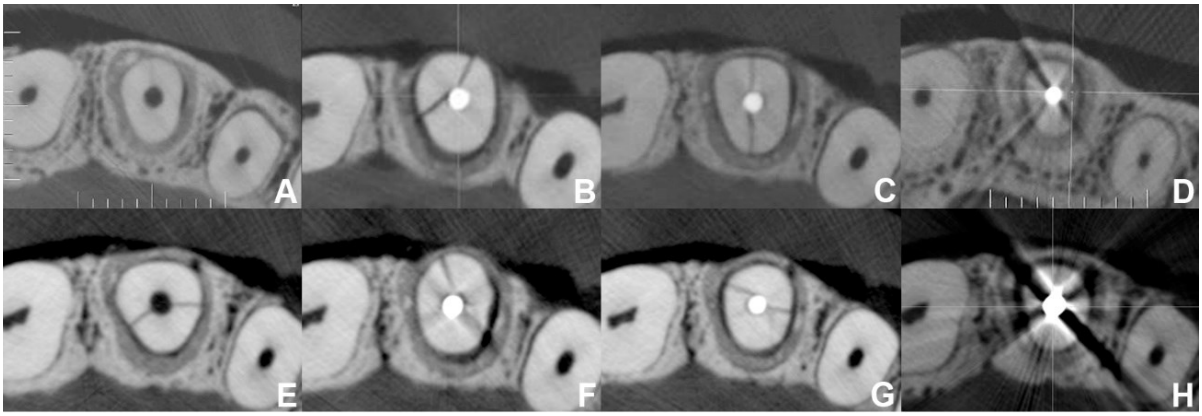

Figure 5. Representative images of the CBCT scans with the BAR filter, in root canals with no fillings (A), gutta-percha (B), fiberglass post (C), and metal post (D); and without the BAR filter, in roots with no fillings (E), gutta-percha (F), fiberglass post (G), and metal post H).

Discussion

It is well known that high-density materials impair CBCT images. Root canal fillings and intracanal posts cause imaging artifacts, such as beam hardening, that reduce the image quality (9). The presence of artifacts hinders the visualization of fracture lines, and might also mimic the presence of VRFs, increasing the likelihood of both false-negatives and false-positive diagnoses (10, 12-14, 17, 18). However, removing root canal fillings and intracanal posts in non-fractured teeth might weaken the root structure, and increase the risk of developing a VRF (19). Hence, to avoid unnecessary treatments in teeth with suspicion of VRFs, the use of metal artifact reduction (MAR) algorithms and filters to improve the diagnosis of VRF in root-filled teeth has been assessed (11, 12, 14). Therefore, the present study evaluated the influence of a novel artifact reduction filter for CBCT images, BAR (e-vol DX software, CDT software), for the diagnosis of experimentally induced vertical root fractures. We found that the application of the BAR filter to the CBCT images did not improve, nor impaired, the diagnostic accuracy of VRFs. There was no difference regarding the values of AUC, accuracy, sensitivity, and specificity. Thus, the null hypothesis was accepted.

The mechanism of the e-vol DX BAR filter is based on enhancing gray-scale contrast, using the maximum dynamic range of the DICOM file (20). This reduces the white contrast artifacts, known as blooming artifacts, which are hyperdense halos around high-density materials such as gutta-percha and metal posts (21). Although the BAR filter has been shown to successfully aid the evaluation of neighboring areas of dense artifact-forming materials (11, 20, 21), it does not reduce the hyper and hypodense streaks and bands caused by the beam-hardening in CBCT acquisitions. This severely impairs image reconstruction in the vicinity of high-density materials (10). Thus, as the anatomical evaluation of these areas is hindered, misinterpretations might occur, leading to serious consequences that affect further endodontic treatments and tooth survival. In our study, it was observed that, although beam-hardening artifacts impaired image quality, in complete VRFs, it was possible to detect most of the fracture lines in multiplanar reconstructions of teeth with either gutta-percha, fiberglass posts, or metal posts.

Several strategies have been developed to minimize the effects of imaging artifacts on the diagnosis of endodontic complications with CBCT. Some CBCT devices use MAR algorithms at the moment of the acquisition, to reduce the variability of grey values and improve the contrast-to-noise ratio. However, it was shown that MAR algorithms slightly impaired the

diagnostic performance of CBCT in laboratory studies (22). Also, several other studies assessed the use of MAR filters on DICOM viewers, after standard CBCT images acquisition. The results are somewhat inconsistent, and in both studies, the improvement in diagnostic accuracy was dependent on the CBCT device that was used (11, 14). According to our findings, without the MAR filter, regardless of the intracanal material, CBCT scans were highly accurate to detect complete VRFs. This agrees with several studies that used high-resolution CBCT images to assess teeth with no fillings (10, 13, 17, 23), gutta-percha (11, 13, 17, 24), fiberglass posts (10, 13), and metal posts (11, 17). In contrast, some studies observed a decrease in diagnostic values when assessing root canals with gutta-percha (9) and metal posts (10, 13).

Differences might be observed in the current literature regarding the diagnostic performance of CBCT. VRFs detection might be widely varied across *in vivo* (25, 26) and *in vitro* (7, 9-14, 17, 18, 21, 23, 24, 27-29) studies. Several factors must be taken into account, regarding acquisition parameters (i.e., voxel and FOV size, CBCT device, tube current, and tube voltage), as well as patient-related factors (i.e., motion artifacts, fracture pattern), which increases the heterogeneity among studies (8). Thus, it is important for *in vitro* studies to simulate situations that provide valuable information to clinical practice. According to Andraws Yalda et al., differences in anthropomorphic model designs (i.e., acrylic block, human skull, human skull with 5 mm wax, human skull immersed in water) do not affect the diagnostic accuracy of root fractures using this CBCT scans (27). However, the authors did not assess *in vivo* diagnostic accuracy. It seems unreasonable to extrapolate the findings of studies that assessed fractured teeth embedded in acrylic resin blocks. Thus, in this study, we simulated the clinical conditions of a CBCT scan as close as possible in an experimental model.

Imaging artifacts such as beam hardening reduce the image quality and increase the likelihood of false-positive results because it mimics fracture lines in CBCT images (9, 17). Our results showed that the presence of high-density intracanal materials did not affect the diagnostic performance of CBCT scans in detecting the absence of fractures. The overall specificity was very high (above 85%), which means that few false-positive diagnoses were found. This corroborates with most of the published laboratory studies that evaluated CBCT scans for the diagnosis of VRFs (11, 13, 18, 24, 29, 30). Some studies reported elevated rates of false positives in the presence of gutta-percha or metal posts. This highlights the importance of using conservative approaches regarding the identification of possible fracture lines.

Clinically, false-positive diagnoses lead to unnecessary and irreversible procedures, such as tooth extractions (1).

In this study, we found that the fracture pattern was the most important factor regarding the detection of VRFs. The diagnostic sensitivity of CBCT images for incomplete VRFs was extremely lower compared to complete fractures, in all intracanal conditions. The results vary considerably in the literature regarding the diagnostic performance of CBCT scans in the detection of incomplete VRFs in teeth with no fillings (9, 10, 23, 29), and root canal fillings (9, 10, 29). The mean sensitivity values varied from 27 to 93% (23, 29), and 26 to 69% (9, 10), respectively. Regarding the presence of intracanal posts, the mean sensitivity values vary from 48 to 73% in teeth with fiberglass posts (10, 30), and from 28 to 46% in teeth with metal posts (10, 29).

Incipient VRFs often are presented as incomplete fractures, with minimal fragment separation. It has been shown in laboratory studies that the widths of incomplete VRFs are much lower than complete fractures (9, 23). Thus, the detection of early VRFs is clinically challenging since the spatial resolution of CBCT images might not allow reconstruction of the fracture lines. These findings are supported by Zhang et al., that found a 33.3% sensitivity at the *in vivo* diagnosis of subtle VRFs in endodontically treated teeth (26).

Caetano et al. recently assessed the use of the BAR filter for the diagnosis of VRFs (11). The authors did not explicitly describe the induction of either complete or incomplete fractures. However, it is described that after fracture, each root fragment was bonded with cyanoacrylate. Hence, it should be considered that all specimens presented complete VRFs. The images were also acquired in a Prexion 3D device, with the same voxel size. Their findings corroborate our results, as the sensitivity and specificity were very high (above 86%), with no significant differences regarding the use of the BAR filter, and intracanal material – no fillings, gutta-percha, and metal post. The AUC values were also similar between the assessment with the BAR filter (no fillings: 0.928; gutta-percha: 0.962; metal post: 0.921), or without (no fillings: 0.964; gutta-percha: 0.982; metal post: 0.949), with no significant difference. The authors also compared the diagnosis of VRFs using the Kodak 9000 3D (Eastman Kodak Company, Rochester, New York, USA) and OP300 (Instrumentarium Kavo Kerr, Tuusula, Finland) devices, and concluded that the Prexion 3D device had the best performance.

Arguments regarding the effective dose of radiation involved in the acquisition protocol of this study might be raised, due to the increased acquisition time and continuous

radiation exposure, set by the Prexion 3D, at high-resolution mode. According to the ALARA – as low as reasonably achievable – principles, the exposure parameters for CBCT acquisition should be optimized to reduce the patient's radiation dose (31). However, unlike what is claimed by the linear no-threshold hypothesis, advocated by the ALARA model, trustworthy evidence on the carcinogenic risk of imaging-related low-doses, below 100 mSv, is non-existent (31, 32). Since the effective dose from CBCT imaging varies from 0.005 to 1.073 mSv (33), there is no evidence that the ionizing radiation from CBCT scans presents any unsafe potential or biological risk regarding the incidence of cancer or increasing of mortality rates (32).

Prexion 3D provides images with superior diagnostic performance for VRFs, compared to other devices that use pulsed beams, such as i-CAT (28) (Imaging Sciences International, Hatfield, USA), OrthoPhos XG (28) (Sirona Dental System, Bensheim, Germany), Kodak 9000 3D (11) (Eastman Kodak Company, Rochester, New York, USA) and OP300 (11) (Instrumentarium Kavo Kerr, Tuusula, Finland). Thus, an accurate diagnosis should be the main priority, and switching imaging tests, acquisition parameters, or CBCT devices to less accurate options is unjustifiable. Considering that using lower-dose protocols might increase the chances of occurring diagnostic errors, and the radiation doses of CBCT scans are not harmful, it can be concluded that using the ALARA concept might be more prejudicial than beneficial (34).

CBCT scans have been successfully used to identify bone defects associated with VRF (26, 35), which often present J-shaped perirradicular lesions, buccopalatal/lingual cortical loss, or radiolucent halos around the furcation region. In the current study, the diagnosis of VRF was achieved based exclusively on the detection of fracture lines. However, the diagnosis of VRFs is often complex and should include a comprehensive analysis of radiographic exams, clinical symptoms, visual inspection, and periodontal evaluation (1). Additional strategies might also include the use of operating microscopes, the application of dyes, or transillumination to identify fracture lines (4). The lack of incorporation of patient-related factors and clinical signs and/or symptoms is an inherent limitation of *in vitro* studies. With that in mind, the results should be interpreted with caution, and further *in vivo* investigations must be conducted to corroborate our findings.

Conclusion

Considering the findings of this experimental study, the use of the BAR filter did not improve the diagnostic accuracy of VRFs. The intracanal materials also did not influence the diagnosis. However, the fracture pattern highly impacted on the diagnostic accuracy of VRFs. The detection of VRFs was severely impaired at the assessment of incomplete VRFs, when compared to the complete fracture pattern.

Acknowledgements

This work was supported by the "Coordenação de Aperfeiçoamento de Pessoal de Nível Superior (CAPES)" in the form of a scholarship [grant code 001]. The authors declare that they have no conflict of interest.

References

1. Rivera EM, Walton RE. Longitudinal tooth cracks and fractures: an update and review. Endodontic Topics 2015;33(1):14-42. https://doi.org/10.1111/etp.12085
2. Fuss Z, Lustig J, Tamse A. Prevalence of vertical root fractures in extracted endodontically treated teeth. Int Endod J 1999;32(4):283-286. https://doi.org/:10.1046/j.1365-2591.1999.00208.x
3. Yoshino K, Ito K, Kuroda M, Sugihara N. Prevalence of vertical root fracture as the reason for tooth extraction in dental clinics. Clin Oral Investig 2015;19(6):1405-1409. https://doi.org/:10.1007/s00784-014-1357-4
4. Patel S, Bhuva B, Bose R. Present status and future directions: vertical root fractures in root filled teeth. Int Endod J 2022;55 Suppl 3:804-826. https://doi.org/:10.1111/iej.13737
5. Khasnis SA, Kidiyoor KH, Patil AB, Kenganal SB. Vertical root fractures and their management. J Conserv Dent 2014;17(2):103-110. https://doi.org/:10.4103/0972-0707.128034
6. Tsesis I, Kamburoglu K, Katz A, Tamse A, Kaffe I, Kfir A. Comparison of digital with conventional radiography in detection of vertical root fractures in endodontically treated maxillary premolars: an ex vivo study. Oral Surg Oral Med Oral Pathol Oral Radiol Endod 2008;106(1):124-128. https://doi.org/:10.1016/j.tripleo.2007.09.007
7. Chang E, Lam E, Shah P, Azarpazhooh A. Cone-beam Computed Tomography for Detecting Vertical Root Fractures in Endodontically Treated Teeth: A Systematic Review. J Endod 2016;42(2):177-185. https://doi.org/:10.1016/j.joen.2015.10.005
8. Salineiro FCS, Kobayashi-Velasco S, Braga MM, Cavalcanti MGP. Radiographic diagnosis of root fractures: a systematic review, meta-analyses and sources of heterogeneity. Dentomaxillofac Radiol 2017;46(8):20170400. https://doi.org/:10.1259/dmfr.20170400
9. Patel S, Brady E, Wilson R, Brown J, Mannocci F. The detection of vertical root fractures in root filled teeth with periapical radiographs and CBCT scans. Int Endod J 2013;46(12):1140-1152. https://doi.org/:10.1111/iej.12109
10. Neves FS, Freitas DQ, Campos PS, Ekestubbe A, Lofthag-Hansen S. Evaluation of cone-beam computed tomography in the diagnosis of vertical root fractures: the influence of imaging modes and root canal materials. J Endod 2014;40(10):1530-1536. https://doi.org/:10.1016/j.joen.2014.06.012
11. Caetano AP, Sousa TO, Oliveira MR, Evanglista K, Bueno JM, Silva MA. Accuracy of three cone-beam CT devices and two software systems in the detection of vertical root fractures. Dentomaxillofac Radiol 2021;50(3):20200334. https://doi.org/:10.1259/dmfr.20200334
12. De Martin ESD, Campos CN, Pires Carvalho AC, Devito KL. Diagnosis of Mesiodistal Vertical Root Fractures in Teeth with Metal Posts: Influence of Applying Filters in Cone-beam Computed Tomography Images at Different Resolutions. J Endod 2018;44(3):470-474. https://doi.org/:10.1016/j.joen.2017.08.030
13. de Rezende Barbosa GL, Sousa Melo SL, Alencar PN, Nascimento MC, Almeida SM. Performance of an artefact reduction algorithm in the diagnosis of in vitro vertical root fracture in four different root filling conditions on CBCT images. Int Endod J 2016;49(5):500-508. https://doi.org/:10.1111/iej.12477
14. Saati S, Eskandarloo A, Falahi A, Tapak L, Hekmat B. Evaluation of the efficacy of the metal artifact reduction algorithm in the detection of a vertical root fracture in endodontically treated teeth in cone-beam computed tomography images: An in vitro study. Dent Med Probl 2019;56(4):357-363. https://doi.org/:10.17219/dmp/109902

15. Cohen JF, Korevaar DA, Altman DG, Bruns DE, Gatsonis CA, Hooft L, et al. STARD 2015 guidelines for reporting diagnostic accuracy studies: explanation and elaboration. BMJ Open 2016;6(11):e012799. https://doi.org/:10.1136/bmjopen-2016-012799
16. DeLong ER, DeLong DM, Clarke-Pearson DL. Comparing the areas under two or more correlated receiver operating characteristic curves: a nonparametric approach. Biometrics 1988;44(3):837-845. https://doi.org/:10.2307/2531595
17. Melo SL, Bortoluzzi EA, Abreu M, Jr., Correa LR, Correa M. Diagnostic ability of a cone-beam computed tomography scan to assess longitudinal root fractures in prosthetically treated teeth. J Endod 2010;36(11):1879-1882. https://doi.org/:10.1016/j.joen.2010.08.025
18. Pinto MGO, Rabelo KA, Sousa Melo SL, Campos PSF, Oliveira L, Bento PM, et al. Influence of exposure parameters on the detection of simulated root fractures in the presence of various intracanal materials. Int Endod J 2017;50(6):586-594. https://doi.org/:10.1111/iej.12655
19. Garcia-Guerrero C, Mendoza-Beltran W, Roldan-Roldan M, Villa-Machado P, Restrepo-Restrepo F. Vertical root fractures: A time-dependent clinical condition. A case-control study in two colombian populations. J Clin Exp Dent 2021;13(11):e1104-e1111. https://doi.org/:10.4317/jced.58701
20. Bueno MR, Azevedo BC, Estrela C. A Critical Review of the Differential Diagnosis of Root Fracture Line in CBCT scans. Braz Dent J 2021;32(5):114-128. https://doi.org/:10.1590/0103-6440202104742
21. Gregoris Rabelo LE, Bueno MDR, Costa M, de Musis CR, Estrela CRA, Guedes OA, et al. Blooming artifact reduction using different cone-beam computed tomography software to analyze endodontically treated teeth with intracanal posts. Comput Biol Med 2021;136:104679. https://doi.org/:10.1016/j.compbiomed.2021.104679
22. Fontenele RC, Machado AH, de Oliveira Reis L, Freitas DQ. Influence of metal artefact reduction tool on the detection of vertical root fractures involving teeth with intracanal materials in cone beam computed tomography images: A systematic review and meta-analysis. Int Endod J 2021;54(10):1769-1781. https://doi.org/:10.1111/iej.13569
23. Brady E, Mannocci F, Brown J, Wilson R, Patel S. A comparison of cone beam computed tomography and periapical radiography for the detection of vertical root fractures in nonendodontically treated teeth. Int Endod J 2014;47(8):735-746. https://doi.org/:10.1111/iej.12209
24. Wanderley VA, Neves FS, Nascimento MCC, Monteiro GQM, Lobo NS, Oliveira ML, et al. Detection of Incomplete Root Fractures in Endodontically Treated Teeth Using Different High-resolution Cone-beam Computed Tomographic Imaging Protocols. J Endod 2017;43(10):1720-1724. https://doi.org/:10.1016/j.joen.2017.05.017
25. Dias DR, Iwaki LCV, de Oliveira ACA, Martinhao FS, Rossi RM, Araujo MG, et al. Accuracy of High-resolution Small-volume Cone-Beam Computed Tomography in the Diagnosis of Vertical Root Fracture: An In Vivo Analysis. J Endod 2020;46(8):1059-1066. https://doi.org/:10.1016/j.joen.2020.04.015
26. Zhang L, Wang T, Cao Y, Wang C, Tan B, Tang X, et al. In Vivo Detection of Subtle Vertical Root Fracture in Endodontically Treated Teeth by Cone-beam Computed Tomography. J Endod 2019;45(7):856-862. https://doi.org/:10.1016/j.joen.2019.03.006
27. Andraws Yalda F, Clarkson RJ, Davies J, Rout PGJ, Sengupta A, Horner K. Does anthropomorphic model design in ex vivo studies affect diagnostic accuracy for dental root fracture using CBCT? Dentomaxillofac Radiol 2020;49(7):20200093. https://doi.org/:10.1259/dmfr.20200093

28. Freitas ESA, Marmora B, Barriviera M, Panzarella FK, Raitz R. CBCT Performance and Endodontic Sealer Influence in the Diagnosis of Vertical Root Fractures. J Contemp Dent Pract 2019;20(5):552-556. https://doi.org/:10.1007/s00784-018-2558-z
29. Wanderley VA, Nascimento EHL, Gaeta-Araujo H, Oliveira-Santos C, Freitas DQ, Oliveira ML. Combined Use of 2 Cone-beam Computed Tomography Scans in the Assessment of Vertical Root Fracture in Teeth with Intracanal Material. J Endod 2021;47(7):1132-1137. https://doi.org/:10.1016/j.joen.2021.04.001
30. Ferreira RI, Bahrami G, Isidor F, Wenzel A, Haiter-Neto F, Groppo FC. Detection of vertical root fractures by cone-beam computerized tomography in endodontically treated teeth with fiber-resin and titanium posts: an in vitro study. Oral Surg Oral Med Oral Pathol Oral Radiol 2013;115(1):e49-57. https://doi.org/:10.1016/j.oooo.2012.06.012
31. Cohen MD. ALARA, image gently and CT-induced cancer. Pediatr Radiol 2015;45(4):465-470. https://doi.org/:10.1007/s00247-014-3198-3
32. Siegel JA, Pennington CW, Sacks B. Subjecting Radiologic Imaging to the Linear No-Threshold Hypothesis: A Non Sequitur of Non-Trivial Proportion. J Nucl Med 2017;58(1):1-6. https://doi.org/:10.2967/jnumed.116.180182
33. Ludlow JB, Timothy R, Walker C, Hunter R, Benavides E, Samuelson DB, et al. Effective dose of dental CBCT-a meta analysis of published data and additional data for nine CBCT units. Dentomaxillofac Radiol 2015;44(1):20140197. https://doi.org/:10.1259/dmfr.20140197
34. Cohen MD. Point: Should the ALARA Concept and Image Gently Campaign Be Terminated? J Am Coll Radiol 2016;13(10):1195-1198. https://doi.org/:10.1016/j.jacr.2016.04.023
35. Alaugaily I, Azim AA. CBCT Patterns of Bone Loss and Clinical Predictors for the Diagnosis of Cracked Teeth and Teeth with Vertical Root Fracture. J Endod 2022;48(9):1100-1106. https://doi.org/:10.1016/j.joen.2022.06.004

Figure legends

Figure 1. Flow diagram showing the acquisition of the reference standard (i.e., direct visualization of the fracture line) and index test (CBCT scans), before and after incomplete and complete VRFs. Adapted from STARD 2015 flow diagram (Cohen et al. 2016).

Figure 2. ROC curves for the comparison between the CBCT assessment method, with or without BAR filter, for each intracanal material, in teeth with complete VRFs.

Figure 3. ROC curves for the comparison between the CBCT assessment method, with or without BAR filter, for each intracanal material, in teeth with incomplete VRFs.

Figure 4. ROC curves for the overall comparison between the CBCT assessment method, with or without BAR filter, for each intracanal material, in teeth with both complete and incomplete fracture patterns.

Figure 5. Representative images of the CBCT scans with the BAR filter, in root canals with no fillings (A), gutta-percha (B), fiberglass post (C), and metal post (D); and without the BAR filter, in roots with no fillings (E), gutta-percha (F), fiberglass post (G), and meta post H).

Supplemental material 1. STARD 2015 Checklist.

Section & Topic	No	Item	Reported on page #
TITLE OR ABSTRACT	**1**	Identification as a study of diagnostic accuracy using at least one measure of accuracy (such as sensitivity, specificity, predictive values, or AUC)	46
ABSTRACT	**2**	Structured summary of study design, methods, results, and conclusions (for specific guidance, see STARD for Abstracts)	46
INTRODUCTION	**3**	Scientific and clinical background, including the intended use and clinical role of the index test	47-48
	4	Study objectives and hypotheses	48
METHODS *Study design*	**5**	Whether data collection was planned before the index test and reference standard were performed (prospective study) or after (retrospective study)	49
Participants	**6**	Eligibility criteria	49
	7	On what basis potentially eligible participants were identified (such as symptoms, results from previous tests, inclusion in registry)	Not applicable
	8	Where and when potentially eligible participants were identified (setting, location and dates)	Not applicable
	9	Whether participants formed a consecutive, random or convenience series	50-51
Test methods	**10a**	Index test, in sufficient detail to allow replication	52-53
	10b	Reference standard, in sufficient detail to allow replication	52
	11	Rationale for choosing the reference standard (if alternatives exist)	Not applicable
	12a	Definition of and rationale for test positivity cut-offs or result categories of the index test, distinguishing pre-specified from exploratory	Not applicable
	12b	Definition of and rationale for test positivity cut-offs or result categories of the reference standard, distinguishing pre-specified from exploratory	Not applicable
	13a	Whether clinical information and reference standard results were available to the performers/readers of the index test	53
	13b	Whether clinical information and index test results were available to the assessors of the reference standard	53
Analysis	**14**	Methods for estimating or comparing measures of diagnostic accuracy	53-54
	15	How indeterminate index test or reference standard results were handled	54
	16	How missing data on the index test and reference standard were handled	Not applicable
	17	Any analyses of variability in diagnostic accuracy, distinguishing pre-specified from exploratory	54
	18	Intended sample size and how it was determined	48
RESULTS *Participants*	**19**	Flow of participants, using a diagram	51
	20	Baseline demographic and clinical characteristics of participants	Not applicable

	21a	Distribution of severity of disease in those with the target condition	Not applicable
	21b	Distribution of alternative diagnoses in those without the target condition	Not applicable
	22	Time interval and any clinical interventions between index test and reference standard	Not applicable
Test results	**23**	Cross tabulation of the index test results (or their distribution) by the results of the reference standard	54-57
	24	Estimates of diagnostic accuracy and their precision (such as 95% confidence intervals)	54-57
	25	Any adverse events from performing the index test or the reference standard	Not applicable
DISCUSSION	**26**	Study limitations, including sources of potential bias, statistical uncertainty, and generalisability	63
	27	Implications for practice, including the intended use and clinical role of the index test	63
OTHER INFORMATION	**28**	Registration number and name of registry	Not applicable
	29	Where the full study protocol can be accessed	Not applicable
	30	Sources of funding and other support; role of funders	64

6 ARTIGO 3

Diagnostic accuracy of cone beam computed tomography for vertical root fractures detection and its associated factors: a systematic review and meta-analyses of in vitro studies

Luiz Carlos de Lima Dias-Junior[1], Eduardo Antunes Bortoluzzi[1], Lucas da Fonseca Roberti Garcia[1].

[1] Department of Dentistry, Federal University of Santa Catarina (UFSC), Florianópolis, SC, Brazil.

[2] Department of Diagnosis & Oral Health, Division of Endodontics, School of Dentistry, University of Louisville, Louisville, KY, USA.

Artigo formatado conforme normas do periódico **Clinical Oral Investigations**.

Abstract

Introduction: This systematic review investigated the different factors associated with the diagnostic accuracy of VRFs with cone-beam computed tomography (CBCT) scans, assessed by *in vitro* studies.

Materials and methods: Studies were screened from PubMed, Embase, Scopus, Web of Science, and Lilacs, up to January 2022. The included studies assessed the diagnostic accuracy of CBCT scans for laboratory-induced VRFs. The quality assessment of the included studies was performed using the QUADAS-2 tool. Meta-analyses were performed using the bivariate model with random effects to produce summary sensitivity and specificity with a 95% confidence interval. The influence of confounding factors on the accuracy of CBCT images was investigated by meta-regression models. Covariates were added to the bivariate model, to assess the impact on sensitivity, specificity, or both. The quality of evidence of each meta-analysis was assessed using the GRADE approach.

Results: Eighty-five studies were included. Eighteen studies presented a low risk of bias, twenty-two moderate risk, and forty-five high risk. CBCT scans presented a higher sensitivity for the diagnosis of complete VRFs, compared to incomplete fractures. The presence of metal posts impaired both sensitivity and specificity. Smaller voxel sizes favored the detection of VRFs in teeth with metal posts.

Conclusions: In laboratory settings, the diagnosis of VRFs by CBCT images is mainly affected by the fracture pattern, presence of intracanal materials, and voxel size.

Clinical relevance: Considering the that the diagnosis of VRFs are often complex, it is crucial to comprehend the main factors associated with the diagnostic accuracy of CBCT images.

Keywords: Artifacts, Cone-Beam Computed Tomography, Diagnosis, Meta-Analysis, Systematic Review, Tooth Fractures

Introduction

Vertical root fractures (VRF) extend along the vertical axis of the tooth root toward the apex [1]. The fractures are longitudinally oriented and might be a partial or complete rupture of the tooth root [1]. This type of fracture is more commonly found in endodontically treated teeth, with a reported prevalence ranging from 10.9%-31.7% in extracted teeth [2, 3]. Early detection and management of VRFs are essential to avoid unnecessary and inappropriate treatment, and minimize undesirable consequences, such as perirradicular bone loss [4].

Accurate diagnosis of VRFs is challenging since they may develop slowly [5]. Clinical examination might provide limited information due to the lack of specific signs and symptoms [5], which might include swelling, increased tooth mobility, tenderness to percussion or biting, or evidence of fracture lines [6]. In addition, the examination of periapical radiographs is limited due to their two-dimensional nature and superimposition of images [7].

Usually, VRFs occur in the buccolingual plane, and less commonly in the mesiodistal plane [6]. The presence of intracanal materials (i.e., root filling materials and intracanal retainers) make it difficult to visualize the vertical fracture line, especially the initial or incomplete ones [8]. There is minimal separation between fragments making diagnosis even more challenging [8]. Pathognomonic signs of VRFs such as deep and narrow periodontal probing depth, or J-shaped radiographic lesions, are often observed at advanced stages, when the root fragments are largely separated [4].

Radiographic evaluation of VRFs may be improved with the use of cone-beam computed tomography (CBCT), due to the possibility of the acquisition of 3-dimensional images with micrometric resolution and the absence of overlapping [9]. CBCT scans have been highly recommended in endodontics for the diagnosis of contradictory or non-specific clinical signs, including in the suspicion of VRFs[7]. However, several technical factors might influence the quality and accuracy of CBCT images such as voxel and field-of-view (FOV) sizes, tube current, and voltage [10].

Patient-related factors also impact image quality, such as the presence of high-density intracanal materials that generate imaging artifacts, which may obscure structures adjacent to such materials, jeopardizing the detection of VRFs [11, 12]. The presence of gutta-percha and intracanal posts causes beam-hardening artifacts, that present two distinct manifestations: streaking and cupping artifacts [10]. Sharpness filters and metal artifact reduction (MAR) tools have been developed to reduce the impact of these radiodense materials on diagnostic accuracy

and improve CBCT image quality. However, the results from studies that evaluated these tools are still controversial [13-22].

Many factors may influence the VRF diagnosis. This systematic review investigated the different factors associated with the diagnostic accuracy of VRFs by CBCT scans. *In vivo* studies on VRFs diagnostic accuracy are still scarce and there is limited information available in the literature, with high methodological heterogeneity. Therefore, only *in vitro* studies were included and, due to the large number of data available, it was possible to evaluate each factor individually and analyze its influence on the diagnostic accuracy of CBCT images. Therefore, this systematic review aimed to answer the focused question "Which are the factors associated with the diagnostic accuracy of CBCT for the detection of VRFs?".

Materials and methods

Protocol and registration

This review was conducted following the Cochrane Handbook for Systematic Reviews of Diagnostic Test Accuracy. The reporting of this systematic review and meta-analysis complies with the Preferred Reporting Items for Systematic Reviews and Meta-Analyses of Diagnostic Test Accuracy (PRISMA-DTA) guidelines [23]. See **Appendix 1** for the PRISMA-DTA checklist. The study protocol was registered in the International Prospective Register of Systematic Reviews (PROSPERO) database (registration number CRD42020207094).

Search strategy

The literature search covered the following electronic databases: PubMed, Embase, Scopus, Web of Science, and Lilacs. We searched for unpublished studies and gray literature on ProQuest, Open Grey, and Google Scholar (the first 100 items). Also, as an additional method for the identification of studies, experts were consulted for possibly eligible articles, and the reference lists of the included studies were screened.

The literature search was executed until January 17th, 2022, with no restriction on language or date of publication. The complete search strategies used in each database are presented in **Appendix 2**.

Eligibility criteria

Inclusion criteria

The inclusion criteria were created based on the PIRDS strategy [24], as follows:

- Participants (P): human extracted teeth;
- Index Test (I): CBCT scans;
- Reference Test (R): visual inspection of extracted teeth with or without the aid of magnification, transillumination, and/or stains;
- Diagnostic (D): vertical root fractures;
- Study design (S): *in vitro* studies assessing the diagnostic accuracy of VRF with CBCT scans.

Exclusion criteria

The following exclusion criteria were adopted:

1. Studies with primary human teeth or animal teeth;
2. Studies that included teeth with incomplete root formation;
3. Studies that did not evaluate CBCT as the index test;
4. Studies that did not investigate the diagnostic accuracy of VRFs;
5. Studies with fracture simulation that are not consistent with the real aspect of VRFs;
6. *In vivo* studies;
7. Reviews, letters, case reports, and case series.

Study Selection

Study selection was performed in a two-phase process. Firstly, two trained reviewers independently screened the titles and abstracts (L.C.L.D.J. and D.L.S.). All records were assessed according to the inclusion and exclusion criteria, and the articles that met the eligibility criteria were retrieved for full-text reading. Any disagreement was resolved by discussion, or by consulting a third reviewer (A.P.B.). Similarly, in phase two, inclusion criteria were applied to the studies' full text and any discrepancies were settled by discussion between reviewers.

Data extraction

Data from the included studies were extracted by two independent reviewers (L.C.L.D.J. and D.L.S.). The following data were extracted from the studies and inserted into a structured form: name of the first author; year of publication; country of the first author; sample

size; type of teeth; method of fracture induction; type of fracture (i.e., complete or incomplete); experimental groups and subgroups; CBCT device; acquisition parameters for the CBCT scans; application of image filters or acquisition algorithms; root canal conditions (i.e., no filling, root canal filling, metal post, fiberglass post, or other); simulation of *in vivo* conditions (i.e., use of human skull or mandible); diagnostic results in terms of sensitivity and specificity values, and true-positive (TP), false-positive (FP), false-negative (FN), and true-negative (TN) rates; and main conclusions. For studies that did not report the TP, FP, TN, FN rates, they were calculated based on the sensitivity, specificity, and prevalence values, and sample size, using the calculator in Review Manager 5.4 software (Cochrane Collaboration, Oxford, UK). In cases of missing information or data, the corresponding authors of the studies were contacted by e-mail with up to five attempts at a one-week interval. Disagreements from data extraction were resolved by discussion with a third author (A.P.B.). See **Appendix 3** for the complete extraction form with all the data collected from the included studies summarized in a table.

Quality assessment of the included studies

Two reviewers (L.C.L.D.J. and D.L.S.) independently assessed the quality of the included studies. The Quality Assessment of Diagnostic Accuracy Studies 2 (QUADAS-2) tool [25] was adapted to this systematic review because some questions (i.e., randomization of patients and threshold of the index test) were not applicable for *in vitro* studies.

QUADAS-2 assesses the methodological quality of diagnostic accuracy studies based on four major domains regarding the risk of bias: patient selection, index test, reference standard test, and flow and timing; and three domains regarding the applicability concerns: patient selection, index test, and reference standard test. 'Review specific' descriptions of how the QUADAS-2 items were contextualized and implemented in our systematic review are detailed in **Appendix 4**.

In each aspect, if the answer to the leading questions were “yes”, then it was given a “low” risk of bias and applicability concern judgment. If any answer was “unclear”, then it was judged to have “some concerns” regarding the risk of bias and applicability concerns. Similarly, if any of the answers were “no”, the domain was judged as “high” for risk of bias and applicability concerns. Discrepancies between reviewers were discussed and settled with the assistance of three experts (C.S.T., L.F.R.G. and E.A.B.).

Quality of evidence

The quality of evidence of each outcome (factor) was assessed using the GRADE (Grading of Recommendations, Assessment, Development, and Evaluation) approach. GRADE is used to substantiate intervention recommendations with four levels of evidence quality, ranging from high to very low [26]. Two reviewers (L.C.L.D.J. and A.P.B.) independently assessed the following categories: risk of bias, inconsistency, indirectness, imprecision, and publication bias; using the GRADEpro GDT software (https://www.gradepro.org). The experts (C.S.T., L.F.R.G. and E.A.B.) were consulted to settle disagreements between reviewers.

Statistical Analysis

Initially, comparative analyses included all studies with relevant data, by direct or indirect evidence. Meta-analyses were performed using the bivariate model with random effects to produce summary sensitivity (SSe) and specificity (SSp) [27]. We investigated the factors associated with the accuracy of CBCT scans by meta-regression, adding covariates to the bivariate model to assess the association with sensitivity or specificity, or both. Significant differences in test performance were evaluated by a likelihood ratio test comparing models with and without covariate terms for sensitivity and specificity. The models were fitted using the "glmer" function in the "lme4" package for R version 4.1.3 software (R Foundation for Statistical Computing, Vienna, Austria. URL: https://www.R-project.org/). For each analysis, summary ROC curves were plotted using Review Manager 5.4 software (Cochrane Collaboration, Oxford, UK). We assessed inter-study heterogeneity through the chi-squared-based Q-test and inconsistency index (I^2). A significance level of 5% was adopted for all analyses.

Results

Study selection

After electronic searches, we identified 4067 records on the five different databases accessed in this study. Duplicates records were identified, and 1500 studies were removed, resulting in 2567 articles that were screened by a comprehensive evaluation of titles and abstracts (phase 1). For full-text assessment (phase 2), 110 records were retrieved for being considered potentially useful, of which we excluded 28 articles (see the reasons for exclusion in **Appendix 5**), resulting in 82 included studies. An additional search on grey literature, consult

of experts, and reference list of selected studies provided 184 possibly eligible articles, of which 3 studies met the eligibility criteria after full-text assessment. Thus, 85 articles were selected to answer the questions proposed by this systematic review. See **Figure 1** for the detailed process of studies identification, inclusion, and exclusion, in the PRISMA 2020 flow diagram [28].

Study characteristics

The publication years of the included studies ranged from 2009 to 2022. A total of 4982 teeth were analyzed. The methods of VRF included hammer and pin [13, 16, 22, 29-55], hammer and chisel [15, 56-62], bench vise [63], universal testing machine [8, 12, 14, 17-19, 21, 64-97] and post or pin turned into the canal [20, 86, 98, 99]. Out of the 85 articles, 25 investigated complete fractures [8, 13, 15, 16, 22, 32-34, 40, 42, 43, 46, 58-62, 65, 67, 70, 78, 82, 84, 90, 99]. Twenty-seven studies investigated incomplete fractures [8, 12, 19, 20, 34-36, 38, 40, 56, 57, 63, 65, 71, 73, 75, 80, 82-86, 93-95, 98, 99], 12 included both types of fracture [14, 21, 30, 47, 50, 53, 69, 72, 74, 86, 92, 96] and 29 were unclear regarding which type of fracture was produced [17, 29, 31, 37, 39, 41, 44, 45, 48-52, 54, 55, 64, 66-68, 76, 77, 79, 81, 88, 89, 91, 97, 100, 101]. To simulate *in vivo* conditions, these teeth were placed in the sockets of dry human mandible or skull [8, 12, 14-19, 21, 29, 35, 37, 38, 41-43, 47, 51-53, 56, 58-61, 65-73, 75, 76, 78-80, 82, 84, 85, 88, 89, 93-97], ovine mandible [55], gypsum stone blocks [48, 62, 63, 83, 98, 101], bovine rib sockets [13, 20, 22, 31-33, 46, 49], acrylic blocks [34, 36, 57, 64, 74, 81, 86, 90-92], macerated bone artificial sockets [50] and wax models [87].

Investigation groups included teeth with no root canal filling [8, 12, 14, 16-19, 29, 30, 35, 39, 40, 42-44, 47, 48, 52, 53, 56-62, 66, 70, 71, 75, 76, 79-82, 85, 88, 93, 94, 97, 101], gutta-percha with or without root canal sealer [12-16, 20, 22, 29, 30, 32, 33, 35, 36, 38, 39, 41-49, 51, 53, 57-59, 62, 64, 72, 74-78, 80, 82, 84, 85, 89, 94, 95, 98, 99], metal post [12, 14-17, 20, 29, 31, 34-36, 42-45, 47, 50, 53-55, 57, 65, 69, 75, 77, 78, 80-83, 86, 87, 89-92, 94, 97, 98, 100], fiber post [16, 47, 50, 53, 54, 67, 68, 75, 82, 97], bioceramic root canal filling material [64], and zirconium based root canal filling material [72].

Image acquisition was performed with a variety of CBCT devices set with kilovoltage ranging from 120 kVp to 60 kVp, voxel size from 0.075 mm to 0.4 mm, and field of view (FOV) size from 23×23 cm to 4×4 cm. In 14 of the included studies, a variety of metal artifact reduction (MAR) algorithms were applied during image acquisition [13, 16, 18, 20-22, 49, 65, 71, 73, 83, 90, 98, 100]. Image filters were also evaluated. Two studies applied artifact reduction filters to

the acquired images [14, 49], and four studies used sharpness filters in the images [15, 17, 19, 46]. The characteristic of each included study is presented in **Appendix 2**.

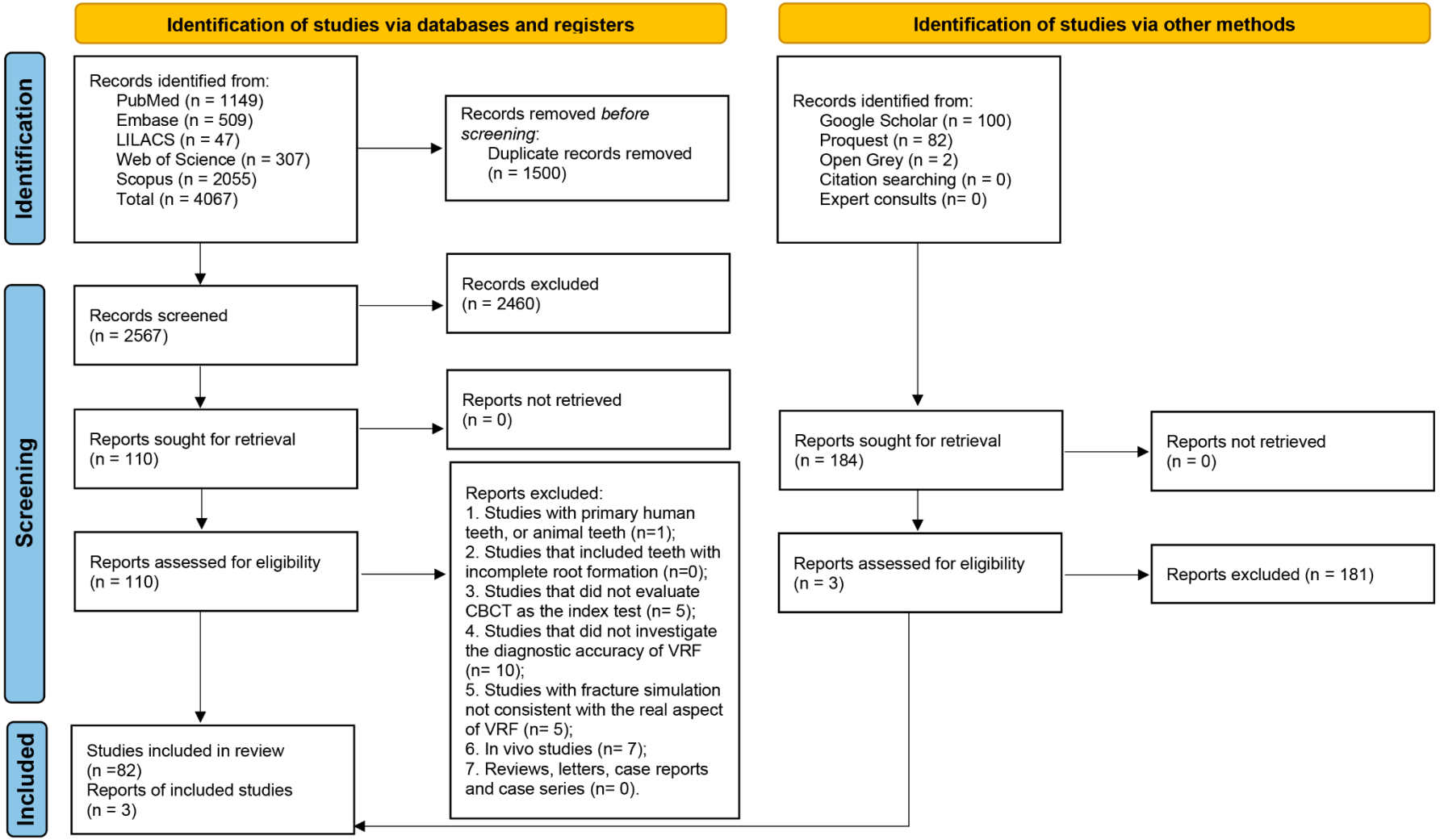

Figure 1. PRISMA 2020 flow diagram.

Quality Assessment

The summarized results for risk of bias and applicability concerns assessment of the 85 included studies are presented in **Figure 2**. Overall, only 18 of the included studies presented a low risk of bias and applicability concerns [14, 16, 19, 21, 22, 35, 42, 43, 47, 56, 59, 61, 65, 67, 68, 72, 75, 89]. Twenty-two studies presented a moderate risk of bias due to unclear or no description of sample size calculation and the use of bovine bone and acrylic or gypsum blocks for simulation of *in vivo* conditions [8, 12, 15, 17, 18, 20, 38, 52, 53, 58, 69, 74, 76, 78, 79, 82, 84, 85, 93-96]. Additionally, the 45 remaining studies presented a high risk of bias especially due to the lack of baseline evaluation of the teeth [13, 32, 33, 41, 46, 49, 64, 70, 71, 73, 90, 100], issues with index test methodology, such as the absence of *in vivo* conditions simulation (isolated tooth) and lack of examiners blinding [29-31, 34, 36, 39-41, 44, 45, 48, 50, 51, 57, 60, 63, 77, 80, 81, 83, 86, 87, 90-92, 98-101]. High risk was also considered when there was no description of the reference test [13, 32, 33, 37, 39, 41, 46, 48, 49, 51, 64, 66, 70, 88, 97, 98, 100, 101] and final inspection was performed only on part of the sample (fractured or non-fractured teeth) [13, 31-33, 37, 39, 41, 46, 48, 49, 51, 66, 70, 71, 73, 77, 88, 90, 91, 98-101]. The detailed quality assessment of the included studies is shown in **Figure 3**.

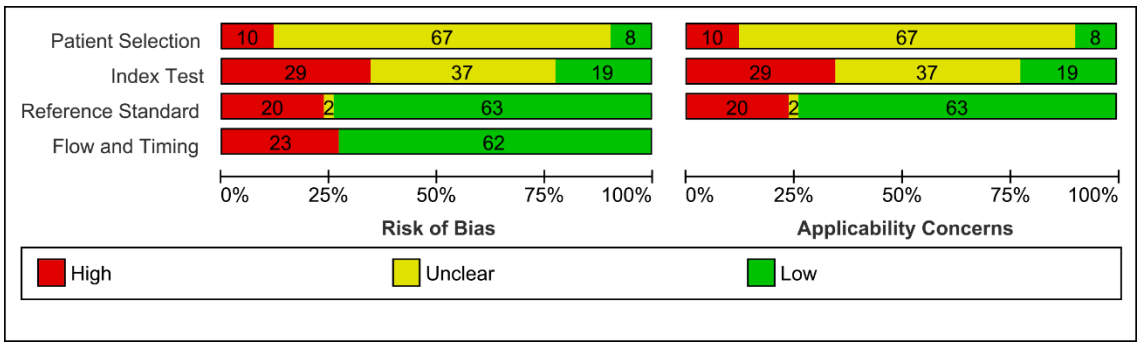

Figure 2. Summarized results of the quality assessment for the included studies.

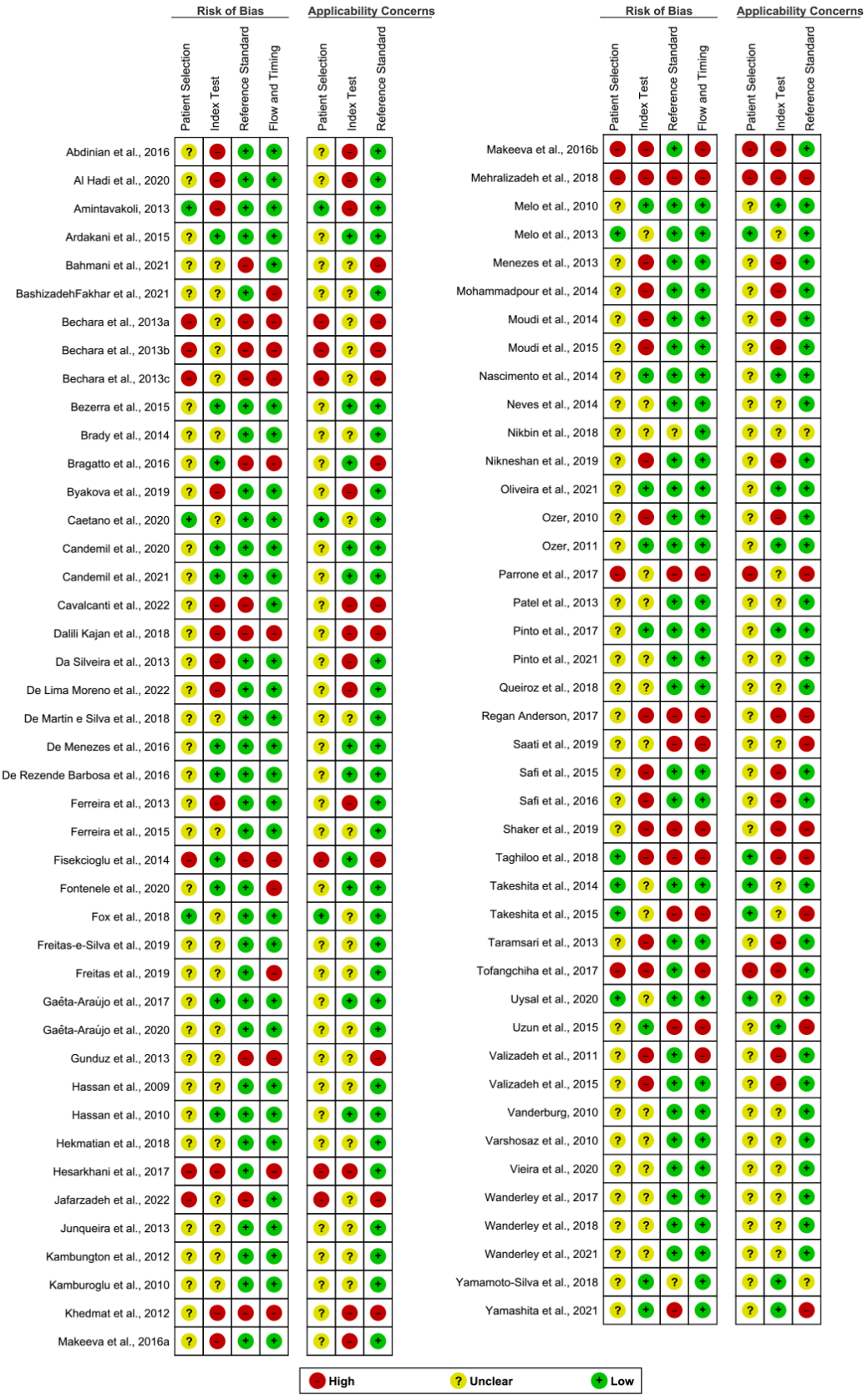

Figure 3. Detailed results of the quality assessment according to the QUADAS-2 appraisal tool for diagnostic accuracy studies.

Synthesis of the results

The possible factors associated with the diagnostic accuracy of CBCT scans for VRFs identified from the primary studies were fracture pattern (i.e., complete, or incomplete); acquisition parameters (FOV and voxel sizes, tube current, tube voltage); intracanal materials; image enhancement filters; MAR algorithms; CBCT device; tooth position within FOV; and the presence of adjacent dental implants.

Fracture pattern

In this section, we present the results for comparison of the diagnostic accuracy of complete and incomplete VRFs. Overall, the meta-analyses included 4351 teeth in 4 studies that directly compared the fracture patterns [8, 65, 82, 84], 10 studies that assessed only complete VRFs [16, 22, 42, 43, 58, 59, 61, 67, 75, 78], and 7 studies that assessed only incomplete VRFs [12, 18-20, 35, 94]. It was observed that complete VRFs presented a higher sensitivity (SSe= 0.724; 95% CI, 0.646—0.79) than the incomplete pattern (SSe= 0.588; 95% CI, 0.487—0.682) (p=0.03084; I^2= 86.5%). There was no significant difference (p=0.141) regarding the specificity of complete (SSp= 0.835; 95% CI, 0.78—0.879) or incomplete VRFs (SSp= 0.763; 95% CI, 0.673—0.835; I^2= 82.3%).

Next, for a sensitivity analysis, the meta-analyses were conducted according to the root canal conditions. For root canals with no filling (i.e., empty canals), we performed a meta-analysis that included 1271 teeth, in 2 studies with direct comparisons between complete and incomplete VRFs [8, 82], five studies that assessed only complete VRFs [16, 42, 43, 61, 75], and 5 studies that assessed only incomplete VRFs [12, 18, 19, 35, 94]. There was a statistically significant (Chi-square=17.01; p=0.0045) difference in the diagnostic accuracy according to the fracture pattern. The sensitivity of complete VRFs (SSe= 0.867; 95% CI, 0.698—0.949) was significantly higher (Chi-square=17.0; p=0.0019) compared to the incomplete fracture pattern (SSe= 0.674; 95% CI, 0.492—0.816; I^2= 90.1%). The specificity did not differ (Chi-square=0.2442; p=0.6212) between complete (SSp= 0.909; 95% CI, 0.822—0.956) and incomplete (SSp= 0.887; 95% CI, 0.653—0.97; I^2= 85.3%) VRFs (Fig. 4.2).

Regarding teeth with root canal filling (i.e., gutta-percha and sealer), the meta-analysis included 1368 teeth, in 2 studies with direct comparisons [82, 84], 6 studies that assessed only complete VRFs [16, 22, 42, 43, 75, 78], and 5 studies that assessed only incomplete VRFs [12, 20, 35, 94, 95]. The results revealed that there was no difference in the diagnostic accuracy of

complete and incomplete VRFs (Chi-square: 2.18; p=0.336). Both sensitivity (SSe= 0.682; 95% CI, 0.602—0.753) and specificity (SSp= 0.816; 95% CI, 0.69—0.898) of the complete fractures were similar to the sensitivity (SSe= 0.584; 95% CI, 0.354—0.783; I^2= 82.7%) and specificity (SSp= 0.757; 95% CI, 0.67—0.828; I^2= 81.2%) of the incomplete pattern (Fig. 4.3).

The meta-analysis for the root canals with metal posts included 846 teeth, in 2 studies with direct comparisons [65, 82], 5 studies that evaluated only complete VRFs [16, 42, 43, 75, 78], and 4 studies that evaluated only incomplete VRFs [12, 20, 35, 94]. There were no significant differences in the diagnostic accuracy between the two fracture patterns (Chi-square: 8.41; p=0.135), in terms of sensitivity (SSe= 0.543; 95% CI, 0.461—0.623; and 0.481; 95% CI, 0.398—0.566; I^2= 31.9%; for complete and incomplete VRFs, respectively) or specificity (SSp= 0.705; 95% CI, 0.582—0.804; and 0.594; 95% CI, 0.509—0.674; I^2= 71.9%; for complete and incomplete VRFs, respectively) (Fig. 4.4).

It was not possible to assess the differences in diagnostic accuracy between complete and incomplete fractures in root canals with other intracanal materials, such as fiberglass posts, due to the lack of primary studies.

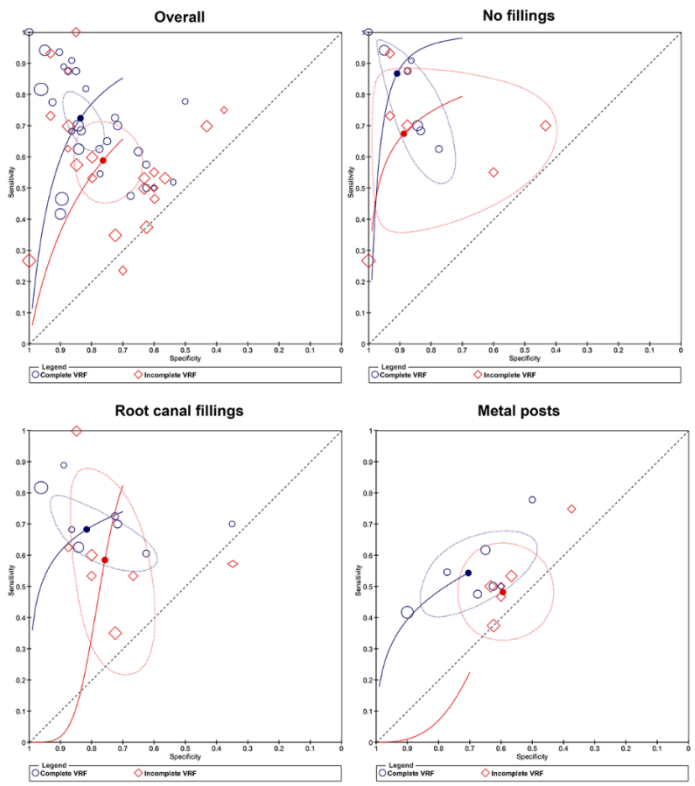

Figure 4. SROC plots of the meta-analyses for the overall comparison between complete and incomplete VRFs, and in root canals with no fillings, gutta-percha, and metal posts.

CBCT scan voxel size

The investigation of the influence of the spatial resolution in the diagnostic accuracy of VRFs was performed with different thresholds for the differentiation between high and low resolutions, using the voxel size as parameter. The meta-analyses were divided according to the presence of intracanal materials.

- ***Threshold for high resolution: 0.2 mm^3***

The voxel size of 0.2 mm^3 was set as the threshold for high resolution at the initial meta-analysis, thus, any voxel size below this value was considered "low resolution". The meta-analysis of root canals with no filling included 1933 teeth, in 2 studies with low resolutions [42, 61], and 18 studies with high resolutions [8, 12, 14, 16-19, 21, 35, 42, 43, 47, 52, 53, 61, 75, 82, 94]. There was no significant difference (Chi-square=2.87; p=0.7192) between high (SSe= 0.798; 95% CI, 0.716—0.86; SSp= 0.833; 95% CI, 0.76—0.887) and low resolutions (SSe= 0.781; 95% CI, 0.415—0.947; I^2= 79.7%; SSp= 0.883; 95% CI, 0.722—0.956; I^2= 77.7%) in the diagnostic accuracy.

Similarly, there was no difference (Chi-square=3.5524; p=0.1693) in root canals obturated with gutta-percha, regarding the use of high (SSe= 0.725; 95% CI, 0.634—0.8; SSp= 0.796; 95% CI, 0.731—0.848) or low resolutions (SSe= 0.641; 95% CI, 0.474—0.78; I^2= 81.2%; SSp= 0.919; 95% CI, 0.692—0.983; I^2= 83%). The meta-analysis included 2236 teeth, in 3 studies with low resolutions [22, 42, 78] and 19 studies with high resolutions [12, 14, 16, 20-22, 35, 42, 43, 47, 53, 72, 74, 75, 78, 82, 84, 94, 95].

The meta-analysis of root canals with metal posts included 1910 teeth, in 2 studies with low resolutions [42, 78], and 18 studies with high resolutions [12, 14, 16, 17, 20, 21, 35, 42, 43, 47, 53, 65, 69, 75, 78, 82, 94, 96]. There were also no significant differences (Chi-square=0.5745; p=0.7503) between high (SSe= 0.588; 95% CI, 0.501—0.67; SSp= 0.697; 95% CI, 0.624—0.762) and low (SSe= 0.564; 95% CI, 0.407—0.709; I^2= 76.1%; SSp= 0.615; 95% CI, 0.456—0.753; I^2= 73.1%) resolutions for the diagnostic accuracy of VRFs.

- ***Threshold for high resolution: 0.16 mm^3***

When using the voxel size of 0.16 mm^3 as the threshold for high spatial resolution, the meta-analysis of teeth with no fillings included 8 studies with low resolution [12, 16, 17, 19, 42, 43, 61, 94], and 11 studies with high resolution[8, 14, 18, 21, 35, 47, 52, 53, 61, 75, 82].

There was no significant difference (Chi-square=0.069; p=0.9661) between high (SSe= 0.75; 95% CI, 0.66—0.822; SSp= 0.878; 95% CI, 0.744—0.947) and low resolution (SSe= 0.772; 95% CI, 0.635—0.869; I^2= 79.2%; SSp= 0.868; 95% CI, 0.793—0.918; I^2= 84.1%).

The meta-analysis of root canals obturated with gutta-percha included 8 studies with low resolutions [12, 16, 22, 42, 43, 74, 78, 94], and 14 studies with high resolutions [14, 20-22, 35, 47, 53, 72, 74, 75, 78, 82, 84, 95]. There was also no significant difference (Chi-square=0.3559; p=0.837) between high (SSe= 0.731; 95% CI, 0.621—0.818; SSp= 0.803; 95% CI, 0.714—0.868) and low resolutions (SSe= 0.715; 95% CI, 0.619—0.795; I^2= 77.3%; SSp= 0.833; 95% CI, 0.731—0.902; I^2= 82.6%).

Regarding the presence of metal posts, the meta-analysis included 9 studies with low resolutions [12, 16, 17, 42, 43, 65, 78, 94, 96], and 11 studies with high resolutions [14, 20, 21, 35, 47, 53, 69, 75, 78, 82, 96], and there was no difference (Chi-square=5.2581; p=0.07215) between high (SSe= 0.646; 95% CI, 0.538—0.741; SSp= 0.674; 95% CI, 0.584—0.753) and low resolutions (SSe= 0.501; 95% CI, 0.424—0.577; I^2= 76.3%; SSp= 0.727; 95% CI, 0.617—0.815; I^2= 73.3%).

- ***Threshold for high resolution: 0.125 mm^3***

The meta-analyses considering the voxel size of 0.125 mm^3 as the threshold for high spatial resolution, revealed that the diagnostic accuracy of teeth with no fillings still did not differ (Chi-square=3.2918; p=0.1928) between high (SSe= 0.767; 95% CI, 0.668—0.844; SSp= 0.916; 95% CI, 0.833—0.96) and low resolutions (SSe= 0.749; 95% CI, 0.635—0.836; I^2= 79.2%; SSp= 0.813; 95% CI, 0.683—0.897; I^2= 84.1%). The meta-analysis included 10 studies with low resolutions [12, 16, 18, 19, 36, 42, 43, 52, 61, 94] and 9 studies with high resolutions [8, 14, 21, 35, 47, 53, 61, 75, 82].

Gutta-percha filled canals also presented no difference (Chi-square=0.9673; p=0.6165), in a meta-analysis with 10 studies with high resolution [12, 16, 20, 22, 42, 43, 74, 78, 84, 94] (SSe= 0.765; 95% CI, 0.629—0.862; SSp= 0.83; 95% CI, 0.766—0.88) and 12 studies with low resolution [14, 21, 22, 35, 47, 53, 72, 74, 75, 78, 82, 95] (SSe= 0.694; 95% CI, 0.627—0.753; I^2= 76.5%; SSp= 0.792; 95% CI, 0.666—0.88; I^2= 82.6%).

The meta-analysis of root canals with metal posts included 11 studies with low resolution [12, 16, 17, 20, 42, 43, 65, 69, 78, 94, 96] (SSe= 0.521; 95% CI, 0.443—0.598; SSp= 0.717; 95% CI, 0.628—0.791), and 9 studies with high resolution [14, 21, 35, 47, 53, 75, 78,

82, 96] (SSe= 0.688; 95% CI, 0.555—0.795; I^2= 76.5%; SSp= 0.671; 95% CI, 0.553—0.77; I^2= 73.6%). It was observed a higher sensitivity for high-resolution CBCT scans (Chi-square=6.2572; p=0.01237). There was no difference regarding the specificity (Chi-square=0.2437; p=0.6216).

- ***Threshold for high resolution: 0.1 mm^3***

Using the voxel size of 0.1 mm^3 as the threshold, the meta-analysis of root canals with no filling included 11 studies with low resolutions [8, 12, 16-19, 42, 43, 52, 61, 94] (SSe= 0.717; 95% CI, 0.567—0.83; SSp= 0.855; 95% CI, 0.718—0.932), and 8 studies with high resolutions [8, 14, 21, 35, 47, 53, 75, 82] (SSe= 0.823; 95% CI, 0.705—0.9; I^2= 87.3%; SSp= 0.902; 95% CI, 0.816—0.951; I^2= 84.1%), and no difference (Chi-square=2.0356; p=0.3614) was observed regarding the diagnostic accuracy of VRF.

Gutta-percha-filled root canals also presented no difference (Chi-square=0.1371; p=0.9337), in a meta-analysis with 10 studies with low resolution [12, 16, 20, 22, 42, 43, 74, 78, 84, 94] (SSe= 0.707; 95% CI, 0.633—0.771; SSp= 0.795; 95% CI, 0.67—0.881) and 10 studies with high resolution [14, 21, 35, 47, 53, 72, 74, 75, 82, 95] (SSe= 0.701; 95% CI, 0.58—0.799; I^2= 76.4%; SSp= 0.801; 95% CI, 0.74—0.851; I^2= 84.3%).

The meta-analysis of root canals with metal posts included 11 studies with low resolutions [12, 16, 17, 20, 42, 43, 65, 69, 78, 94, 96] (SSe= 0.534; 95% CI, 0.467—0.6; SSp= 0.715; 95% CI, 0.628—0.789), and 8 studies with high resolutions [14, 21, 35, 47, 53, 75, 82, 96] (SSe= 0.676; 95% CI, 0.54—0.788; I^2= 77.5%; SSp= 0.683; 95% CI, 0.565—0.781; I^2= 74.4%), and presented no significant difference (Chi-square=4.5413; p=0.1032) regarding the spatial resolution.

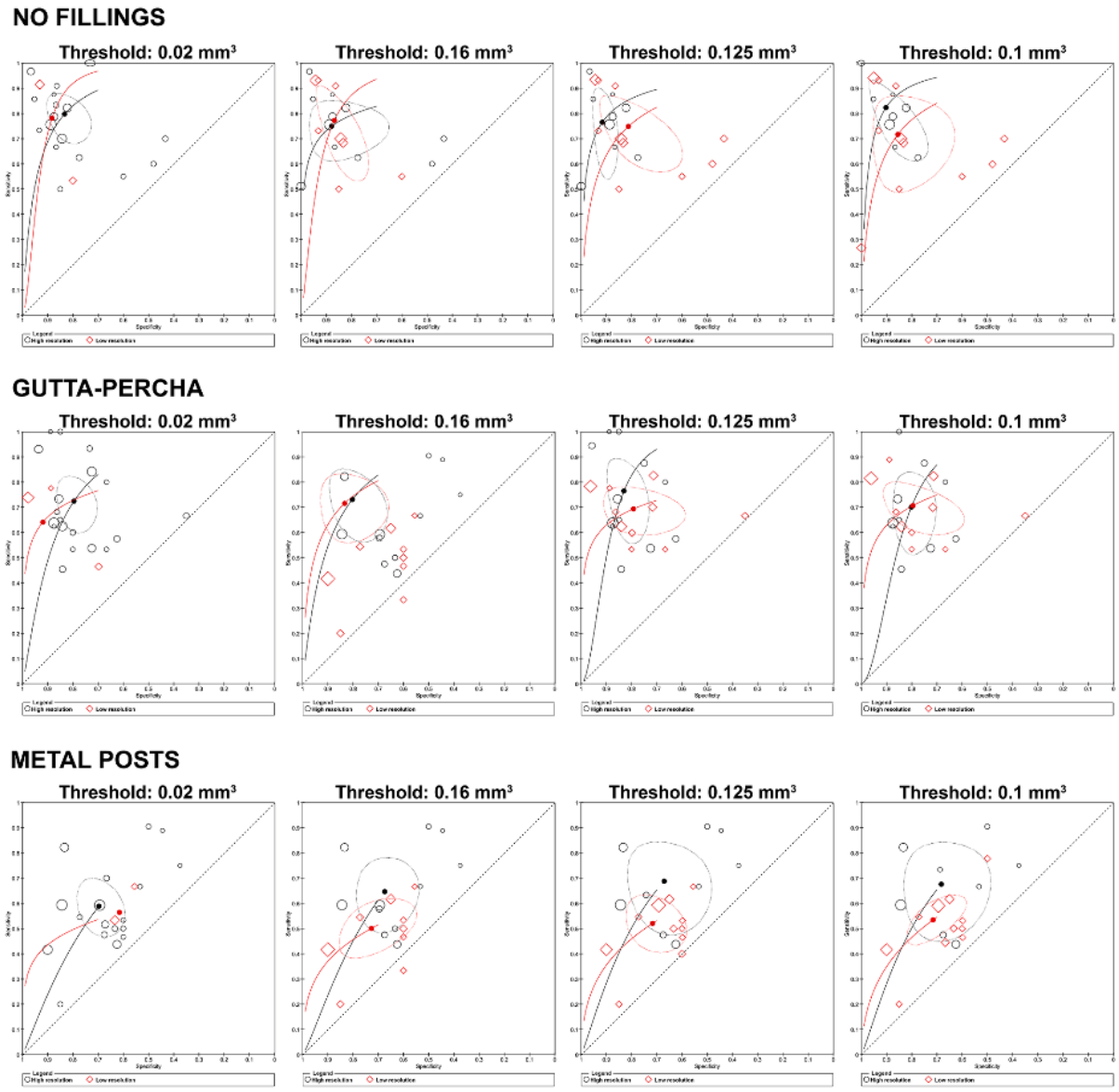

Figure 5. SROC plots of the meta-analyses for the comparisons between high and low spatial resolution considering different thresholds of voxel size, in root canals with no fillings, gutta-percha, and metal posts.

Presence of intracanal materials

The effect of intracanal materials on the diagnostic accuracy of VRFs was assessed using empty root canals as the comparator for the meta-analyses of each material. Sensitivity analyses were conducted, when possible, to assess the influence of the type of fracture (i.e., complete, or incomplete) on the diagnostic accuracy of VRF.

- ***No filling x gutta-percha***

The meta-analysis that compared empty root canals and root canals obturated with gutta-percha included 3683 teeth in 12 studies that compared both intracanal conditions [12, 14, 16, 21, 35, 42, 43, 47, 75, 76, 82, 94], 7 studies that assessed empty root canals [8, 17-19, 52, 56, 61], and 7 studies with gutta-percha-filled root canals [20, 22, 72, 74, 78, 84, 95]. There was no significant difference between the diagnostic accuracy of teeth with empty canals (SSe= 0.755; 95% CI, 0.676—0.819; SSp= 0.877; 95% CI, 0.8—0.927) or with gutta-percha-based root canal fillings (SSe= 0.721; 95% CI, 0.627—0.798; I^2= 81.7%; SSp= 0.803; 95% CI, 0.735—0.856; I^2= 84%) (Chi-square= 3.2638; p=0. 1956). However, the sensitivity analysis demonstrated that in the presence of complete VRFs, there was a significant difference in the diagnostic accuracy of empty root canals (SSe= 0.861; 95% CI, 0.704—0.942; SSp= 0.902; 95% CI, 0.823—0.948) and root filled canals (SSe= 0.699; 95% CI, 0.623—0.765; SSp= 0.8; 95% CI, 0.648—0.896), in both sensitivity (Chi-square=15.086; p=0.004526) and specificity (Chi-square=14.111; p=0.006948). In contrast, teeth with incomplete VRFs presented no difference (Chi-square=2.7482; p=0.2531) in the diagnostic accuracy of empty root canals (SSe= 0.748; 95% CI, 0.549—0.879; SSp= 0.908; 95% CI, 0.731—0.973) or root filled canals (SSe= 0.618; 95% CI, 0.41—0.79; SSp= 0.735; 95% CI, 0.598—0.838).

- ***No filling x metal posts***

The meta-analysis comparing empty root canals and root canals with metal posts included 3038 teeth in 12 studies that compared both situations [12, 14, 16, 17, 21, 35, 42, 43, 47, 75, 82, 94], 7 studies that assessed empty root canals [8, 18, 19, 52, 56, 61, 76], and 5 studies with metal posts [20, 65, 69, 78, 96]. It was found that teeth with metal posts present a lower diagnostic accuracy (SSe= 0.569; 95% CI, 0.489—0.645; SSp= 0.7; 95% CI, 0.628—0.764) than teeth with no root canal fillings (SSe= 0.755; 95% CI, 0.676—0.819; I^2= 83.6%; SSp= 0.877; 95% CI, 0.8—0.927; I^2= 83.9%), in terms of sensitivity (Chi-square= 9.9106; p=0.001643) and specificity (Chi-square= 9.8339; p= 0.001713). These findings were also confirmed by the sensitivity analysis according to the fracture patterns, and the results were similar for both complete and incomplete VRFs, with a significant difference between empty root canals and root canals with metal posts.

- ***No filling x fiberglass posts***

The diagnostic accuracy of teeth with fiberglass posts (SSe= 0.785; 95% CI, 0.671—0.867; SSp= 0.85; 95% CI, 0.775—0.903) did not differ from teeth with no root canal fillings (SSe= 0.755; 95% CI, 0.676—0.819; I^2= 78.3%; SSp= 0.877; 95% CI, 0.8—0.927; I^2= 81.4%), in terms of either sensitivity or specificity (Chi-square=0.5218; p=0.7704). The meta-analysis included 2127 teeth in 4 studies that compared both clinical situations [16, 47, 75, 82], 15 studies with empty root canals [8, 12, 14, 17-19, 21, 35, 42, 43, 52, 56, 61, 76, 94], and 1 study with fiberglass posts [67]. It was not possible to conduct a sensitivity analysis due to the lack of primary studies with separate analyses for complete and incomplete VRFs.

Also, it was not possible to assess the influence of bioceramic root-filling material [64], and zirconium-based root-filling material [72] on the diagnostic accuracy of VRFs due to the limited number of primary studies.

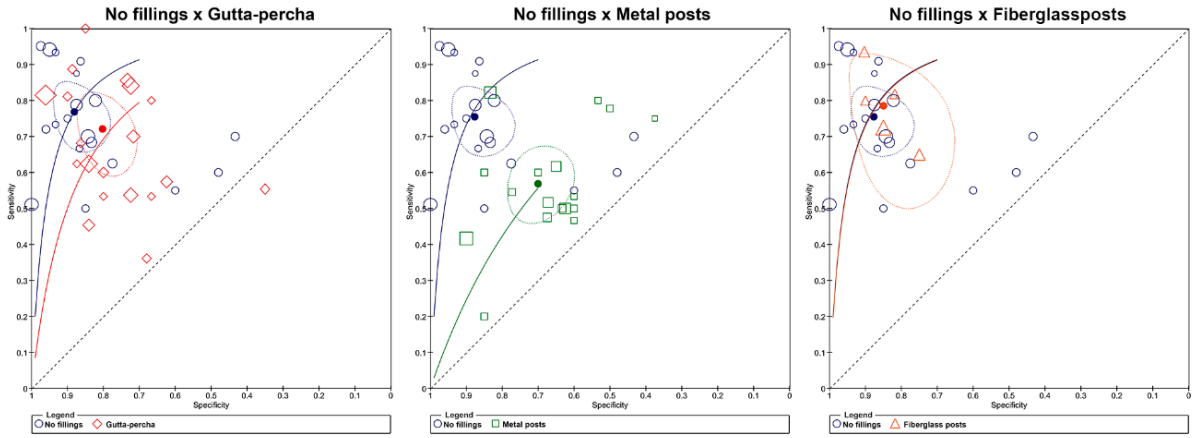

Figure 6. SROC plots of the meta-analyses for the comparisons between different intracanal materials, using root canal with no fillings as comparator.

Image enhancement filters

Three studies evaluated the use of sharpness filters in the i-CAT vision software (Imaging Sciences International, Hatfield, PA, USA). The filters were sharpen [15, 17, 19], hard [15], sharpen mild [17, 19], sharpen 3x3 [17, 19], s9 [17, 19], smooth [17], smooth 3x3 [17], sharpen super mild [17], angio sharpen medium 5x5 [17], angio sharpen high 5x5 [17], and shadow 3x3 [17]. The Adaptive Image Noise Optimiser filter (AINO, Planmeca, Helsinki, Finland) was also assessed by one study [46]. The use of enhancement filters in CBCT images demonstrated no influence on the diagnosis of VRFs in teeth with no fillings [17, 19], root canal filling [15, 46] (i.e., gutta-percha), or metal posts [15, 17]. Therefore, the evidence suggests that their use is not justified.

The use of artifact reduction filters was assessed by two different studies, in teeth with no filling [14], root canal filling [14, 49] (i.e., gutta-percha), and metal posts [14]. The filters were: MATLAB artifact removal software [49] (MathWorks Inc, Natick, MA, USA); and Blooming Artifact Reduction filter [14] (BAR, e-Vol DX, CDT software, Bauru, SP, Brazil). The results were not consistent, and although some level of improvement in diagnostic accuracy was observed in both studies, it was dependent on the CBCT device that was used.

It was not possible to perform meta-analyses to assess the influence of image enhancement filters on the diagnostic accuracy of VRFs due to the limited number of primary studies.

MAR algorithms

Several studies investigated the diagnostic accuracy of CBCT scans acquired with metal artifact reduction algorithms using the standard CBCT scans as comparators [13, 16, 18, 20-22, 49, 65, 71, 73, 83, 90, 98, 100]. The algorithms evaluated were: ProMax MAR algorithm [13, 20, 49, 73, 83, 90] (Planmeca, Helsinki, Finland); Master 3D MAR algorithm [13] (Vatech, Hwaseong, South Korea); Picasso Trio MAR algorithm [65] (Vatech, Hwaseong, South Korea); Pax-i3D MAR algorithm [98] (Vatech Co., Ltd., Gyeonggi-do, South Korea); EasyDent4 MAR algorithm [16] (E-WOO, Giheung-gu, South Korea); OP300 MAR algorithm [18, 21, 71] (Instrumentarium, Tuusula, Finland); Cranex 3D MAR algorithm [49] (Soredex, Tuusula, Finland); SMAR algorithm[100] (Scanora 3D, Soredex, Tuusula, Finland); i-CAT MAR algorithm [22] (Imaging Sciences International, Hatfield, PA, USA). The algorithms were applied in teeth with no fillings [16, 20, 21], root canal fillings [13, 16, 20-22, 49, 98], metal posts [16, 20, 21, 65, 83, 90, 98, 100], and fiberglass posts [16, 20]. Two studies evaluated the use of MAR algorithms for dental implants adjacent to the fractured teeth [71, 73], and one study assessed teeth with metal posts adjacent to the fractured teeth [18].

The results were very distinct among the included studies. Five studies found no difference in the diagnostic accuracy of VRFs with or without MAR algorithms [16, 22, 49, 83, 90, 100], while 2 studies reported an improved diagnostic accuracy when the algorithm was used [20, 98]. However, in 3 studies, the use of MAR algorithms demonstrated a negative impact on the diagnostic accuracy of VRFs, compared to CBCT scans without algorithms [13, 21, 65].

It was not possible to perform meta-analyses to assess the influence of MAR algorithms on the diagnostic accuracy of VRFs due to the limited number of primary studies, and high heterogeneity among included studies.

CBCT device

The influence of the CBCT device on the diagnostic accuracy of VRF was evaluated by several studies [8, 13, 14, 33, 36-38, 49, 51, 53, 59, 67, 74, 86, 96]. The CBCT devices evaluated were: ProMax (Planmeca) [13, 33, 49, 67]; Master 3D (Vatech) [13, 33]; 3D Accuitomo-XYZ (J. Morita) [59], 3D Accuitomo 170 (J. Morita) [8, 37, 51]; i-CAT (Imaging Sciences International) [8, 36, 59, 74, 96]; Prexion 3D (Teracom) [14, 74]; OP300 (Instrumentarium) [14, 53]; CS 9300 (Carestream) [67]; CS 9000 3D (Carestream) [14, 53], NewTom GO (Quantitative Radiology) [67], NewTom 3G (Quantitative Radiology) [37, 38, 49, 51, 59], NewTom VGI (Quantitative Radiology) [86], Scanora 3D (Soredex) [36, 59, 86]; Orthophos XG (Sirona Dental System) [74]; Galileos 3D (Sirona Dental System) [59]; Iluma Ultra (Imtec Imaging) [38]; Cranex 3D (Soredex) [49]; and Eagle 3D (Dabi Atlante) [96].

It is hard to extrapolate the findings of the included studies because different comparisons were performed in each one, with different intracanal materials, and acquisition parameters (i.e., FOV and voxel sizes, tube current, tube voltage). Therefore, it was not possible to perform meta-analyses to assess the influence of the CBCT devices on the diagnostic accuracy of VRFs due to the high heterogeneity among included studies.

FOV size

The influence of the FOV size was assessed by 5 studies, in teeth with root canal filling and metal posts. Small FOVs assessed by the studies included: 4×4 [51, 85]; 5×5 [69]; 6×6 [45, 51]; and 10×7.5 [87] cm^3; while large FOVs included 8×8 [69]; 10×10 [85]; 13×14[87]; 15×15 [51]; 18×16 [45]; and 22×22 [51] cm^3. The voxel size associated with the CBCT scan varied from 0.08 to 0.3 mm^3. In all studies, it was observed that small-volume CBCT scans presented higher diagnostic accuracy for VRFs than CBCT scans with large FOVs.

It was not possible to perform meta-analyses to assess the influence of the FOV sizes on the diagnostic accuracy of VRFs due to the limited number of primary studies and high methodological heterogeneity among the included studies.

Position within FOV

Three studies assessed the influence of the position of the suspected tooth within the FOV, on the diagnostic accuracy of VRF. The studies evaluated teeth with no filling [20], root canal filling [20], metal posts [20, 69, 92] and fiberglass posts [20]. The FOV sizes varied from 5×5 to 15×15 cm^3, whilst the voxel size varied between 0.16-0.2 mm^3. It was consensus among all studies that the central positioning of the suspected tooth increased diagnostic accuracy.

It was not possible to perform meta-analyses to assess the influence of the positioning within FOV on the diagnostic accuracy of VRFs due to the limited number of primary studies.

Tube current

Seven studies evaluated the association of the CBCT tube current and the diagnostic accuracy of VRFs [18, 41, 47, 69, 71, 75, 87], in teeth with no filling [18, 47, 71, 75], root canal filling [41, 47, 75], metal posts [47, 69, 75, 87] and fiberglass posts [47, 75]. The voxel sizes varied from 0.1 to 0.25 mm^3. In the majority of studies, there was no influence of lower or higher tube currents in the diagnostic task [7, 18, 47, 69, 71, 75]. Conversely, one study the increase in tube current improved diagnostic accuracy [41], while another found better diagnostic performance with lower tube current [87].

It is hard to extrapolate the findings of the included studies because different comparisons were performed in each one, with different intracanal materials, and acquisition parameters (i.e., FOV and voxel sizes, tube voltage). It was not possible to perform meta-analyses to assess the influence of the tube current on the diagnostic accuracy of VRFs due to the limited number of primary studies, and high heterogeneity among included studies.

Tube voltage

Four studies assessed the influence of the CBCT tube voltage on the diagnostic accuracy of VRFs, in teeth with no filling [47, 73], root canal filling [41, 47], fiberglass posts [47], and metal posts [31, 47]. The voxel sizes varied from 0.1 to 0.15 mm^3. In 2 studies [47, 73], the variations in tube voltage did not alter the diagnostic accuracy. In contrast, in 1 study 60 kVp performed better than 85 kVp [41], and in another study, 80 kVp performed better than 92 kVp [31].

It is hard to extrapolate the findings of the included studies because different comparisons were performed in each one, with different intracanal materials, and acquisition

parameters (i.e., FOV and voxel sizes, tube voltage). It was not possible to perform meta-analyses to assess the influence of the tube voltage on the diagnostic accuracy of VRFs due to the limited number of primary studies, and high heterogeneity among included studies.

Metallic objects inside the FOV

Five studies [18, 67, 68, 71, 73] evaluated the influence of the presence of metallic objects (i.e., metal posts, dental implants) adjacent to the investigation tooth. The voxel sizes varied from 0.08 to 0.15 mm^3. The includes studies used titanium implants [67, 68], zirconium-oxide implants [71, 73], nickel-chromium metal posts [18], and cobalt-chromium metal posts [67, 68] to generate artifacts. The results are somewhat inconsistent. Three studies reported a decreased diagnostic accuracy in the presence of metallic objects [18, 71, 73], and 2 studies found no difference regarding the presence of such objects [67, 68].

It is hard to extrapolate the findings of the included studies because different comparisons were performed in each one, with different metallic objects, intracanal materials, and acquisition parameters (i.e., FOV and voxel sizes, tube voltage and tube current, application of MAR algorithms). It was not possible to perform meta-analyses to assess the influence of the tube voltage on the diagnostic accuracy of VRFs due to the limited number of primary studies, and high heterogeneity among included studies.

It was not possible to assess the influence of other possible factors in the diagnostic accuracy of VRFs using CBCT scans, as only one study was available. These factors are bioceramic root-filling material [64]; zirconium-based root-filling material [72]; and DICOM viewer software [43].

Quality of evidence

The assessment of the quality of evidence based on the GRADE approach revealed a "very low" certainty of evidence for the meta-analyses that evaluated the influence of the fracture type, voxel size, and intracanal materials. The downgrade was applied at the domains of indirectness, due to the *in vitro* nature of the primary studies, and inconsistency, due to the high statistical heterogeneity among the included studies. Further details regarding the GRADE assessments are available in the summary-of-findings table (**Table 1**).

Table 1. GRADE's summary-of-findings table.

Outcomes	Risk of bias	Indirectness	Inconsistency	Imprecision	Publication bias	Other bias	Certainty of the evidence (GRADE)
Type of fracture							
Complete x Incomplete	not serious	very serious[a]	serious[b]	not serious	undetected	undetected	⊕◯◯◯ VERY LOW [a,b]
Voxel size							
High resolution x Low resolution	not serious	very serious[a]	serious[b]	not serious	undetected	undetected	⊕◯◯◯ VERY LOW [a,b]
Intracanal materials							
No fillings x Root canal filling	not serious	very serious[a]	serious[b]	not serious	undetected	undetected	⊕◯◯◯ VERY LOW [a,b]
No fillings x Metal posts	not serious	very serious[a]	serious[b]	not serious	undetected	undetected	⊕◯◯◯ VERY LOW [a,b]
No fillings x Fiberglass posts	not serious	very serious[a]	serious[b]	not serious	undetected	undetected	⊕◯◯◯ VERY LOW [a,b]

Explanations: a. Because of the *in vitro* methodology; b. High statistical and methodological heterogeneity.

Discussion

Diagnosing VRFs is difficult in dental practice as it is identified in most clinical situations by a combination of signs, symptoms, and radiographic findings. There is no consensus on the diagnostic accuracy of CBCT images for VRFs, and many factors might be involved. Studies have evaluated the influence of the intracanal materials [12, 14-17, 20, 21, 29, 30, 35, 36, 39, 42-45, 47, 48, 50, 53, 57, 64, 72, 75-78, 80-82, 85, 89, 94, 97, 98], fracture pattern [8, 34, 40, 65, 82, 84, 99], image acquisition parameters [12, 13, 15, 18, 22, 31-33, 38, 41, 42, 45-47, 50, 51, 57, 61, 63, 66, 69, 71, 73, 75, 78, 85, 87, 95, 96], and other factors. Current evidence regarding *in vivo* detection of VRFs is very limited [102], and it would be impossible to identify the factors involved in diagnostic accuracy using only these studies. Hence, since there is a high volume of data in published articles, the present systematic review focused on *in vitro* studies that evaluated the diagnosis of VRF by CBCT imaging. We intended to screen the main factors that might optimize CBCT imaging for the diagnosis of VRFs and guide further laboratory and clinical investigations. Meta-analyses were performed to assess the influence of each factor on sensitivity and specificity values in the diagnosis of VRFs. The quality of evidence was also assessed for each factor.

The effect of intracanal materials on the diagnostic accuracy of VRFs was assessed, using non-endodontically treated teeth for comparison. It was observed that the presence of root canal filling caused a reduction in sensitivity and specificity values only in teeth with complete VRFs. This may be explained by the fracture width of complete and incomplete VRFs. The mean gap between fragments of incomplete VRFs is much lower than complete ones [8, 84]. Hence, the effects of imaging artifacts caused by gutta-percha are much more prejudicial when assessing complete VRFs, which would be visible in the absence of artifacts. In contrast, incipient fractures [82, 84, 99], with minimal separation between fragments [4, 103], are not easily detected by CBCT images, as the spatial resolution might not allow the reconstruction of the fracture lines, regardless of the presence of root canal filling. Conversely, it was observed that the presence of metal posts caused a reduction in both sensitivity and specificity values, in teeth with either complete or incomplete VRFs. These findings were expected because the beam-hardening artifacts are more prominent in the presence of materials containing chemical elements with higher atomic numbers [10]. The high radiodensity of metal posts severely affect image quality [45, 86]. Our findings corroborate with Dias et al. [104], which recently analyzed

in vivo VRFs, and found that intracanal posts limited the diagnostic performance of CBCT images.

Also, regarding imaging artifacts, the influence of metallic objects inside the FOV on the diagnosis of VRFs has been investigated [18, 67, 68, 71, 73]. Nickel-chromium [18] and cobalt-chromium [67, 68] metal posts, and dental implants composed mainly of titanium [67, 68] or zirconium [71, 73] were analyzed. Three studies reported that the presence of metallic objects impaired the diagnostic performance of CBCT images [18, 71, 73]. Specificity is significantly lower in the presence of zirconium implants [71, 73]. The artifacts formed in adjacent areas may mimic fracture lines, generating false-positive diagnoses. In opposition, two studies reported no influence of cobalt-chromium posts or titanium implants on the diagnosis of VRF in adjacent teeth [67, 68]. The studies presented low methodological heterogeneity. All included studies used dry human mandibles as phantoms, and high-resolution CBCT images, with voxel sizes that ranged from 0.08 to 0.15 mm^3. Perhaps other factors also influenced the diagnostic task, such as fracture pattern, CBCT device, and tube current and voltage. The influence of metallic objects within the FOV should be further investigated.

The final quality of CBCT images is affected by several technical factors. Changes in the acquisition parameters have been thoroughly evaluated by several studies, in terms of tube current [18, 41, 47, 69, 71, 75, 87], tube voltage [31, 41, 47, 73], and FOV size [45, 51, 69, 85, 87], however, no consensus was found. Regarding the FOV size, it is consensus that small FOVs present superior diagnostic performance in comparison with the large ones [45, 51, 69, 85, 87]. Most studies found no discrepancies in the diagnostic accuracy of VRFs when varying the tube current in non-endodontically treated teeth [18, 47, 71, 75], root-filled teeth [47, 75], and teeth with metal [47, 69, 75] and fiberglass posts [47, 75]. In contrast, one study reported better diagnostic performance with increased tube current in root-filled teeth [41], and in another study, the diagnosis of teeth with metal posts was improved with a reduction in tube current [87]. Changes in tube voltage also provided controversial results. Two studies reported no difference in the detection of VRFs with varied tube voltage, regardless of the intracanal material [47, 73]. Conversely, other two studies reported that a reduction in tube voltage improved the diagnostic accuracy of VRFs, in root-filled teeth [41], and roots with metal posts [31]. Adjustments in tube current and voltage cause variations in the emitted radiation, as they modify the beam energy, penetrability, and the number of photons that reach the CBCT detector [105]. Bearing this in mind, variations in acquisition parameters are focused on reducing the

effective radiation dose, following the ALARA - as low as reasonably achievable - principles [106, 107]. However, there is no reliable evidence that the effective dose of CBCT scans presents any biological risk, regarding the incidence of cancer or raising the mortality rates [106, 107]. Hence, further research efforts should focus solely on developing strategies and tools that may improve CBCT image quality.

The main factor that influences the spatial resolution of CBCT images is the voxel size. The meta-analyses that evaluated the influence of the voxel size were divided according to different thresholds set for high and low resolutions. According to our findings, a minimum voxel size of 0.125 mm^3 should be considered to optimize VRF diagnosis in teeth with metal posts. However, it is important to clarify that only the sensitivity was improved with higher spatial resolutions. The specificity was unchanged with voxel-size variations. The summarized specificity for teeth with metal posts was 0.7 (95% CI, 0.628—0.764). A lower specificity is observed in the presence of false-positive diagnoses. False-positive rates are raised in teeth with metal posts due to the presence of artifacts that mimic the presence of fracture lines [15, 42, 50, 78, 96]. Since most teeth with VRF are extracted [4, 103], clinicians should be cautious when assessing VRFs in teeth with metal posts [10, 39, 84]. Direct visualization of the fracture line by surgery might be necessary to validate the diagnosis [6, 103]. Conversely, the diagnosis of VRFs in teeth filled with gutta-percha, or non-root-filled teeth, does not seem to be influenced by the voxel size, according to our results. PradeepKumar et al. [102] recently assessed the diagnostic accuracy of *in vivo* VRFs by meta-analysis, for root-filled teeth. The meta-regression did not identify the voxel size as a possible confounding factor.

Some CBCT units offer MAR algorithms options for image reconstruction. The use of MAR algorithms remains controversial. Most of the studies reported that there is no influence on the diagnostic accuracy of VRF when using these tools [16, 22, 49, 83, 90, 100]. In some studies, the MAR algorithms impaired diagnostic performance [13, 21, 65]. Since subtle VRFs present small hypodense lines, which are very similar to an artifact streak, the image enhancement provided by the MAR algorithms did not improve diagnostic accuracy [108]. The mechanism of MAR algorithms includes interpolation-based sinogram corrections, which replace the projection data of metal objects with surrounding data in the sinogram [16]. However, studies have reported incomplete artifact correction [109], secondary artifact formation [109], and loss of information surrounding high-density materials [13]. Conversely, two studies reported that MAR algorithms improved the diagnostic sensitivity of VRFs [20,

98]. However, the main improvement reported in these studies occurred in teeth without root canal filling. Hence, the applicability of MAR algorithms for the diagnosis of VRFs is, at minimum, questionable. It is important to consider that most of the included studies assessing AR tools presented a high or moderate risk of bias [13, 18, 20, 49, 73, 83, 90, 98, 100]. The main concerns regarding the risk of bias were the lack of a baseline evaluation to exclude previously fractured teeth, incomplete description of the reference standard test (i.e., direct visualization, magnification, transillumination), or restriction of the reference standard test to the fractured teeth.

Enhancement filters also have been assessed to reduce the impact of imaging artifacts. Filters differ from MAR algorithms as they are applied to an acquired image, and not during CBCT acquisition. The mechanism is based on increasing or decreasing image characteristics, such as sharpness and noise. It has been shown that applying enhancement filters in tomographic images did not improve the diagnostic accuracy of VRFs [15, 17, 19, 46]. Alternatively, some enhancement filters use different mechanisms, based on enhancing gray-scale contrast, to reduce artifacts in CBCT images [14, 49]. Although it has been demonstrated that these filters improved image quality [110, 111], there is no change in the hyper and hypodense streaks and bands caused by the beam-hardening in CBCT acquisitions. The evidence regarding the diagnostic accuracy of CBCT images with artifact removal filters is uncertain. Saati et al. [49] evaluated the MATLAB artifact removal filter in root-filled teeth, using NewTom 3G, Promax 3D, and Cranex 3D. The MATLAB filter improved the diagnostic accuracy when using the Cranex 3D images. However, the authors did not describe the type of fracture that was evaluated (i.e., complete, or incomplete), and the voxel size provided by each CBCT unit. Similarly, Caetano et al. [14] also evaluated an artifact removal filter, e-vol DX BAR filter, in non-endodontically treated teeth, root-filled teeth, and metal posts. The BAR filter improved the overall accuracy of the 9000 3D device (from 62% to 74%). However, the accuracy was still lower than the OP300 and Prexion 3D units (86%, and 96%, respectively), regardless of the application of the BAR filter (87%, and 92%, respectively). Hence, it seems that using different CBCT devices has more impact on the final image quality, than the application of enhancement filters.

Regarding the diagnostic accuracy provided by different CBCT devices, several units have been compared [8, 13, 14, 33, 36-38, 49, 51, 53, 59, 67, 74, 86, 96]. It has been argued that the technology of CBCT detectors affects image quality in terms of spatial resolution,

dynamic range, and contrast resolution [59]. Detectors based on image intensifier tube/charged coupled device combinations (IIT/CCD) presented inferior diagnostic performance compared to flat-panel detectors (FPD) in some studies [37, 59], while others found no difference [38, 49, 51]. It was not possible to perform a meta-analysis, because the studies present high methodological heterogeneity. There are important differences among the included studies in the fracture pattern, intracanal materials, and acquisition parameters, which directly impact the image quality, and diagnostic performance. Nevertheless, the majority of the included studies obtained CBCT images on FPD-based devices [8, 12-22, 29-51, 53-75, 77-97, 99-101], and a few studies used ITT/CCD devices [37, 38, 49, 51, 52, 59, 76, 98].

Regarding the quality assessment of the included studies, most of the studies presented a high risk of bias. The main reason why several studies presented high risk of bias was the reference standard test adopted by them. Low risk of bias was recognized for studies that described that all specimens were analyzed before and after fracture induction, using at least one method to assist the direct visualization of the fracture lines: magnification of any type, transillumination, or application of stains [8, 12, 14-19, 21, 22, 29-31, 34-36, 38, 40, 42-45, 47, 50, 52-54, 56-61, 63, 65, 67-69, 71-84, 86, 87, 89-93, 95, 99]. Unclear risk of bias was decided for studies that solely described the reference standard as direct visualization [20, 85, 94, 96]. However, several studies did not describe the reference standard test [13, 32, 33, 46, 70, 97], or did not evaluate all specimens with the test [37, 39, 41, 48, 49, 51, 64, 66, 71, 73, 77, 88, 90, 91, 98-101], and thus, were considered as high risk of bias. The diagnostic accuracy of an index test is determined after establishing the presence or absence of the target condition in the sample with the reference standard test. As several tests may be available to detect the same condition, the authors should describe the methods used for both index and reference standard tests in sufficient detail to allow replication [112]. Differences in test protocols potentially affect the variability in accuracy measures among studies.

Also, a high risk of bias was attributed to several studies due to the lack of anthropomorphic model designs [12, 30, 34, 36, 39, 40, 44, 45, 48-50, 57, 63, 77, 81, 83, 86, 87, 90-92, 97-101], to simulate the clinical condition of a CBCT scan. Andraws Yalda et al. [113] recently investigated the influence of different phantom designs on the diagnosis of root fractures. The authors evaluated five models (i.e., acrylic resin block, human skull, skull covered in wax, skull immersed in water, skull immersed in water with cervical vertebrae), and found no difference among the experimental designs. However, the authors did not compare

the *in vitro* models with an *in vivo* assessment. *In vivo*, a CBCT scan is affected by scattering artifacts and image noise, due to the x-ray attenuation by the patient's soft and hard tissues. Acquiring images without any simulation of the clinical condition provides a level of contrast and a contrast-to-noise ratio that is impossible to achieve in any *in vivo* scenario. Hence, it is not plausible to assume that images taken from teeth in acrylic resin or gypsum blocks represent a valid simulation of real CBCT scans for the diagnosis of VRFs.

The GRADE appraisal revealed a very-low certainty of evidence for the meta-analyses that evaluated the influence of the fracture pattern, voxel size, and intracanal materials. The downgrading occurred because we included only *in vitro* studies in this systematic review. Many comparisons were performed with indirect evidence, and inconsistency, as there was a significant statistical and methodological heterogeneity among the included studies. There was no downgrading due to the risk of bias because rigorous criteria were applied during the quality analysis with QUADAS-2, and studies with high risk were not included in the meta-analyses. Imprecision was also not considered, since there was a significant sample size involved in all included studies. Publication bias or other forms of bias were not detected. Although very strict criteria were used to select studies for the meta-analyses, it is important to consider that this systematic review focused on *in vitro* studies. Hence, the impact of several aspects regarding fracture patterns, and CBCT acquisition were identified. However, further clinical investigations should be conducted to validate the findings of this review.

Conclusions

The diagnosis of VRFs by CBCT images is mainly affected by the fracture pattern, presence of intracanal materials, and voxel size, in laboratory settings. The diagnostic accuracy of incomplete VRFs is lower than complete VRFs. Metal posts and root canal filling also reduce diagnostic accuracy. A minimum voxel size of 0.125 mm^3 is beneficial for the diagnosis of VRFs, in the presence of metal posts. Evidence suggests that image-enhancement filters and MAR algorithms do not affect VRFs diagnosis. Other factors should be further evaluated to establish an association with the diagnosis of VRFs. Additional strategies and tools for the diagnosis of VRFs should be developed, especially for incomplete fractures and teeth containing root canal filling materials or metal posts.

Funding: This work was supported by the “Coordenação de Aperfeiçoamento de Pessoal de Nível Superior (CAPES)” in the form of a scholarship [grant code 001].

Conflict of Interest: The authors declare that they have no conflict of interest.

References

1. American Association of Endodontists (2008) Endodontics: colleagues for excellence—cracking the cracked tooth code: detection and treatment of various longitudinal tooth fractures. https://www.aae.org/specialty/wp-content/uploads/sites/2/2017/07/ecfesum08.pdf. Accessed 17 january 2022
2. Fuss Z, Lustig J, Tamse A (1999) Prevalence of vertical root fractures in extracted endodontically treated teeth. Int Endod J 32(4):283-286. https://doi.org/10.1046/j.1365-2591.1999.00208.x
3. Yoshino K, Ito K, Kuroda M, Sugihara N (2015) Prevalence of vertical root fracture as the reason for tooth extraction in dental clinics. Clin Oral Investig 19(6):1405-1409. https://doi.org/10.1007/s00784-014-1357-4
4. Patel S, Bhuva B, Bose R (2022) Present status and future directions: vertical root fractures in root filled teeth. Int Endod J 55(Suppl 3):804-826. https://doi.org/10.1111/iej.13737
5. Cohen S, Berman LH, Blanco L, Bakland L, Kim JS (2006) A demographic analysis of vertical root fractures. J Endod 32(12):1160-1163. https://doi.org/10.1016/j.joen.2006.07.008
6. von Arx T, Bosshardt D (2017) Vertical root fractures of endodontically treated posterior teeth: A histologic analysis with clinical and radiographic correlates. Swiss Dent J 127(1):14-23
7. Oliveira ML, Candemil AP, Freitas DQ, Haiter-Neto F, Wenzel A, Spin-Neto R (2021) Objective assessment of the combined effect of exomass-related- and motion artefacts in cone beam CT. Dentomaxillofac Radiol 50(1):20200255. https://doi.org/10.1259/dmfr.20200255
8. Brady E, Mannocci F, Brown J, Wilson R, Patel S (2014) A comparison of cone beam computed tomography and periapical radiography for the detection of vertical root fractures in nonendodontically treated teeth. Int Endod J 47(8):735-746. https://doi.org/10.1111/iej.12209
9. Salineiro FCS, Kobayashi-Velasco S, Braga MM, Cavalcanti MGP (2017) Radiographic diagnosis of root fractures: a systematic review, meta-analyses and sources of heterogeneity. Dentomaxillofac Radiol 46(8):20170400. https://doi.org/10.1259/dmfr.20170400
10. Schulze R, Heil U, Gross D, Bruellmann DD, Dranischnikow E, Schwanecke U, Schoemer E (2011) Artefacts in CBCT: a review. Dentomaxillofac Radiol 40(5):265-273. https://doi.org/10.1259/dmfr/30642039
11. Chang E, Lam E, Shah P, Azarpazhooh A (2016) Cone-beam Computed Tomography for Detecting Vertical Root Fractures in Endodontically Treated Teeth: A Systematic Review. J Endod 42(2):177-185. https://doi.org/10.1016/j.joen.2015.10.005
12. Wanderley VA, Nascimento EHL, Gaeta-Araujo H, Oliveira-Santos C, Freitas DQ, Oliveira ML (2021) Combined Use of 2 Cone-beam Computed Tomography Scans in the Assessment of Vertical Root Fracture in Teeth with Intracanal Material. J Endod 47(7):1132-1137. https://doi.org/10.1016/j.joen.2021.04.001
13. Bechara B, McMahan CA, Moore WS, Noujeim M, Teixeira FB, Geha H (2013a) Cone beam CT scans with and without artefact reduction in root fracture detection of endodontically treated teeth. Dentomaxillofac Radiol 42(5):20120245. https://doi.org/10.1259/dmfr.20120245
14. Caetano AP, Sousa TO, Oliveira MR, Evanglista K, Bueno JM, Silva MA (2021) Accuracy of three cone-beam CT devices and two software systems in the detection of

vertical root fractures. Dentomaxillofac Radiol 50(3):20200334. https://doi.org/10.1259/dmfr.20200334
15. De Martin e Silva D, Campos CN, Pires Carvalho AC, Devito KL (2018) Diagnosis of Mesiodistal Vertical Root Fractures in Teeth with Metal Posts: Influence of Applying Filters in Cone-beam Computed Tomography Images at Different Resolutions. 44(3):470-474. https://doi.org/10.1016/j.joen.2017.08.030.
16. de Rezende Barbosa GL, Sousa Melo SL, Alencar PN, Nascimento MC, Almeida SM (2016) Performance of an artefact reduction algorithm in the diagnosis of in vitro vertical root fracture in four different root filling conditions on CBCT images. Int Endod J 49(5):500-508. https://doi.org/10.1111/iej.12477
17. Ferreira LM, Visconti M, Nascimento HA, Dallemolle RR, Ambrosano GM, Freitas DQ (2015) Influence of CBCT enhancement filters on diagnosis of vertical root fractures: a simulation study in endodontically treated teeth with and without intracanal posts. 44(5):20140352. https://doi.org/10.1259/dmfr.20140352.
18. Gaêta-Araujo H, de Oliveira Reis L, Leandro Nascimento EH, Oliveira-Santos N, Oliveira-Santos C (2020) Influence of metal post in adjacent teeth in the detection of vertical root fracture using CBCT with different acquisition parameters. J Endod 46(11):1655-1661. https://doi.org/10.1016/j.joen.2020.08.013
19. Nascimento MC, Nejaim Y, de Almeida SM, Bóscolo FN, Haiter-Neto F, Sobrinho LC, Silva EJ (2014) Influence of cone beam CT enhancement filters on diagnosis ability of longitudinal root fractures. Dentomaxillofac Radiol 43(3):20130374. https://doi.org/10.1259/dmfr.20130374
20. Nikbin A, Kajan ZD, Taramsari M, Khosravifard N (2018) Effect of object position in the field of view and application of a metal artifact reduction algorithm on the detection of vertical root fractures on cone-beam computed tomography scans: An in vitro study. Imaging Sci Dent 48(4):245-254. https://doi.org/10.5624/isd.2018.48.4.245
21. Oliveira MR, Sousa TO, Caetano AF, de Paiva RR, Valladares-Neto J, Yamamoto-Silva FP, Silva MAG (2021) Influence of CBCT metal artifact reduction on vertical radicular fracture detection. Imaging Sci Dent 51(1):55-62. https://doi.org/10.5624/isd.20200191
22. Uysal S, Akcicek G, Yalcin ED, Tuncel B, Dural S (2021) The influence of voxel size and artifact reduction on the detection of vertical root fracture in endodontically treated teeth. Acta Odontol Scand 79(5):354-358. https://doi.org/10.1080/00016357.2020.1859611
23. McInnes MDF, Moher D, Thombs BD, McGrath TA, Bossuyt PM, and the P-DTAG, Clifford T, Cohen JF, Deeks JJ, Gatsonis C, Hooft L, Hunt HA, Hyde CJ, Korevaar DA, Leeflang MMG, Macaskill P, Reitsma JB, Rodin R, Rutjes AWS, Salameh JP, Stevens A, Takwoingi Y, Tonelli M, Weeks L, Whiting P, Willis BH (2018) Preferred Reporting Items for a Systematic Review and Meta-analysis of Diagnostic Test Accuracy Studies: The PRISMA-DTA Statement. JAMA 319(4):388-396. https://doi.org/10.1001/jama.2017.19163
24. Campbell JM, Klugar M, Ding S, Carmody DP, Hakonsen SJ, Jadotte YT, White S, Munn Z (2015) Diagnostic test accuracy: methods for systematic review and meta-analysis. Int J Evid Based Healthc 13(3):154-162. https://doi.org/10.1097/XEB.0000000000000061
25. Whiting PF, Rutjes AW, Westwood ME, Mallett S, Deeks JJ, Reitsma JB, Leeflang MM, Sterne JA, Bossuyt PM, Group Q- (2011) QUADAS-2: a revised tool for the quality assessment of diagnostic accuracy studies. Ann Intern Med 155(8):529-536. https://doi.org/10.7326/0003-4819-155-8-201110180-00009
26. Guyatt GH, Oxman AD, Schunemann HJ, Tugwell P, Knottnerus A (2011) GRADE guidelines: a new series of articles in the Journal of Clinical Epidemiology. J Clin Epidemiol 64(4):380-382. https://doi.org/10.1016/j.jclinepi.2010.09.011

27. Reitsma JB, Glas AS, Rutjes AW, Scholten RJ, Bossuyt PM, Zwinderman AH (2005) Bivariate analysis of sensitivity and specificity produces informative summary measures in diagnostic reviews. J Clin Epidemiol 58(10):982-990. https://doi.org/10.1016/j.jclinepi.2005.02.022
28. Page MJ, McKenzie JE, Bossuyt PM, Boutron I, Hoffmann TC, Mulrow CD, Shamseer L, Tetzlaff JM, Akl EA, Brennan SE, Chou R, Glanville J, Grimshaw JM, Hrobjartsson A, Lalu MM, Li T, Loder EW, Mayo-Wilson E, McDonald S, McGuinness LA, Stewart LA, Thomas J, Tricco AC, Welch VA, Whiting P, Moher D (2021) The PRISMA 2020 statement: an updated guideline for reporting systematic reviews. BMJ 372(n71. https://doi.org/10.1136/bmj.n71
29. Abdinian M, Razavian H, Jenabi N (2016) In Vitro Comparison of Cone Beam Computed Tomography with Digital Periapical Radiography for Detection of Vertical Root Fracture in Posterior Teeth. J Dent (Shiraz) 17(2):84-90
30. Al Hadi D, Parekh S, Naeem W, Luke AM, Mathew S (2020) Detection of Vertical Root Fractures Using Three Different Imaging Modalities: An In Vitro Study. J Contemp Dent Pract 21(5):549-553
31. BashizadehFakhar H, Bolhari B, Shamshiri AR, Amini S, Ranji PJDH (2021) Diagnostic Accuracy of Cone-Beam Computed Tomography at Different Tube Voltages for Vertical Root Fractures in Endodontically Treated Teeth with Metallic Posts. Dent. Hypotheses 12(3):132. https://doi.org/10.4103/denthyp.denthyp_107_21
32. Bechara B, McMahan CA, Nasseh I, Geha H, Hayek E, Khawam G, Raad M, Noujeim M (2013b) Number of basis images effect on detection of root fractures in endodontically treated teeth using a cone beam computed tomography machine: an in vitro study. Oral Surg Oral Med Oral Pathol Oral Radiol 115(5):676-681. https://doi.org/10.1016/j.oooo.2013.01.026
33. Bechara B, McMahan CA, Noujeim M, Faddoul T, Moore WS, Teixeira FB, Geha H (2013c) Comparison of cone beam CT scans with enhanced photostimulated phosphor plate images in the detection of root fracture of endodontically treated teeth. Dentomaxillofac Radiol 42(7):20120404. https://doi.org/10.1259/dmfr.20120404
34. Byakova SF, Novozhilova NE, Makeeva IM, Grachev VI, Kasatkina IV (2019) The detection of vertical root fractures in post-core restored teeth ith cone-beam CT: In vivo and ex vivo. Dentomaxillofac Radiol 48(6):20180327. https://doi.org/10.1259/dmfr.20180327.
35. de Menezes RF, de Araujo NC, Rosa J, Carneiro VSM, Neto APD, Costa V, Moreno LM, Miranda JM, de Albuquerque DS, Albuquerque M, dos Santos RA, Gerbi M (2016) Detection of vertical root fractures in endodontically treated teeth in the absence and in the presence of metal post by cone-beam computed tomography. BMC Oral Health 16(48):1-6. https://doi.org/10.1186/s12903-016-0207-y.
36. Ferreira RI, Bahrami G, Isidor F, Wenzel A, Haiter-Neto F, Groppo FC (2013) Detection of vertical root fractures by cone-beam computerized tomography in endodontically treated teeth with fiber-resin and titanium posts: an in vitro study. Oral Surg Oral Med Oral Pathol Oral Radiol 115(1):e49-57. https://doi.org/10.1016/j.oooo.2012.06.012
37. Gunduz K, Avsever H, Orhan K, Çelenk P, Ozmen B, Cicek E, Egrioglu E, Karaçaylı Ü (2013) Comparison of intraoral radiography and cone-beam computed tomography for the detection of vertical root fractures: An in vitro study. Oral Radiol 29(1):6-12. https://doi.org/10.1007/s11282-012-0098-9
38. Kamburoğlu K, Murat S, Yüksel SP, Cebeci AR, Horasan S (2010) Detection of vertical root fracture using cone-beam computerized tomography: an in vitro assessment. Oral

Surg Oral Med Oral Pathol Oral Radiol Endod 109(2):e74-81. https://doi.org/10.1016/j.tripleo.2009.09.005
39. Khedmat S, Rouhi N, Drage N, Shokouhinejad N, Nekoofar MH (2012) Evaluation of three imaging techniques for the detection of vertical root fractures in the absence and presence of gutta-percha root fillings. Int Endod J 45(11):1004-1009. https://doi.org/10.1111/j.1365-2591.2012.02062.x
40. Makeeva IM, Byakova SF, Novozhilova NE, Adzhieva EK, Golubeva GI, Grachev VI, Kasatkina IV (2016a) Detection of artificially induced vertical root fractures of different widths by cone beam computed tomography in vitro and in vivo. Int Endod J 49(10):980-989. https://doi.org/10.1111/iej.12549
41. Mehralizadeh S, Khalilak Z, Entezari S (2018) Effect of different exposure settings on the diagnosis of vertical root fractures on cone-beam computed tomography images. Biosci. Biotech. Res. Comm 11(1):117-121. https://doi.org/10.21786/bbrc/11.1/16
42. Melo SL, Bortoluzzi EA, Abreu M, Jr., Corrêa LR, Corrêa M (2010) Diagnostic ability of a cone-beam computed tomography scan to assess longitudinal root fractures in prosthetically treated teeth. J Endod 36(11):1879-1882. https://doi.org/10.1016/j.joen.2010.08.025
43. Melo SLS, Haiter-Neto F, Correa LR, Scarfe WC, Farman AG (2013) Comparative diagnostic yield of cone beam CT reconstruction using various software programs on the detection of vertical root fractures. Dentomaxillofac Radiol 42(9):20120459. https://doi.org/10.1259/dmfr.20120459
44. Moudi E, Haghanifar S, Madani Z, Alhavaz A, Bijani A, Bagheri M (2014) Assessment of vertical root fracture using cone-beam computed tomography. Imaging Sci Dent 44(1):37-41. https://doi.org/10.5624/isd.2014.44.1.37
45. Moudi E, Haghanifar S, Madani Z, Bijani A, Nabavi ZS (2015) The effect of metal artifacts on the identification of vertical root fractures using different fields of view in cone-beam computed tomography. Imaging Sci Dent 45(3):147-151. https://doi.org/10.5624/isd.2015.45.3.147
46. Parrone MT, Bechara B, Deahl ST, 2nd, Ruparel NB, Katkar R, Noujeim M (2017) Cone beam computed tomography image optimization to detect root fractures in endodontically treated teeth: an in vitro (phantom) study. Oral Surg Oral Med Oral Pathol Oral Radiol 123(5):613-620. https://doi.org/10.1016/j.oooo.2017.01.010
47. Pinto MGO, Rabelo KA, Melo SLS, Campos PSF, Oliveira L, Bento PM, Melo DP (2017) Influence of exposure parameters on the detection of simulated root fractures in the presence of various intracanal materials. Int Endod J 50(6):586-594. https://doi.org/10.1111/iej.12655.
48. Regan Anderson M (2017) Stationary intraoral tomosynthesis imaging for vertical root fracture detection. Dissertation, University of Minnesota
49. Saati S, Eskandarloo A, Falahi A, Tapak L, Hekmat B (2019) Evaluation of the efficacy of the metal artifact reduction algorithm in the detection of a vertical root fracture in endodontically treated teeth in cone-beam computed tomography images: An in vitro study. Dent Med Probl 56(4):357-363. https://doi.org/10.17219/dmp/109902
50. Taramsari M, Kajan ZD, Bashirzadeh P, Salamat F (2013) Comparison of high-resolution and standard zoom imaging modes in cone beam computed tomography for detection of longitudinal root fracture: An in vitro study. Imaging Sci Dent 43(3):171-177. https://doi.org/10.5624/isd.2013.43.3.171
51. Uzun I, Gunduz K, Celenk P, Avsever H, Orhan K, Canitezer G, Ozmen B, Cicek E, Egrioglu E (2015) Comparing the Effect of Different Voxel Resolutions for Assessment of

Vertical Root Fracture of Permanent Teeth. Iran J Radiol 12(3):e18290. https://doi.org/10.5812/iranjradiol.18290
52. Vanderburg A (2010) In-vitro assessment of cone beam computed tomography in the detection of fractures in the vertical plane. Dissertation, University of North Carolina
53. Vieira LEM, de Lima ED, Peixoto LR, Pinto MGO, Melo SLS, Oliveira ML, Silva KR, Bento PM, de Melo DP (2020) Assessment of the Influence of Different Intracanal Materials on the Detection of Root Fracture in Birooted Teeth by Cone-beam Computed Tomography. J Endod 46(2):264-270. https://doi.org/10.1016/j.joen.2019.10.028
54. de Lima Moreno JJ, Boessio Vizzotto M, da Silveira Tiecher PF, Arús NA, Arriola-Guillén LE, Dias da Silveira HL (2022) Impact of intracanal post-material on vertical root fractures diagnosis: A high-resolution cone-beam computed tomography study. J Int Oral Health 14(1):71-77. https://doi.org/10.4103/jioh.Jioh_209_21
55. Jafarzadeh M, Ansari S, Sharifishoshtari S (2022) In vitro diagnostic accuracy of cone-beam computed tomography with variable gamma values for detection of vertical root fractures in teeth with prefabricated metal posts. Dent Res J (Isfahan) 19(7. https://doi.org/10.4103/1735-3327.336692
56. Ardakani FE, Razavi SH, Tabrizizadeh M (2015) Diagnostic value of cone-beam computed tomography and periapical radiography in detection of vertical root fracture. Iran Endod J 10(2):122-126. https://doi.org/10.22037/iej.v10i2.7410
57. da Silveira PF, Vizzotto MB, Liedke GS, da Silveira HL, Montagner F, da Silveira HE (2013) Detection of vertical root fractures by conventional radiographic examination and cone beam computed tomography - an in vitro analysis. Dent Traumatol 29(1):41-46. https://doi.org/10.1111/j.1600-9657.2012.01126.x
58. Hassan B, Metska ME, Ozok AR, van der Stelt P, Wesselink PR (2009) Detection of vertical root fractures in endodontically treated teeth by a cone beam computed tomography scan. J Endod 35(5):719-722. https://doi.org/10.1016/j.joen.2009.01.022
59. Hassan B, Metska ME, Ozok AR, van der Stelt P, Wesselink PR (2010) Comparison of Five Cone Beam Computed Tomography Systems for the Detection of Vertical Root Fractures. J Endod 36(1):126-129. https://doi.org/10.1016/j.joen.2009.09.013
60. Ozer SY (2010) Detection of vertical root fractures of different thicknesses in endodontically enlarged teeth by cone beam computed tomography versus digital radiography. J Endod 36(7):1245-1249. https://doi.org/10.1016/j.joen.2010.03.021
61. Ozer SY (2011) Detection of Vertical Root Fractures by Using Cone Beam Computed Tomography with Variable Voxel Sizes in an In Vitro Model. J Endod 37(1):75-79. https://doi.org/10.1016/j.joen.2010.04.021.
62. Cavalcanti MGP, Salineiro FC, Barros FM, Barros FBA (2022) Influence of endodontic sealers artifacts in the detection of vertical root fractures. Braz Dent J 33(1):22-30. https://doi.org/10.1590/0103-6440202204392
63. Amintavakoli N (2013) The Effect of Cone Beam CT Voxel Size on the Identification of Vertical and Horizontal Root Fractures: An In-vitro Study. Dissertation, University of Toronto
64. Bahmani A, Karkehabadi H, Shokri A, Farhadian M (2021) Performance of bioceramic-based root filling material with artifact reduction properties in the detection of vertical root fractures using cone-beam computed tomography. Open Dent. J. 15(1):170-175. https://doi.org/10.2174/1874210602115010170
65. Bezerra IS, Neves FS, Vasconcelos TV, Ambrosano GM, Freitas DQ (2015) Influence of the artefact reduction algorithm of Picasso Trio CBCT system on the diagnosis of vertical

root fractures in teeth with metal posts. Dentomaxillofac Radiol 44(6):20140428. https://doi.org/10.1259/dmfr.20140428
66. Bragatto F, Iwaki Filho L, Kasuya A, Chicarelli M, Queiroz A, Takeshita W, Iwaki L (2016) Accuracy in the diagnosis of vertical root fractures, external root resorptions, and root perforations using cone-beam computed tomography with different voxel sizes of acquisition. J Conserv Dent 19(6):573-577. https://doi.org/10.4103/0972-0707.194029.
67. Candemil AP, Mangione F, Vasconcelos KF, Oenning AC, Jacobs R, Freitas DQ, Haiter-Neto F, Salmon B, Oliveira ML (2021a) Influence of the exomass on the detection of simulated root fracture in cone-beam CT - an ex-vivo study. Dentomaxillofac Radiol 50(4):20200450. https://doi.org/10.1259/dmfr.20200450
68. Candemil AP, Salmon B, Vasconcelos KF, Oenning AC, Jacobs R, Freitas DQ, Haiter-Neto F, Mangione F, Oliveira ML (2021b) Cone beam CT optimisation for detection of vertical root fracture with metal in the field of view or the exomass. Sci Rep 11(1):19155. https://doi.org/10.1038/s41598-021-98345-6
69. de Oliveira Pinto MG, Melo SLS, Suassuna FCM, Marinho LE, Leite J, Batista AUD, Bento PM, Melo DP (2021) Influence of size of field of view (FOV), position within the FOV, and scanning mode on the detection of root fracture and observer's perception of artifacts in CBCT images. Dentomaxillofac Radiol 50(6):20200563. https://doi.org/10.1259/dmfr.20200563
70. Fisekcioglu E, Dolekoglu S, Ilguy M, Ersan N, Ilguy D (2014) In vitro detection of dental root fractures with cone beam computed tomography (CBCT). Iran J Radiol 11(1):e11485. https://doi.org/10.5812/iranjradiol.11485
71. Fontenele RC, Farias Gomes A, Nejaim Y, Freitas DQ (2020) Do the tube current and metal artifact reduction influence the diagnosis of vertical root fracture in a tooth positioned in the vicinity of a zirconium implant? A CBCT study. Clin Oral Investig 25(4):2229-2235. https://doi.org/10.1007/s00784-020-03538-4
72. Fox A, Basrani B, Lam EWN (2018) The Performance of a Zirconium-based Root Filling Material with Artifact Reduction Properties in the Detection of Artificially Induced Root Fractures Using Cone-beam Computed Tomographic Imaging. J Endod 44(5):828-833. https://doi.org/10.1016/j.joen.2018.02.007
73. Freitas DQ, Vasconcelos TV, Noujeim M (2019) Diagnosis of vertical root fracture in teeth close and distant to implant: an in vitro study to assess the influence of artifacts produced in cone beam computed tomography. Clin Oral Investig 23(3):1263-1270. https://doi.org/10.1007/s00784-018-2558-z
74. Freitas-e-Silva A, Mármora B, Barriviera M, Panzarella FK, Raitz R (2019) CBCT performance and endodontic sealer influence in the diagnosis of vertical root fractures. J Contemp Dent Pract 20(5):552-556. https://doi.org/10.5005/jp-journals-10024-2556
75. Gaeta-Araujo H, de Souza GQS, Freitas DQ, de Oliveira-Santos C (2017) Optimization of Tube Current in Cone-beam Computed Tomography for the Detection of Vertical Root Fractures with Different Intracanal Materials. J Endod 43(10):1668-1673. https://doi.org/10.1016/j.joen.2017.04.003
76. Hekmatian E, Karbasi Kheir M, Fathollahzade H, Sheikhi M (2018) Detection of Vertical Root Fractures Using Cone-Beam Computed Tomography in the Presence and Absence of Gutta-Percha. Sci World J 2018(1920946):1-6. https://doi.org/10.1155/2018/1920946
77. Hesarkhani A, Masoomi F, Mohammadi A, Jamshidifar A (2017) Study of Metal Artifacts of Different Alloys of Casting Posts in Diagnosis of Vertical Root Fracture in CBCT. Int J Adv Biotechnol Res 8(3):1971-1977

78. Junqueira RB, Verner FS, Campos CN, Devito KL, do Carmo AM (2013) Detection of vertical root fractures in the presence of intracanal metallic post: a comparison between periapical radiography and cone-beam computed tomography. J Endod 39(12):1620-1624. https://doi.org/10.1016/j.joen.2013.08.031
79. Kambungton J, Janhom A, Prapayasatok S, Pongsiriwet S (2012) Assessment of vertical root fractures using three imaging modalities: Cone beam CT, intraoral digital radiography and film. Dentomaxillofac Radiol 41(2):91-95. https://doi.org/10.1259/dmfr/49798768
80. Menezes RFd, Santos RAd, Rosa JMS, Costa VS (2013) Diagnóstico de fraturas radiculares verticais em dentes tratados endodonticamente, com ou sem a presença de núcleos metálicos fundidos, empregando-se a tomografia computadorizada cone beam. Dent Press Endod 3(2):59-63
81. Mohammadpour M, Bakhshalian N, Shahab S, Sadeghi S, Ataee M, Sarikhani S (2014) Effect of titanium and stainless steel posts in detection of vertical root fractures using NewTom VG cone beam computed tomography system. Imaging Sci Dent 44(2):89-94. https://doi.org/10.5624/isd.2014.44.2.89
82. Neves FS, Freitas DQ, Campos PSF, Ekestubbe A, Lofthag-Hansen S (2014) Evaluation of cone-beam computed tomography in the diagnosis of vertical root fractures: The influence of imaging modes and root canal materials. J Endod 40(10):1530-1536. https://doi.org/10.1016/j.joen.2014.06.012
83. Nikneshan S, Javaheri P, Hadian H (2019) Effect of artifact reduction on the diagnosis of vertical root fracture in teeth with posts using CBCT. Iran J Radiol 16(4):e85626. https://doi.org/10.5812/iranjradiol.85626
84. Patel S, Brady E, Wilson R, Brown J, Mannocci F (2013) The detection of vertical root fractures in root filled teeth with periapical radiographs and CBCT scans. Int Endod J 46(12):1140-1152. https://doi.org/10.1111/iej.12109
85. Queiroz PM, Santaella GM, Capelozza ALA, Rosalen PL, Freitas DQ, Haiter-Neto F (2018) Zoom Reconstruction Tool: Evaluation of Image Quality and Influence on the Diagnosis of Root Fracture. J Endod 44(4):621-625. https://doi.org/10.1016/j.joen.2017.10.011
86. Safi Y, Aghdasi MM, Ezoddini-Ardakani F, Beiraghi S, Vasegh Z (2015) Effect of metal artifacts on detection of vertical root fractures using two cone-beam computed tomography systems. Iran Endod J 10(3):193-198. https://doi.org/10.7508/iej.2015.03.010
87. Safi Y, Hosseinpour S, Aziz A, Bamedi M, Malekashtari M, Vasegh Z (2016) Effect of Amperage and Field of View on Detection of Vertical Root Fracture in Teeth with Intracanal Posts. Iran Endod J 11(3):202-207. https://doi.org/10.7508/iej.2016.03.011
88. Takeshita WM, Chicarelli M, Iwaki LCV (2015) Comparison of diagnostic accuracy of root perforation, external resorption and fractures using cone-beam computed tomography, panoramic radiography and conventional & digital periapical radiography. Indian J Dent Res 26(6):619-626. https://doi.org/10.4103/0970-9290.176927
89. Takeshita WM, Iwaki LCV, Da Silva MC, Sabio S, Albino PRF (2014) Comparison of periapical radiography with cone beam computed tomography in the diagnosis of vertical root fractures in teeth with metallic post. J Conserv Dent 17(3):225-229. https://doi.org/10.4103/0972-0707.131781
90. Tofangchiha M, Adel M, Tavakolian E, Ghaffari P, Jabbarian R (2017) The effect of metal artifacts reduction algorithm on diagnostic accuracy of vertical root fracture by cone beam computed tomography an in vitro study. Sch J Dent Sci 4(3):115-120. https://doi.org/10.36347/sjds.2017.v04i03.007

91. Valizadeh S, Khosravi M, Azizi Z (2011) Diagnostic accuracy of conventional, digital and Cone Beam CT in vertical root fracture detection. Iran Endod J 6(1):15-20. https://doi.org/10.22037/iej.v6i1.2025
92. Valizadeh S, Vasegh Z, Rezapanah S, Safi Y, Khaeazifard MJ (2015) Effect of object position in cone beam computed tomography field of view for detection of root fractures in teeth with intra-canal posts. Iran J Radiol 12(4):e25272. https://doi.org/10.5812/iranjradiol.25272
93. Varshosaz M, Tavakoli MA, Mostafavi M, Baghban AA (2010) Comparison of conventional radiography with cone beam computed tomography for detection of vertical root fractures: an in vitro study. J Oral Sci 52(4):593-597. https://doi.org/10.2334/josnusd.52.593
94. Wanderley VA, Freitas DQ, Haiter-Neto F, Oliveira ML (2018) Influence of Tooth Orientation on the Detection of Vertical Root Fracture in Cone-beam Computed Tomography. J Endod 44(7):1168-1172. https://doi.org/10.1016/j.joen.2018.04.006
95. Wanderley VA, Neves FS, Nascimento MCC, Monteiro GQD, Lobo NS, Oliveira ML, Neto J, Araujo LF (2017) Detection of Incomplete Root Fractures in Endodontically Treated Teeth Using Different High-resolution Cone-beam Computed Tomographic Imaging Protocols. J Endod 43(10):1720-1724. https://doi.org/10.1016/j.joen.2017.05.017
96. Yamamoto-Silva FP, Siqueira CFD, Silva M, Fonseca RB, Santos AA, Estrela C, Silva BSD (2018) Influence of voxel size on cone-beam computed tomography-based detection of vertical root fractures in the presence of intracanal metallic posts. Imaging Sci Dent 48(3):177-184. https://doi.org/10.5624/isd.2018.48.3.177
97. Yamashita FC, Yamashita AL, Romanichen IMM, Tolentino ES, Sabio S, Chicarelli M, Iwaki LCV (2021) Accuracy of cone-beam CT in detecting vertical root fractures in teeth with post-endodontic restorations: An in vitro study. Acta Sci. Health Sci. 43(https://doi.org/10.4025/actascihealthsci.v43i1.55832
98. Dalili Kajan Z, Taramsari M, Khosravi Fard N, Khaksari F, Moghasem Hamidi F (2018) The Efficacy of Metal Artifact Reduction Mode in Cone-Beam Computed Tomography Images on Diagnostic Accuracy of Root Fractures in Teeth with Intracanal Posts. Iran Endod J 13(1):47-53. https://doi.org/10.22037/iej.v13i1.17352
99. Makeeva IM, Byakova SF, Adzhieva EK, Golubeva GI, Grachev VI, Kasatkina IV (2016b) [Detection of vertical root fractures by cone beam CT]. Stomatologiia (Mosk) 95(6):9-11. https://doi.org/10.17116/stomat20169569-11
100. Shaker I, Mohamed N, Abdelsamad A (2019) Effect of applying metal artifact reduction algorithm in cone beam computed tomography in detection of vertical root fractures of teeth with metallic post versus digital intraoral radiography. Saudi Endod J 9(1):51-55. https://doi.org/10.4103/sej.sej_56_18
101. Taghiloo H, Shokri H, Esmaeili F, Taghiloo S, Dehghani AH, Rahbar M (2018) Comparison of digital diagnostic value and cone beam computed tomography (CBCT) in determining vertical root fracture in single-root teeth. Pesqui Bras Odontopediatria Clinic Integr 18(1):1-10. https://doi.org/10.4034/PBOCI.2018.181.97
102. PradeepKumar AR, Shemesh H, Nivedhitha MS, Hashir MMJ, Arockiam S, Uma Maheswari TN, Natanasabapathy V (2021) Diagnosis of Vertical Root Fractures by Cone-beam Computed Tomography in Root-filled Teeth with Confirmation by Direct Visualization: A Systematic Review and Meta-Analysis. J Endod 47(8):1198-1214. https://doi.org/10.1016/j.joen.2021.04.022
103. Rivera EM, Walton RE (2015) Longitudinal tooth cracks and fractures: an update and review. Endodontic Topics 33(1):14-42. https://doi.org/https://doi.org/10.1111/etp.12085

104. Dias DR, Iwaki LCV, de Oliveira ACA, Martinhao FS, Rossi RM, Araujo MG, Hayacibara RM (2020) Accuracy of High-resolution Small-volume Cone-Beam Computed Tomography in the Diagnosis of Vertical Root Fracture: An In Vivo Analysis. J Endod 46(8):1059-1066. https://doi.org/10.1016/j.joen.2020.04.015
105. Oliveira ML, Freitas DQ, Ambrosano GM, Haiter-Neto F (2014) Influence of exposure factors on the variability of CBCT voxel values: a phantom study. Dentomaxillofac Radiol 43(6):20140128. https://doi.org/10.1259/dmfr.20140128
106. Cohen MD (2015) ALARA, image gently and CT-induced cancer. Pediatr Radiol 45(4):465-470. https://doi.org/10.1007/s00247-014-3198-3
107. Siegel JA, Pennington CW, Sacks B (2017) Subjecting Radiologic Imaging to the Linear No-Threshold Hypothesis: A Non Sequitur of Non-Trivial Proportion. J Nucl Med 58(1):1-6. https://doi.org/10.2967/jnumed.116.180182
108. Fontenele RC, Machado AH, de Oliveira Reis L, Freitas DQ (2021) Influence of metal artefact reduction tool on the detection of vertical root fractures involving teeth with intracanal materials in cone beam computed tomography images: A systematic review and meta-analysis. Int Endod J 54(10):1769-1781. https://doi.org/10.1111/iej.13569
109. Prell D, Kyriakou Y, Beister M, Kalender WA (2009) A novel forward projection-based metal artifact reduction method for flat-detector computed tomography. Phys Med Biol 54(21):6575-6591. https://doi.org/10.1088/0031-9155/54/21/009
110. Gregoris Rabelo LE, Bueno MDR, Costa M, de Musis CR, Estrela CRA, Guedes OA, Gavini G, Estrela C (2021) Blooming artifact reduction using different cone-beam computed tomography software to analyze endodontically treated teeth with intracanal posts. Comput Biol Med 136(104679. https://doi.org/10.1016/j.compbiomed.2021.104679
111. Estrela C, Costa MVC, Bueno MR, Rabelo LEG, Decurcio DA, Silva JA, Estrela CRA (2020) Potential of a New Cone-Beam CT Software for Blooming Artifact Reduction. Braz Dent J 31(6):582-588. https://doi.org/10.1590/0103-6440202005899
112. Cohen JF, Korevaar DA, Altman DG, Bruns DE, Gatsonis CA, Hooft L, Irwig L, Levine D, Reitsma JB, de Vet HC, Bossuyt PM (2016) STARD 2015 guidelines for reporting diagnostic accuracy studies: explanation and elaboration. BMJ Open 6(11):e012799. https://doi.org/10.1136/bmjopen-2016-012799
113. Andraws Yalda F, Clarkson RJ, Davies J, Rout PGJ, Sengupta A, Horner K (2020) Does anthropomorphic model design in ex vivo studies affect diagnostic accuracy for dental root fracture using CBCT? Dentomaxillofac Radiol 49(7):20200093. https://doi.org/10.1259/dmfr.20200093

Figure legends

Figure 1. PRISMA 2020 flow diagram.

Figure 2. Summarized results of the quality assessment for the included studies.

Figure 3. Detailed results of the quality assessment according to the QUADAS-2 appraisal tool for diagnostic accuracy studies.

Figure 4. SROC plots of the meta-analyses for the overall comparison between complete and incomplete VRFs, and in root canals with no fillings, gutta-percha, and metal posts.

Figure 5. SROC plots of the meta-analyses for the comparisons between high and low spatial resolution considering different thresholds of voxel size, in root canals with no fillings, gutta-percha, and metal posts.

Figure 6. SROC plots of the meta-analyses for the comparisons between different intracanal materials, using root canal with no fillings as comparator.

Appendix 1. PRISMA-DTA checklist.

Section/topic	#	PRISMA-DTA Checklist Item	Reported on page #
TITLE / ABSTRACT			
Title	1	Identify the report as a systematic review (+/- meta-analysis) of diagnostic test accuracy (DTA) studies.	71
Abstract	2	Abstract: See PRISMA-DTA for abstracts.	72
INTRODUCTION			
Rationale	3	Describe the rationale for the review in the context of what is already known.	73-74
Clinical role of index test	D1	State the scientific and clinical background, including the intended use and clinical role of the index test, and if applicable, the rationale for minimally acceptable test accuracy (or minimum difference in accuracy for comparative design).	73-74
Objectives	4	Provide an explicit statement of question(s) being addressed in terms of participants, index test(s), and target condition(s).	74
METHODS			
Protocol and registration	5	Indicate if a review protocol exists, if and where it can be accessed (e.g., Web address), and, if available, provide registration information including registration number.	74-75
Eligibility criteria	6	Specify study characteristics (participants, setting, index test(s), reference standard(s), target condition(s), and study design) and report characteristics (e.g., years considered, language, publication status) used as criteria for eligibility, giving rationale.	75-76
Information sources	7	Describe all information sources (e.g., databases with dates of coverage, contact with study authors to identify additional studies) in the search and date last searched.	75
Search	8	Present full search strategies for all electronic databases and other sources searched, including any limits used, such that they could be repeated.	Appendix 2
Study selection	9	State the process for selecting studies (i.e., screening, eligibility, included in systematic review, and, if applicable, included in the meta-analysis).	76
Data collection process	10	Describe method of data extraction from reports (e.g., piloted forms, independently, in duplicate) and any processes for obtaining and confirming data from investigators.	77
Definitions for data extraction	11	Provide definitions used in data extraction and classifications of target condition(s), index test(s), reference standard(s) and other characteristics (e.g. study design, clinical setting).	77
Risk of bias and applicability	12	Describe methods used for assessing risk of bias in individual studies and concerns regarding the applicability to the review question.	77-78
Diagnostic accuracy measures	13	State the principal diagnostic accuracy measure(s) reported (e.g. sensitivity, specificity) and state the unit of assessment (e.g. per-patient, per-lesion).	77-79
Synthesis of results	14	Describe methods of handling data, combining results of studies and describing variability between studies. This could include, but is not limited to: a) handling of multiple definitions of target condition. b) handling of multiple thresholds of test positivity, c) handling multiple index test readers, d) handling of indeterminate test results, e) grouping and comparing tests, f) handling of different reference standards	77-79
Meta-analysis	D2	Report the statistical methods used for meta-analyses, if performed.	78-79

Additional analyses	16	Describe methods of additional analyses (e.g., sensitivity or subgroup analyses, meta-regression), if done, indicating which were pre-specified.	78-79
RESULTS			
Study selection	17	Provide numbers of studies screened, assessed for eligibility, included in the review (and included in meta-analysis, if applicable) with reasons for exclusions at each stage, ideally with a flow diagram.	79
Study characteristics	18	For each included study provide citations and present key characteristics including: a) participant characteristics (presentation, prior testing), b) clinical setting, c) study design, d) target condition definition, e) index test, f) reference standard, g) sample size, h) funding sources	80-81
Risk of bias and applicability	19	Present evaluation of risk of bias and concerns regarding applicability for each study.	83
Results of individual studies	20	For each analysis in each study (e.g. unique combination of index test, reference standard, and positivity threshold) report 2x2 data (TP, FP, FN, TN) with estimates of diagnostic accuracy and confidence intervals, ideally with a forest or receiver operator characteristic (ROC) plot.	Appendix 3
Synthesis of results	21	Describe test accuracy, including variability; if meta-analysis was done, include results and confidence intervals.	85-98
Additional analysis	23	Give results of additional analyses, if done (e.g., sensitivity or subgroup analyses, meta-regression; analysis of index test: failure rates, proportion of inconclusive results, adverse events).	85-98
DISCUSSION			
Summary of evidence	24	Summarize the main findings including the strength of evidence.	107
Limitations	25	Discuss limitations from included studies (e.g. risk of bias and concerns regarding applicability) and from the review process (e.g. incomplete retrieval of identified research).	107-108
Conclusions	26	Provide a general interpretation of the results in the context of other evidence. Discuss implications for future research and clinical practice (e.g. the intended use and clinical role of the index test).	107-108
FUNDING			
Funding	27	For the systematic review, describe the sources of funding and other support and the role of the funders.	108

From: McInnes MDF, Moher D, Thombs BD et al. Preferred Reporting Items for a Systematic Review and Meta-analysis of Diagnostic Test Accuracy Studies: The PRISMA-DTA Statement. JAMA. 2018;319(4):388-396. DOI: 10.1001/jama.2017.19163]

Appendix 2. Database search strategy.

Database	Search
PUBMED	("cone-beam computed tomography"[MeSH Terms] OR "cone beam" OR "cone-beam" OR "cbct" OR "volume computed tomography" OR "volumetric ct" OR "volumetric computed tomography" OR "volume ct" OR "imaging examinations" OR "imaging examination" OR "imaging modalities" OR "imaging modality" OR "diagnostic imaging"[MeSH Terms] OR "diagnostic imaging" OR "imaging modes" OR "imaging mode") AND ("tooth fractures"[MeSH Terms] OR "tooth fractures" OR "tooth fracture" OR "teeth fractures" OR "teeth fracture" OR "root fractures" OR "root fracture" OR "dental fracture" OR "dental fractures" OR "cracked tooth" OR "cracked tooth syndrome"[MeSH Terms] OR "cracked tooth syndrome" OR "cracked teeth" OR "dental cracks")
EMBASE	('cone beam' OR 'cone-beam' OR 'cbct' OR 'volume computed tomography'/exp OR 'volume computed tomography' OR 'volumetric ct'/exp OR 'volumetric ct' OR 'volumetric computed tomography'/exp OR 'volumetric computed tomography' OR 'volume ct'/exp OR 'volume ct' OR 'imaging examinations' OR 'imaging examination' OR 'imaging modalities' OR 'imaging modality' OR 'diagnostic imaging'/exp OR 'diagnostic imaging' OR 'imaging modes' OR 'imaging mode') AND ('tooth fractures'/exp OR 'tooth fractures' OR 'tooth fracture'/exp OR 'tooth fracture' OR 'teeth fractures' OR 'teeth fracture' OR 'root fractures' OR 'root fracture'/exp OR 'root fracture' OR 'dental fracture'/exp OR 'dental fracture' OR 'dental fractures' OR 'cracked tooth' OR 'cracked tooth syndrome'/exp OR 'cracked tooth syndrome' OR 'cracked teeth' OR 'dental cracks')
SCOPUS	(TITLE-ABS-KEY("cone beam" OR "cone-beam" OR "cbct" OR "volume computed tomography" OR "volumetric ct" OR "volumetric computed tomography" OR "volume ct" OR "imaging examinations" OR "imaging examination" OR "imaging modalities" OR "imaging modality" OR "diagnostic imaging" OR "imaging modes" OR "imaging mode") AND ALL ("tooth fractures" OR "tooth fracture" OR "teeth fractures" OR "teeth fracture" OR "root fractures" OR "root fracture" OR "dental fracture" OR "dental fractures" OR "cracked tooth" OR "cracked tooth syndrome" OR "cracked teeth" OR "dental cracks"))
WEB OF SCIENCE	(“cone beam” OR “cone-beam” OR “cbct” OR “volume computed tomography” OR “volumetric ct” OR “volumetric computed tomography” OR “volume ct” OR “imaging examinations” OR “imaging examination” OR “imaging modalities” OR “imaging modality” OR “diagnostic imaging” OR “imaging modes” OR “imaging mode”) AND (“tooth fractures” OR “tooth fracture” OR “teeth fractures” OR “teeth fracture” OR “root fractures” OR “root fracture” OR “dental fracture” OR “dental fractures” OR “cracked tooth” OR “cracked tooth syndrome” OR “cracked teeth” OR “dental cracks”)
LILACS	(tw:("cone beam" OR "cone-beam" OR "feixe cônico" OR "feixe-cônico" OR "haz cónico" OR "haz-cónico" OR "cbct" OR "tcfc" OR "tchc" OR "volume computed tomography" OR "volumetric computed tomography" OR "tomografia computadorizada volumétrica" OR "volumetric ct" OR "volume ct" OR "tac volumétrico" OR "tac volumétrica" OR "tc volumétrica" OR "tc volumétrico" OR "imaging examinations" OR "imaging examination" OR "imaging modalities" OR "imaging modality" OR "diagnostic imaging" OR "diagnóstico por imagem" OR "imageamento" OR "imageologia" OR "imagiologia" OR "radiodiagnóstico" OR "Imagen Clínica" OR "imaging modes" OR "imaging mode" OR "modo de imagem" OR "modos de imagem" OR "modos de imagens" OR "modo de imagens" OR "modo de imagen" OR "modos de imagen" OR "modo de imágenes")) AND (tw:("tooth fractures" OR "tooth fracture" OR "teeth fractures" OR "teeth fracture" OR "dental fracture" OR "dental fractures" OR "fratura dental" OR "fratura dentária" OR "fraturas dentárias" OR "fraturas dos dentes" OR "fraturas de dentes" OR "fratura de dente" OR "fracturas de los dientes" OR "fractura dental" OR

	"fracturas dentales" OR "fractura de diente" OR "root fractures" OR "root fracture" OR "fratura radicular" OR "fraturas radiculares" OR "fratura da raiz" OR "fraturas das raízes" OR "fractura de raíz" OR "fractura de raíces" OR "fractura radicular" OR "fracturas radiculares" OR "cracked tooth" OR "cracked tooth syndrome" OR "cracked teeth" OR "dente quebrado" OR "síndrome de dente quebrado" OR "síndrome de diente fisurado" OR "dente trincado" OR "dente fissurado" OR "dente gretado" OR "diente roto" OR "diente quebrado"))
PROQUEST DISSERTATIONS & THESES	NOFT (“cone beam” OR “cone-beam” OR “cbct” OR “volume computed tomography” OR “volumetric ct” OR “volumetric computed tomography” OR “volume ct” OR “imaging examinations” OR “imaging examination” OR “imaging modalities” OR “imaging modality” OR “diagnostic imaging” OR “imaging modes” OR “imaging mode”) AND (“tooth fractures” OR “tooth fracture” OR “teeth fractures” OR “teeth fracture” OR “root fractures” OR “root fracture” OR “dental fracture” OR “dental fractures” OR “cracked tooth” OR “cracked tooth syndrome” OR “cracked teeth” OR “dental cracks”)
OPEN GREY	(“cone beam” OR “cone-beam” OR “cbct” OR “volume computed tomography” OR “volumetric ct” OR “volumetric computed tomography” OR “volume ct” OR “imaging examinations” OR “imaging examination” OR “imaging modalities” OR “imaging modality” OR “diagnostic imaging” OR “imaging modes” OR “imaging mode”) AND (“tooth fractures” OR “tooth fracture” OR “teeth fractures” OR “teeth fracture” OR “root fractures” OR “root fracture” OR “dental fracture” OR “dental fractures” OR “cracked tooth” OR “cracked tooth syndrome” OR “cracked teeth” OR “dental cracks”)
GOOGLE SCHOLAR	("cbct" OR "cone beam" OR "cone-beam") AND ("root fracture" OR "root fractures" OR "tooth fracture" OR "teeth fracture" OR "tooth fractures" OR "teeth fractures" OR "dental fracture" OR "dental fractures" OR "cracked teeth" OR "cracked tooth")

Appendix 3 - Summary of descriptive characteristics of included studies (n=82).

Author, Year;	Sample size/tooth type	Method of VRF induction	Type of fracture	Groups and subgroups	CBCT device	Acquisition parameters	Application of filters/ algorithms	Root canal conditions	Simulation of in vivo conditions	Findings		Main conclusions
										Sens	Spec	
Abdinian et al 2016 Iran	120 mandibular teeth (60 premolars 60 molars)	hammer and pin	Unclear	According to the root canal conditions (n=40): A) no filling B) root canal filling (gutta-percha and sealer) C) root canal filling + metal post + cement	Cranex 3D (SoredexOy, Tuusula, Finland)	89 kV, 6 mA FOV: 8x4 cm Voxel size: 0.2mm	None	A) no filling B) root canal filling (gutta-percha and sealer) C) root canal filling + metal post + cement	Dry human mandible	A1) 1.00 A2) 0.80 A3)0.70	A1) 0.90 A2) 0.60 A3) 0.65	No significant difference between CBCT and a set of three DPRs with different angulations for VRF detection in posterior teeth.
Al Hadi et al 2020 United Arab Emirates	60 single-rooted teeth (lower premolars)	hammer and nail; UTM	Complete and incomplete (varied sample)	According to the root canal conditions (n=45): A) no filling B) root canal filling (gutta-percha and sealer)	CS 9000 3D (Carestream Dental, Rochester, NY)	60 kVp 5 mA FOV: 3.7x5 cm Voxel size: 0.076mm	None	A) no filling B) root canal filling (gutta-percha and sealer)	None.	A) 1.00 B) 0.933	A) 1.00 B) 1.00	CBCT presented higher sensitivity in detection of VRFs in comparison with periapical radiographs.
Amintavakoli , 2013 Canada	30 teeth (incisors, premolars, and molars)	bench vise	Incomplete	According to the voxel size: A) 0.076-mm B) 0.1 mm C) 0.2 mm D) 0.3 mm	Kodak 9000 3D (Kodak Dental Systems, Carestream Health, Rochester, NY, EUA)	65 kVp 2.5 mA FOV: NR Voxel size: A) 0.076mm B) 0.1 mm C) 0.2 mm D) 0.3 mm	None	no filling	Gypsum stone blocks	A) 0.64 B) 0.667 C) 0.613 D) 0.507	A) 0.706 B) 0.76 C) 0.706 D) 0.746	The 0.1-mm voxel size may be the most optimal for this task balancing image noise and contrast.
Ardakani et al 2015 Iran	80 single-rooted teeth	Hammer and chisel	Incomplete	None.	Promax 3D (Planmeca, Helsinki, Finland)	66 kVp 8 mA FOV: 8x8 cm Voxel: NR	None.	no filling	Dry human mandible and skull	0.975	0.95	The accuracy of CBCT in detection of vertical root fracture are higher than periapical radiography.

Bahmani et al. 2021 Iran	100 mandibular premolars	UTM	Unclear	According to the root filling material: A) gutta-percha + sealer B) bioceramic root filling material	Cranex 3D (SoredexOy, Tuusula, Finland)	90 kVp 10 mA FOV: 6x8 cm Voxel size: 0.2mm	None	A) gutta-percha + sealer B) bioceramic root filling material	Acrylic blocks	A) 0.84 B) 0.93	A) 0.78 B) 0.95	The accuracy of CBCT in detection of vertical root fracture was higher with the bioceramic root filling material.
BashizadehFakhar et al. 2021 Iran	60 single-rooted teeth	Hammer and pin	Unclear	According to the acquisition parameter (kilovoltage): A) 80 kVp B) 92 kVp	Promax 3D (Planmeca, Helsinki, Finland)	A) 80 kVp B) 92 kVp 4 mA FOV: 5,5x10 cm Voxel size: 0.15mm	None	Root canal filling (gutta-percha + sealer) and metal post	Bovine rib sockets	A) 0.86 B) 0.6	A) 0.333 B) 0.3	The tube voltage of 80 kVp were more efficient in the diagnosis VRF.
Bechara et al. 2013a United States	66 single-rooted teeth	Hammer and pin	Complete	According to the CBCT device: A) Promax Planmeca B) Picasso Master 3D	A) Promax 3D (Planmeca, Helsinki, Finland) B) Picasso Master 3D (EWOO technology, Republic of Korea)	kVp: NR mA: NR FOV: A) 8x8 cm B) 16x7 cm Voxel size: 0.2mm	None.	Root canal filling (gutta-percha)	Bovine rib sockets	A) 0.81 B) 0.61	A) 0.78 B) 0.61	CBCT small FOVs presented the most favorable results.
Bechara et al. 2013b United States	66 single-rooted teeth	Hammer and pin	Complete	According to the CBCT device: A) Promax Planmeca B) Picasso Master 3D According to the imaging mode: 1) original images 2) MAR algorithm	A) Promax 3D (Planmeca, Helsinki, Finland) B) Picasso Master 3D (EWOO technology, Republic of Korea)	kVp: NR mA: NR FOV: A) 8x8 cm B) 16x7 cm Voxel size: 0.2mm	A) Promax Planmeca MAR algorithm B) Picasso Master 3D MAR algorithm	Root canal filling (gutta-percha)	Bovine rib sockets	* A1) 0.80 A2) 0.71 B1) 0.61 B2) 0.51	* A1) 0.78 A2) 0.59 B1) 0.61 B2) 0.54	MAR decreased the accuracy of RF detection in endodontically treated teeth.
Bechara et al. 2013c United States	66 single-rooted teeth	Hammer and pin	Complete	According to the scan mode: A) 180° B) 360°	Accuitomo 3D (J. Morita, Kyoto, Japan)	76 kVp 6 mA FOV: 6x6 cm Voxel size: 0.125mm	None.	Root canal filling (gutta-percha)	Bovine rib sockets	* A) 0.7 B) 0.65	* A) 0.6 B) 0.74	Only the specificity is improved by the 360° scan.

Bezerra et al. 2015 Brazil	30 single rooted teeth	UTM	Complete and incomplete	According to the type of fracture: A) Complete B) Incomplete According to the imaging mode: 1) original images 2) ARA	Picasso Trio 3D imaging system (Vatech, Hwaseong, Republic of Korea)	90 kVp 5 mA FOV: 8x5 cm Voxel size: 0.2mm	Picasso Trio MAR algorithm	metal post	Dry human mandible	A1) 0.483 A2) 0.483 B1) 0.450 B2) 0.383	A1) 0.583 A2) 0.433 B1) 0.583 B2) 0.433	ARA had a negative impact on the diagnosis
Brady et al. 2014 United Kingdom	30 mandibular teeth 14 premolars 16 molars	UTM	Complete and Incomplete	According to the type of fracture: A) Complete VRF B) Incomplete VRF According to the CBCT device: 1) 3D Accuitomo 2) i-CAT	1) Accuitomo 3D (J. Morita, Kyoto, Japan) 2) i-CAT Next Generation (Imaging Sciences International, Hatfield, PA)	1) 90 kV 3 mA FOV: 4x4 cm Voxel size: 0.08mm 2) 120 KV 5 mA FOV: 16x4 cm Voxel size: 0.125-mm	None	no filling	Dry human mandible	A1) 0.98 A2) 0.98 B1) 0.27 B2) 0.28	A1) 1.00 A2) 0.99 B1) 0.99 B2) 1.00	The detection of complete fractures was significantly higher for all systems than that of incomplete fractures.
Bragatto et al. 2016 Brazil	20 teeth (premolars)	UTM	Unclear	According to the voxel size: A) 0.125 mm B) 0.2 mm C) 0.25 mm D) 0.3 mm E) 0.4 mm	i-CAT (Imaging Sciences International, Hatfield, PA)	120 kVp FOV: 8x8 cm A) 37.07 mA B) 37.07 mA C) 37.07 mA D) 18.54 mA E) 18.54 mA Voxel size: A) 0.125 mm B) 0.2 mm C) 0.25 mm D) 0.3 mm E) 0.4 mm	None..	no filling	Dry human mandible	A) 1.0 B) 1.0 C) 1.0 D) 0.97 E) 0.97	A) 1.0 B) 1.0 C) 0.9 D) 0.5 E) 0.27	Voxel size 0.125 mm produced images with the best resolution. Voxel sizes of 0.3 and 0.4 should be avoided.
Byakova et al. 2019 Russia	50 single-rooted teeth	hammer and pin	**Complete and Incomplete	According to the fracture width: A) Incomplete B) Complete	Accuitomo 3D (J. Morita, Kyoto, Japan)	90 kVp 4-5 mA FOV: 8x8mm Voxel size: 0.16mm	None	metal post	Acrylic blocks	A) 0.27 B) 0.53	A) 0.56 B) 0.62	Fracture width affected the in vitro detectability. The detectability in vivo was decreased because of low image quality.

Caetano et al. 2020 Brazil	45 single-rooted teeth	**UTM	**Complete and incomplete (varied sample)	According to the root canal conditions: A) no filling B) root canal filling (gutta-percha + sealer) C) root canal filling + metal post According to the CBCT device: 1) Prexion 3D 2) OP300 3) 9000 3D According to the imaging mode and software: a) original images, In Vivo Dental b) AR filter, e-Vol DX	1) Prexion 3D (Yoshida Dental, Tokyo. Japan) 2) OP300 Maxio (Instrumentarim Dental, Tuusula, Finland) 3) Kodak 9000 3D (Kodak Dental Systems, Carestream Health, Rochester, NY, EUA)	1) 90 kVp 4 mA FOV: 5.1x5.1 cm Voxel size: 0.1mm 2) 90 kVp 10 mA FOV: 6x4 cm Voxel size: 0.085mm 3) 70 kVp 10 mA FOV: 5x3.7 cm Voxel size: 0.076mm	Blooming Artifact Reduction filter (BAR), e-Vol DX	A) no filling B) root canal filling (gutta-percha + sealer) C) root canal filling + metal post	Dry human mandible	* a) A1) 1.00 A2) 0.80 A3) 0.67 B1) 0.96 B2) 0.83 B3) 0.40 C1) 0.93 C2) 0.80 C3) 0.73 b) A1) 1.00 A2) 0.76 A3) 0.63 B1) 1.00 B2) 0.93 B3) 0.63 C1) 0.93 C2) 0.86 C3) 0.63	* a) A1) 0.93 A2) 0.90 A3) 0.63 B1) 1.00 B2) 0.86 B3) 0.70 C1) 0.93 C2) 0.96 C3) 0.60 b) A1) 0.83 A2) 0.80 A3) 0.90 B1) 0.90 B2) 0.90 B3) 0.70 C1) 0.83 C2) 0.93 C3) 0.93	The PreXion 3D device is the most accurate when detecting VRF.
Candemil et al. 2020 Brazil	20 single-rooted teeth	UTM	**Complete	According to the CBCT unit: A) CS 9300 B) ProMax C) NewTom According to the presence of metallic objects in the exomass or endomass: 1) None. 2) one object in the exomass 3) two objects in the exomass 4) one object in the exomass and one in the endomass 5) one object in the endomass	A) CS 9300 (Carestream Dental, Rochester, NY) B) Promax 3D (Planmeca, Helsinki, Finland) C) NewTom VG (Quantitative Radiology, Verona, Italy)	A) 90 kVp 100 mA FOV: 5x5 Voxel size: 0.09mm B) 90 kVp 96 mA FOV: 4.5x4.5 Voxel size:0.1mm C) 90 kVp 44.8 mA FOV: 6x7 cm Voxel size: 0.08mm	None	fiberglass post	Dry human mandible	*média A1) 0.9 A2) 0.915* A3) 0.9* A4) 0.915* A5) 0.94* B1) 0.98 B2) 0.965* B3) 0.965* B4) 0.925* B5) 0.9* C1) 0.95 C2) 0.975* C3) 0.95* C4) 0.915* C5) 0.88*	*média A1) 0.93 A2) 0.955* A3) 0.95* A4) 0.88* A5) 0.89* B1) 0.95 B2) 1.00* B3) 0.95* B4) 0.9* B5) 0.865* C1) 0.9 C2) 0.89* C3) 0.98* C4) 0.89* C5) 0.925*	Exomass-related metal artefacts did not influence the diagnosis of simulated VRF in CBCT.

Candemil et al., 2021 Brazil	20 single-rooted teeth	UTM	**Complete	According to the presence of metallic objects in the exomass or endomass: A) one object in the exomass B) two objects in the exomass C) one object in the exomass and one in the endomass D) one object in the endomass According to the acquisiton parameters: 1) 90 kVp, 100 mA 2) 70 kVp, 24 mA	CS 9000 3D (Carestream Dental, Rochester, NY)	1) 90 kVp, 100 mA 2) 70 kVp, 24 mA FOV: 5x5 cm Voxel size: 0.09mm	None	fiberglass post	Dry human mandible	A1) 0.90** A2) 0.77** B1) 0.88** B2) 0.74** C1) 0.84** C2) 0.71** D1) 0.89** D2) 0.64**	A1) 0.96** A2) 0.82** B1) 0.96** B2) 0. 85** C1) 0.90** C2) 0.83** D1) 0.91** D2) 0.90**	The 70 kVp/24 mA presented higher accuracy regardless of the number of metallic objects in the exomass and endomass.
da Silveira et al 2013 Brazil	60 single-rooted teeth	hammer and chisel	Incomplete	According to the root canal conditions: A) no filling B) root canal filling (gutta-percha and sealer) C) root canal filling + metal post + cement According to the voxel size: 1) 0.2 mm 2) 0.3 mm 3) 0.4 mm	i-CAT (Imaging Sciences International, Hatfield, PA)	120 kVp 3-8 mA FOV: 8x8 cm Voxel size: 1) 0.2 mm 2) 0.3 mm 3) 0.4 mm	None.	A) no filling B) root canal filling (gutta-percha and sealer) C) root canal filling + metal post + cement		A1) 0.97 A2) 0.87 A3) 0.76 B1) 0.97 B2) 0.67 B3) 0.6 C1) 0.83 C2) 0.63 C3) 0.57	A1) 1.00 A2) 0.97 A3) 0.8 B1) 0.93 B2) 0.74 B3) 0.7 C1) 0.8 C2) 0.91 C3) 0.59	0.2-voxel presented higher accuracy for teeth with filling and/or a post.

Dalili Kajan et al 2018 Iran	60 single-rooted teeth (premolars)	post turned with a wrench	Incomplete	According to the root canal conditions: A) root canal filling (gutta-percha and sealer) B) root canal filling + metal post + cement According to the imaging mode: algorithm: 1) original images 2) MAR algorithm	Pax-i3D (Orangedental, Biberach an der Riss, Germany)	95 kVp 6 mA FOV: 9x12 cm Voxel size: 0.2mm	Pax-i3D MAR algorithm	A) root canal filling (gutta-percha and sealer) B) root canal filling + metal post + cement	Gypsum stone blocks	A1) 0.4667 A2) 0.8667 B1) 0.4667 B2) 0.6667	A1) 0.5333 A2) 0.4 B1) 0.6667 B2) 0.6667	There were no significant differences between the efficacies of imaging modes.
De Martin e Silva et al. 2018 Brazil	40 single-rooted teeh	Hammer and chisel	**Complete	According to the root canal conditions: A) root canal filling (gutta-percha + sealer) B) root canal filling + metal post According to the voxel sizes: a) 0.25 mm b) 0.3 mm According to the optimization filters: 1) original images 2) Sharpen filter 3) Hard filter	i-CAT (Imaging Sciences International, Hatfield, PA)	120 kVp 5 mA FOV: 6x23 cm Voxel size: NR	Sharpen; Hard; i-CAT Vision software	A) root canal filling (gutta-percha + sealer) B) root canal filling + metal post	Dry human mandible	NR	NR	The presence of a metal post and the voxel size significantly interfere with the diagnosis of VRF. Despite the formation of metal artifacts associated with metallic cores, applying filters did not improve the diagnosis.
De Menezes et al 2016 Brazil	48 single-rooted teeth	Hammer and pin	**Incomplete	According to the root canal conditions: A) no filling B) gutta-percha C) metal post	Prexion (Yoshida Dental, Tokyo. Japan)	90 kV 4 mA FOV: 5x5 cm Voxel size:0.1mm	None.	A) no filling B) gutta-percha C) metal post	Dry human mandible	* A) 0.9166 B) 0.6666 C) 0.7083	* A) 0.8333 B) 0.8333 C) 0.3333	The presence of posts and gutta-percha reduced the sensitivity and the accuracy in detecting the VRF.

De Rezende Barbosa et al., 2016 Brazil	44 single-rooted teeth	Hammer and pin	Complete	According to the imaging mode: A) original images B) MAR algorithm According to the root canal condition: 1) no filling 2) gutta-percha 3) metal post 4) fiberglass post	Picasso Trio (Vatech, Hwaseong, Republic of Korea)	80 kVp 4 mA **FOV: 12x7 cm Voxel size: 0.2mm	MAR algorithm (EasyDent4, E-WOO, Giheung-gu, Republic of Korea)	1) no filling 2) gutta-percha 3) metal post 4) fiber post	Dry human mandible	A1) 0.89 A2) 0.69 A3) 0.54 A4) 0.83 B1) 0.83 B2) 0.60 B3) 0.52 B4) 0.92	A1) 0.87 A2) 0.86 A3) 0.75 A4) 0.84 B1) 0.84 B2) 0.84 B3) 0.84 B4) 0.83	ARA did not influence the diagnosis of root fractures; gold posts reduced the overall CBCT diagnostic ability
Ferreira et al. 2013 Brazil	60 bi-rooted teeth (maxillary premolars)	Hammer and pin	Incomplete	According to the root canal conditions: A) root canal filling (gutta-percha and sealer) + fiber post B) root canal filling + metal post According to the CBCT unit: 1) i-CAT 2) Scanora 3D	1) i-CAT (Imaging Sciences International, Hatfield, PA) 2) Scanora 3D (Soredex, Tuusula, Finland)	1) 120 kVp 36.12 mA FOV: 6x8 cm Voxel size: 0.125mm 2) 85 kVp 8 mA FOV: 6x6 cm Voxel size: 0.133mm	None.	A) root canal filling (gutta-percha and sealer) + fiber post B) root canal filling + metal post	Acrylic blocks	A1) 0.85 A2) 0.73 B1) 0.72 B2) 0.73	A1) 0.74 A2) 0.71 B1) 0.75 B2) 0.76	The diagnostic performance for detecting vertical fractures was higher for roots with fiber-resin than with titanium posts.
Ferreira et al. 2015 Brazil	40 single-rooted teeth	UTM	Unclear	According to the imaging mode (application of filters): A) original images B) sharpen filter C) Sharpen mild filter D) sharpen 3x3 filter E) S9 filter F) smooth filter G) smooth 3x3 filter According to the root canal conditions: 1) no filling 2) metal post	i-CAT (Imaging Sciences International, Hatfield, PA)	kV:NR mA: NR FOV: 8x8 cm Voxel size:0.2mm	A) original images B) sharpen filter C) Sharpen mild filter D) sharpen 3x3 filter E) S9 filter F) smooth filter G) smooth 3x3 filter	1) no filling 2) metal post	Dry human mandible	A1) 0.5 A2) 0.2 B1) 0.48 B2) 0.32 C1) 0.75 C2) 0.28 D1) 0.60 D2) 0.45 E1) 0.55 E2) 0.13 F1) 0.48 F2) 0.18 G1) 0.64 G2) 0.20	A1) 0.85 A2) 0.87 B1) 0.58 B2) 0.62 C1) 0.63 C2) 0.90 D1) 0.70 D2) 0.65 E1) 0.78 E2) 0.98 F1) 0.88 F2) 0.80 G1) 0.70 G2) 0.93	The use of enhancement filters in CBCT images has no influence on the diagnosis of VRFs in teeth with metal posts

Fisekcioglu et al. 2014 Turkey	104 teeth (mixed)	UTM	Complete	None.	ILUMA Ultra (IMTEC Imaging, USA)	120 kVp 3.8 mA FOV: 21.1x14.2 cm Voxel size:0.3mm	None.	no filling	Dry human mandible	0.838*	0.996*	Detailed information about root fractures may be obtained using CBCT.
Fontenele et al. 2020 Brazil	30 single-rooted teeth (mandibular premolars)	UTM	**Incomplete	According to the tube current: A) 4 mA B) 8 mA C) 10 mA According to the imaging mode: 1) original images 2) MAR algorithm According to the presence of an adjacent implant: a) absent b) present	OP300 Maxio (Instrumentarium Dental, Tuusula, Finland)	90kVp mA: A) 4 mA B) 8 mA C) 10 mA FOV: 5x5 cm Voxel size: 0.08mm	OP300 MAR algorithm a) original images b) MAR algorithm	no filling	Dry human mandible	a) A1) 0.613 A2) 0.560 B1) 0.500 B2) 0.680 C1) 0.560 C2) 0.560 b) A1) 0.600 A2) 0.613 B1) 0.627 B2) 0.600 C1) 0.550 C2) 0.654	a) A1) 0.653 A2) 0.653 B1) 0.686 B2) 0.746 C1) 0.773 C2) 0.800 b) A1) 0.573 A2) 0.591 B1) 0.706 B2) 0.627 C1) 0.586 C2) 0.520	The zirconium implants impair the diagnosis of VRF in adjacent teeth. Neither the tube current nor the MAR tool is effective in improving the diagnosis of VRF.
Fox et al. 2018 Canada	176 mandibular premolars	UTM	**Complete and incomplete (varied sample)	According to the root canal conditions: A) gutta-percha + sealer B) zirconium-based cone + sealer	CS 9000 3D (Carestream Dental, Rochester, NY)	70 kVp 3.2 mA FOV:5x3.7 cm Voxel size: 0.076mm	None.	A) gutta-percha + sealer B) zirconium-based cone + sealer	Dry human mandible	A) 0.4659 B) 0.5833	A) 0.8485 B) 0.7386	The Zr group improved the sensitivity of the detection of artificially induced VRFs.

Freitas et al 2019 Brazil	20 single-rooted teeth	UTM	Incomplete	Implant adjacent and MAR algorithm: A) without implant and MAR B) with implant and without MAR C) with implant and MAR According to the kilovoltage: 1) 70 kVp 2) 80 kVp 3) 90 kVp	Promax 3D (Planmeca, Helsinki, Finland)	1) 70 kVp 2) 80 kVp 3) 90 kVp 10 mA FOV: 8x5 cm Voxel size: 0.15mm	ProMax 3D MAR tool	no filling	Dry human mandible	A1) 0.564 A2) 0.558 A3) 0.495 B1) 0.614 B2) 0.577 B3) 0.558 C1) 0.577 C2) 0.545 C3) 0.501	A1) 0.737 A2) 0.815 A3) 0.896 B1) 0.658 B2) 0.707 B3) 0.777 C1) 0.676 C2) 0.832 C3) 0.839	Artifacts produced in the vicinity of teeth with suspected VRF impaired the diagnosis by decreasing the specificity, which was improved using MAR.
Freitas-e-Silva et al. 2019 Brazil	80 single-rooted premolars	UTM	**Complete and incomplete (varied sample)	According to the CBCT unit: A) i-CAT B) Orthophos XG C) Prexion 3D	A) i-CAT (Imaging Sciences International, Hatfield, PA) B) Orthophos XG (Sirona, Bensheim, Germany) C)Prexion 3D (Yoshida Dental, Tokyo. Japan)	A) 120 kV 5 mA FOV: 6x6 cm Voxel size: 0.2mm B) 85 kV 6 mA FOV: 5x5 cm Voxel size: 0.16mm C) 90 kV 4 mA FOV: 5x5 cm Voxel size: 0.075mm	None.	gutta-percha	Acrylic blocks	A) 0.93 B) 0.73 C) 0.88	1) 0.70 2) 0.73 3) 0.75	Endodontic sealers did not influence the detection of VRF. The PreXion device was the most accurate, having the highest specificity value.

Gaêta-Araujo et al. 2017 Brazil	20 single-rooted teeth	UTM	**Complete	According to: Intracanal material: A) no filling B) gutta-percha C) metal post D) fiberglass post According to the tube current: 1) 4 mA 2) 8 mA 3) 10 mA 4) 13 mA	OP300 Maxio (Instrumentarium Dental, Tuusula, Finland)	90 kVp 1) 4 mA 2) 8 mA 3) 10 mA 4) 13 mA FOV: 4x6 cm Voxel size: 0.085mm	None.	A) no filling B) gutta-percha C) metal post D) fiberglass post	Dry human mandible	A1) 0.59 A2) 0.69 A3) 0.62 A4) 0.64 B1) 0.54 B2) 0.60 B3) 0.66 B4) 0.54 C1) 0.47 C2) 0.46 C3) 0.50 C4) 0.43 D1) 0.68 D2) 0.70 D3) 0.56 D4) 0.60	A1) 0.72 A2) 0.80 A3) 0.84 A4) 0.82 B1) 0.60 B2) 0.67 B3) 0.60 B4) 0.62 C1) 0.50 C2) 0.72 C3) 0.80 C4) 0.66 D1) 0.68 D2) 0.70 D3) 0.82 D4) 0.80	For teeth with gutta-percha and metal post, an increased milliampere may lead to increased diagnostic performance of VRF.
Gaêta-Araujo et al. 2020 Brazil	10 single-rooted teeth (mandibular premolars)	UTM	**Incomplete	According to the presence of metal posts in adjacent teeth: a) None. b) one adjacent tooth c) both adjacent teeth According to the tube current: A) 4 mA B) 8 mA C) 10 mA According to the imaging mode: 1) original images 2) MAR algorithm	OP300 Maxio (Instrumentarium Dental, Tuusula, Finland)	90 kVp FOV: 5x5 cm Voxel size: 0.125mm A) 4 mA B) 8 mA C) 10 mA	OP300 MAR algorithm	No filling	Dry human mandible	a) A1) 0.76 A2) 0.70 B1) 0.66 B2) 0.75 C1) 0.56 C2) 0.72 b) A1) 0.62 A2) 0.66 B1) 0.64 B2) 0.64 C1) 0.66 C2) 0.64 c) A1) 0.44 A2) 0.64 B1) 0.62 B2) 0.44 C1) 0.54 C2) 0.54	a) A1) 0.40 A2) 0.32 B1) 0.38 B2) 0.48 C1) 0.50 C2) 0.42 b) A1) 0.32 A2) 0.36 B1) 0.38 B2) 0.52 C1) 0.52 C2) 0.54 c) A1) 0.34 A2) 0.48 B1) 0.64 B2) 0.52 C1) 0.54 C2) 0.58	The presence of both adjacent teeth restored with a metal post impairs VRF detection; however, an increase in tube current up to 8 mA may aid in this diagnostic task. Moreover, the MAR tool does not seem to be efficient in those cases.

Gunduz et al. 2013 Turkey	90 single-rooted teeth	Hammer and pin	Unclear	According to the CBCT device: A) NewTom 3G B) 3D Accuitomo 170	A) NewTom 3G (Quantitative Radiology, Verona, Italy) B) Accuitomo 3D (J. Morita, Kyoto, Japan)	A) 65 kVp 2 mA FOV: 4x4 cm Voxel size: 0.125mm B) 110 kVp Automated adjusted mA FOV: 15x15 cm Voxel size: 0.16mm	None.	no filling	Dry human mandible	NR	NR	The 3D Accuitomo 170 was significantly superior to the NewTom 3G images in the detection of VRFs.
Hassan et al. 2009 Netherlands	80 teeth (40 premolars 40 molars)	Hammer and chisel	**Complete	According to the evaluators: A) Endodontists B) Dental students C) Overall	i-CAT (Imaging Sciences International, Hatfield, PA)	120 KvP 5 mA FOV: 10x16 cm Voxel size: 0.25mm	None.	No filling and gutta-percha filled canals (mixed sample)	Dry human mandible	A) 0.775 B) 0.813 C) 0.794 1) 0.80 2) 0.788	A) 0.913 B) 0.938 C) 0.925 1) 0.975 2) 0.875	The results showed an overall higher accuracy for CBCT scans than PRs for detecting VRF.
Hassan et al. 2010 Netherlands	80 teeth (40 premolars 40 molars)	Hammer and chisel	**Complete	According to the CBCT device: A) NewTom 3G B) i-CAT C) Galileos 3D D) Scanora 3D E) AccuiTomo-XYZ	A) NewTom 3G (Quantitative Radiology, Verona, Italy) B) i-CAT (Imaging Sciences International, Hatfield, PA) C) Galileos 3D (Sirona Bensheim, Germany) D) Scanora 3D (Soredex, Tuusula, Finland) E) AccuiTomo-XYZ (J. Morita, Kyoto, Japan)	A) 110 kVp 2.4 mA FOV: 10x10 cm Voxel size: 0.2mm B) 120 kVp 5 mA FOV: 10x16 cm Voxel size: 0.25mm C) 85 kVp 7 mA FOV: 15x15 cm Voxel size: 0.3mm D) 85 kVp 10 mA FOV: 7.5x10 cm Voxel size: 0.2mm E) 80 kVp	None.	No filling and gutta-percha filled canals (mixed sample)	Dry human mandible.	A) 0.304 B) 0.775 C) 0.188 D) 0.575 E) 0.481	A) 0.95 B) 0.913 C) 0.85 D) 0.85 E) 0.907	Root canal filling presence reduced specificity in all systems.

						3.3 mA FOV: 3x4 cm Voxel size: 0.25mm						
Hekmatian et al. 2018 Iran	50 teeth (mandibular premolars)	UTM	Unclear	According to the root canal filling: A) no filling B) gutta-percha	Galileos 3D (Sirona Bensheim, Germany)	85 kVp 13 mA, Voxel size: NR FOV: 5x5.5 cm	None.	A) no filling B) gutta-percha	Dry human mandible	A) 0.72 B) 0.36*	A) 0.96 B) 0.68	The intracanal filling materials such as gutta-percha reduce the diagnostic ability of the vertical root fractures.
Hesarkhani et al. 2017 Iran	30 single-rooted teeth	UTM	Unclear	According to the root canal conditions: A) root canal filling B) metal post	NR	NR	None.	A) root canal filling B) metal post	NR	A) 0.533 B) 0.215*	A) 0.533 B) 0.217*	The presence of intra-canal posts from any of the alloys used in the study significantly reduces the rate and diagnostic sensitivity of the CBCT.
Junqueira et al. 2013 Brazil	18 single-rooted teeth	Hammer and chisel	Complete	According to the root canal conditions: A) apical filling (gutta-percha + sealer) B) apical filling + metal post According to the voxel sizes: 1) 0.25 mm 2) 0.125 mm	i-CAT (Imaging Sciences International, Hatfield, PA)	120 kVp 8 mA FOV: 5x5 cm Voxel sizes: 1) 0.25 mm 2) 0.125 mm	None.	A) apical filling (gutta-percha + sealer) B) apical filling + metal post	Dry human mandible	A1) 0.78 A2) 1 B1) 0.67 B2) 0.89	A1) 0.89 A2) 0.89 B1) 0.56 B2) 0.45	Voxel size did not significantly influence the diagnosis of vertical root fractures.

Kambungton et al. 2012 Thailand	60 single-rooted teeth	UTM	Unclear	None.	Veraviewepocs 3D (J. Morita, Kyoto, Japan)	70 kVp 3 mA Voxel size: NR FOV: NR	None.	no filling	Dry human mandible	NR	NR	There was no significant difference between intraoral film, a high-resolution complementary metal oxide semiconductor digital imaging system and CBCT in detecting VRFs.
Kamburoglu et al. 2010 Turkey	60 teeth (mandibular premolars)	Hammer and pin	**Incomplete	According to the CBCT device, and acquisition parameter (voxel size): A) NewTom 3G B) Iluma Ultra Cone-Beam, 0.3-mm voxel C) Iluma Ultra Cone-Beam, 0.1-mm voxel	A) NewTom 3G (Quantitative Radiology, Verona, Italy) B) ILUMA Ultra (IMTEC Imaging, USA)	A) 110 kVp FOV: 15x15 cm Voxel size: 0.19mm B) 120 kVp 3.8 mA FOV: 21x14 cm. Voxel size: 0.3mm C) 120 kVp 3.8 mA FOV: 21x14 cm Voxel size: 0.1mm	None.	Root canal filling (gutta-percha and sealer) at the apical root third.	Dry human mandible	NR	NR	Both ultra-resolution Iluma and NewTom 3G images performed better than low-resolution Iluma
Khedmat et al. 2012 Iran	100 single-rooted teeth	Hammer and pin	Unclear	According to the root canal conditions: A) no filling B) gutta-percha	Promax 3D (Planmeca, Helsinki, Finland)	70 kVp 4 mA FOV: 8x8 cm Voxel size: 0.16mm	None.	A) no filling B) gutta-percha	None.	A) 0.92 B) 0.8	A) 0.88 B) 0.64	The presence of gutta-percha reduced the accuracy, sensitivity and specificity of CBCT.

Makeeva et al. 2016a Russia	25 single-rooted teeth	Post screwed into the root canal	**Complete and incomplete	According to the type of fracture: A) Complete B) Incomplete	Accuitomo 3D (J. Morita, Kyoto, Japan)	80 kVp 4 mA FOV: 4x4 cm Voxel size: 0.16mm	None.	no filling	None.	A) 0.96 B) 0.32	A) 0.96 B) 0.96	The sensitivity for VRFs with a width > 150 µm is reliably higher than for visualizing VRFs < 150 µm. The specificity is not significantly different.
Makeeva et al. 2016b Russia	**45 single rooted-teeth	Hammer and pin	**Complete and incomplete	According to the type of fracture: A) Complete B) Incomplete	Accuitomo 3D (J. Morita, Kyoto, Japan)	80 kVp 4 mA FOV: 8x8 cm Voxel size: 0.16mm	None.	root canal filling	None.	A) 1 B) 0.54	A) 0.92 B) 0.93	The detectability of VRFs by CBCT was dependent upon fracture width.
Mehralizadeh et al. 2018 Iran	80 single-rooted teeth (premolars)	Hammer and pin	Unclear	According to the acquisition parameters (mA and kVp) A) 60 kVp, 6 mA B) 86 kVp, 6 mA C) 60 kVp, 10 mA D) 86 kVp, 10 mA	Rotograph Evo 3D (Villa Sistemi Medicali. Buccinasco, Italy	A) 60 kVp, 6 mA B) 86 kVp, 6 mA C) 60 kVp, 10 mA D) 86 kVp, 10 mA Voxel size: NR FOV: NR	None.	Root canal filling (gutta-percha and sealer)	Dry human mandible	NR	NR	kVp min/mA max and kVp min/mA min settings are suitable for the diagnosis of VRFs
Melo et al. 2010 Brazil	180 single-rooted teeth	Hammer and pin	**Complete	According to the root canal condition: A) no filling B) gutta-percha C) metal post According to the acquisition parameter (voxel size): 1) 0.3 mm 2) 0.2 mm	i-CAT (Imaging Sciences International, Hatfield, PA)	120 kVp 3–8 mA FOV: 8x8 cm Voxel sizes: 1) 0.3 mm 2) 0.2 mm	None.	A) no filling B) gutta-percha C) metal post	Dry human skull	A1) 0.53 A2) 0.83 B1) 0.47 B2) 0.93 C1) 0.53 C2) 0.70	A1) 0.80 A2) 0.87 B1) 0.70 B2) 0.73 C1) 0.63 C2) 0.66	The CBCT diagnostic ability was not influenced by the presence of posts or gutta-percha, and the 0.3-mm voxel resolution was not reliable for the investigation of VRFs.

Melo et al. 2013 Brazil	180 single-rooted teeth	Hammer and pin	**Complete	According to the root canal condition: A) no filling B) gutta-percha C) metal post According to the DICOM viewer software: 1) Dolphin v. 11.5 2) InVivoDental v. 5.0 3) KDIS3D v. 2.1.11 4) Xoran	i-CAT (Imaging Sciences International, Hatfield, PA)	120 kVp 8 mA FOV: 8x8 cm Voxel size: 0.2mm	None.	A) no filling B) gutta-percha C) metal post	Dry human skull	A1) 0.71 A2) 0.65 A3) 0.71 A4) 0.73 B1) 0.68 B2) 0.61 B3) 0.63 B4) 0.61 C1) 0.43 C2) 0.41 C3) 0.44 C4) 0.41	A1) 0.88 A2) 0.87 A3) 0.85 A4) 0.79 B1) 0.81 B2) 0.91 B3) 0.78 B4) 0.91 C1) 0.87 C2) 0.91 C3) 0.91 C4) 0.92	The diagnosis of VRF does not depend on the software used to reconstruct the image from CBCT. The diagnostic accuracy is significantly reduced for all software when root canals are restored with metallic posts.
Menezes et al. 2013 Brazil	48 single-rooted teeth	UTM	**Incomplete	According to the root canal conditions: A) no filling B) root canal filling (gutta-percha + sealer) C) metal post	Prexion 3D (Yoshida Dental, Tokyo. Japan)	90kV 4mA FOV: 5x5 cm Voxel size: 0.1mm	None.	A) no filling B) root canal filling (gutta-percha + sealer) C) metal post	Dry human mandible.	A) 0.875 B) 0.625 C) 0.75	A) 0.75 B) 0.875 C) 0.375	CBCT is an excellent tool for the VRF diagnosis. The metal post presence resulted in a high percentage of false positive.
Mohammadpour et al. 2014 Iran	80 single-rooted teeth	UTM	Unclear	According to the root canal conditions: A) no filling B) metal post According to the evaluators: 1) radiologists 2) endodontists 3) overall	NewTom VG (Quantitative Radiology, Verona, Italy)	110 kVp 13.8 mA FOV: 8x12 cm Voxel size: 0.15mm	None.	A) no filling B) metal post	Acrylic blocks	A1) 0.9392 A2) 0.8704 A3) 0.9418 B1) 0.8125* B2) 0.925* B3) 0.8625*	A1) 0.8779 A2) 0.6886 A3) 0.8707 B1) 0.725* B2) 0.725* B3) 0.725*	Intracanal posts significantly decreased the VRF diagnostic values of CBCT.

Moudi et al. 2014 Iran	96 teeth (mandibular premolars and molars)	Hammer and pin	Unclear	According to the root canal conditions: A) no filling B) gutta-percha C) gutta-percha + metal post	NewTom 5G (Quantitative Radiology, Verona, Italy)	110 kVp mA: NR FOV: NR Voxel size: 0.3mm	None.	A) no filling B) gutta-percha C) gutta-percha + metal post	None.	A) 0.88 B) 0.94 C) 0.81	A) 1.0 B) 1.0 C) 1.0	The CBCT scans revealed a high accuracy in the diagnosis of vertical root fractures; the accuracy did not decrease in the presence of gutta-percha.
Moudi et al. 2015 Iran	40 teeth (mandibular premolars and molars)	Hammer and pin	Unclear	According to the root canal conditions: A) gutta-percha B) metal post According to the FOV: 1) 18x16 cm 2) 6x6 cm	NewTom 5G (Quantitative Radiology, Verona, Italy)	110 kV 9.6 mA FOV: 1) 18x16 cm 2) 6x6 cm Voxel size: 0.3mm	None.	A) gutta-percha B) metal post	None.	A1) 0.86 A2) 1,0 B1) 1,0 B2) 0.95	A1) 1,0 A2) 1,0 B1) 0.89 B2) 1,0	The specificity of CBCT decreased with the presence of a pin in the large-FOV group, but not in the small-FOV group.
Nascimento et al. 2014 Brazil	40 teeth (molars)	UTM	Incomplete	According to the optimization filters: A) original images B) sharpen mild C) sharpen super mild D) s9 E) sharpen F) sharpen 3x3 G) angio sharpen medium 5x5 H) angio sharpen high 5x5 I) shadow 3x3	i-CAT (Imaging Sciences International, Hatfield, PA)	120 kVp 8 mA FOV: 8x8 cm Voxel size: 0.2mm	Sharpen Mild, Sharpen Super Mild, S9, Sharpen, Sharpen 3x3, Angio Sharpen Medium 5x5, Angio Sharpen High 5x5, and Shadow 3x3; XoranCAT software	no filling	Dry human mandible	A) 0.568 B) 0.722 C) 0.683 D) 0.788 E) 0.763 F) 0.73 G) 0.696 H) 0.789 I) 0.659	A) 0.583 B) 0.682 C) 0.692 D) 0.702 E) 0.738 F) 0.698 G) 0.765 H) 0.762 I) 0.667	No statistical differences were observed in the diagnosis of VRF when using filters.

Neves et al. 2014 Brazil	30 single-rooted teeth	UTM	a) Complete b) Incomplete	According to the root canal conditions: A) no filling B) gutta-percha C) fiber post D) metal post According to the imaging mode: 1) high-fidelity 2) high-resolution 3) high-speed 4) standard According to the type of fracture: a) Complete b) Incomplete	Accuitomo 3D (J. Morita, Kyoto, Japan)	90 kV 5 mA FOV: 4x4 cm Voxel size: 0.08mm	None.	A) no filling B) gutta-percha C) fiber post D) metal post	Dry human mandible	** a) A1) 0.92 A2) 0.92 A3) 0.86 A4) 0.84 B1) 0.74 B2) 0.82 B3) 0.74 B4) 0.70 C1) 0.88 C2) 0.82 C3) 0.86 C4) 0.86 D1) 0.50 D2) 0.50 D3) 0.54 D4) 0.50 b) A1) 0.76 A2) 0.74 A3) 0.52 A4) 0.76 B1) 0.38 B2) 0.34 B3) 0.36 B4) 0.26 C1) 0.60 C2) 0.56 C3) 0.58 C4) 0.48 D1) 0.28 D2) 0.36 D3) 0.36 D4) 0.36	** a) A1) 0.90 A2) 0.92 A3) 0.86 A4) 0.84 B1) 0.76 B2) 0.72 B3) 0.66 B4) 0.66 C1) 0.84 C2) 0.90 C3) 0.88 C4) 0.78 D1) 0.58 D2) 0.62 D3) 0.58 D4) 0.68 b) A1) 0.90 A2) 0.92 A3) 0.86 A4) 0.84 B1) 0.76 B2) 0.72 B3) 0.66 B4) 0.66 C1) 0.84 C2) 0.90 C3) 0.87 C4) 0.78 D1) 0.58 D2) 0.62 D3) 0.58 D4) 0.68	The CBCT imaging modes had little influence in the diagnosis of complete and incomplete VRFs, whereas the presence of intracanal material had greater impact on the diagnostic ability.
Nikbin et al. 2018 Iran	60 single-rooted teeth (premolars)	Pin and screwdriver	Incomplete	According to the root canal conditions (n=60): A) gutta-percha B) gutta-percha + metal post According to the imaging mode, and specimen positioning (n=60): 1) original images, central position	Promax 3D (Planmeca, Helsinki, Finland)	**Kilovoltage and milliamperage determined automatically. FOV: 5x8 cm Voxel size: 0.16mm	Planmeca MAR algorithm	A) gutta-percha B) gutta-percha + metal post	Bovine rib sockets	* A1) 0.578 A2) 0.5773 A3) 0.7107 A4) 0.689 B1) 0.5777 B2) 0.3777 B3) 0.5333	* A1) 0.822 A2) 0.822 A3) 0.8443 A4) 0.8 B1) 0.622 B2) 0.6887 B3) 0.6443 B4) 0.7107	Diagnostic accuracy was higher with central positioning than with peripheral positioning, irrespective of whether the MAR algorithm was applied.

				2) original images, peripheral position 3) MAR algorithm, central position 4) MAR algorithm, peripheral position						B4) 0.333		
Nikneshan et al. 2019 Iran	62 teeth (premolars)	UTM	Incomplete	According to the imaging mode (n=62): A) original images B) MAR algorithm	Promax 3D (Planmeca, Helsinki, Finland)	74 kVp 12 mA FOV: 8x8 cm Voxel size: 0.15mm	mild artifact reduction algorithm (Promax3d)	Root canal filling (gutta-percha and sealer) + metal post	Gypsum stone blocks	A) 0.742 B) 0.7206	A) 0.8816 B) 0.8176	The artifact reduction option creates no CBCT diagnostic difference in the presence of a post and does not provide better diagnosis of VRFs.
Oliveira et al. 2021 Brazil	45 single-rooted teeth (premolars)	UTM	**Complete and incomplete (varied sample)	According to the root canal conditions: A) no filling B) gutta-percha C) metal post According to the imaging mode: 1) original images 2) MAR algorithm	OP300 Maxio (Instrumentarium Dental, Tuusula, Finland)	90 kVp 10 mA FOV: 6x4 cm Voxel size: 0.085mm	OP300 MAR tool	A) no filling B) gutta-percha C) metal post	Dry human mandible	A1) 0.67 A2) 0.63 B1) 0.77 B2) 0.6 C1) 0.83 C2) 0.67	A1) 0.87 A2) 0.8 B1) 0.67 B2) 0.77 C1) 0.53 C2) 0.23	The OP 300 MAR tool negatively influenced the detection of VRFs in teeth with no root canal filling, gutta-percha, or metallic posts.
Özer, 2010 Turkey	80 teeth (28 incisors, 28 premolars, 24 molars)	Hammer and chisel	Complete	According to the fracture thickness: A) 0.2 mm B) 0.4 mm C) <0.2 mm	i-CAT (Imaging Sciences International, Hatfield, PA)	120 kVp 3 mA FOV: 4x4 cm Voxel size: 0.125mm	None	No filling	Dry human mandible	NR	NR	CBCT scans are effective for detecting VRFs of different thicknesses.

Özer, 2011 Turkey	**60 single-rooted teeth (incisors, premolars and molars)	hammer and chisel	Complete	According to the voxel size: A) 0.4 mm B) 0.3 mm C) 0.2 mm D) 0.125 mm	i-CAT (Imaging Sciences International, Hatfield, PA)	120 kVp 5 mA FOV: 4x4 cm Voxel size: A) 0.4 mm B) 0.3 mm C) 0.2 mm D) 0.125 mm	None.	No filling	Dry human mandible	A) 0.91 B) 0.93 C) 0.97 D) 0.98	A) 0.93 B) 0.93 C) 0.96 D) 0.96	CBCT scans were reliable in detecting simulated VRF, and a 0.2-mm voxel was the best protocol, considering the lower x-ray exposure and good diagnostic performance.
Parrone et al. 2017 United States	40 single-rooted teeth	Hammer and pin	Complete	According to the voxel size: A) 0.075 mm B) 0.1 mm According to the imaging mode: 1) original images 2) optimization filter AINO	Promax 3D (Planmeca, Helsinki, Finland)	90 kV 10 mA FOV: 4x4 cm Voxel sizes: A) 0.075 mm B) 0.1 mm	AINO (Adaptive Image Noise Optimiser) mode.	Root canal filling (gutta-percha)	Bovine rib sockets	A1) 0.97 A2) 0.96 B1) 1 B2) 0.95	A1) 0.83 A2) 0.85 B1) 0.88 B2) 0.91	The voxel size of 0.1 mm mode without filter is recommended for VRF detection in endodontically treated teeth.
Patel et al. 2013 United Kingdom	28 teeth (14 premolars and 14 molars)	UTM	Complete and incomplete	According to the type of fracture: A) Complete (n=40) B) Incomplete (n=27) C) overall (n=47)	Accuitomo 3D (J. Morita, Kyoto, Japan)	90 kVp 3 mA FOV: NR Voxel size: 0.16mm	None.	Gutta-percha	Dry human mandible	A) 0.688 B) 0.533 C) 0.573	A) 0.367 B) 0.367 C) 0.343	The imaging artefacts caused by the gutta-percha root filling within the root canal most probably resulted in the overestimation of VRF with CBCT

Pinto et al. 2017 Brazil	160 single-rooted teeth	Hammer and pin	**Complete and incomplete (mixed)	According to the root canal conditions (n=40): A) no filling B) gutta-percha C) fiber post D) metal post According to the acquisition parameters (electric voltage and tube current) (n=40): 1) 74 kV/12 mA 2) 74 kV/10 mA 3) 74 kV/8 mA 4) 74 kV/6.3 mA 5) 70 kV/12 mA 6) 70 kV/10 mA 7) 70 kV/8 mA 8) 70 kV/6.3 mA	Kodak 9000 3D (Kodak Dental Systems, Carestream Health, Rochester, NY, EUA)	1) 74 kV 12 mA 2) 74 kV 10 mA 3) 74 kV 8 mA 4) 74 kV 6.3 mA 5) 70 kV 12 mA 6) 70 kV 10 mA 7) 70 kV 8 mA 8) 70 kV 6.3 mA FOV: 5x3.75 cm Voxel size: 0.1mm	None.	According to the root canal conditions: A) no filling B) gutta-percha C) fiber post D) metal post	Dry human skull	A1) 73.55 A2) 76.50 A3) 76.50 A4) 76.50 A5) 76.50 A6) 76.50 A7) 79.45 A8) 76.50 B1) 70.60 B2) 70.60 B3) 61.75 B4) 64.70 B5) 70.60 B6) 61.75 B7) 55.85 B8) 58.80 C1) 76.50 C2) 79.45 C3) 79.45 C4) 76.50 C5) 79.45 C6) 76.50 C7) 79.45 C8) 73.55 D1) 58.80 D2) 58.80	A1) 87.00 A2) 87.00 A3) 89.15 A4) 91.35 A5) 89.15 A6) 89.15 A7) 89.15 A8) 89.15 B1) 91.30 B2) 84.80 B3) 87.00 B4) 84.80 B5) 87.00 B6) 89.15 B7) 91.30 B8) 89.15 C1) 87.00 C2) 89.15 C3) 86.95 C4) 89.15 C5) 89.15 C6) 89.15 C7) 84.80 C8) 87.00 D1) 82.65 D2) 87.00	The variations in exposure parameters did not interfere with the diagnosis of VRF, independent of the root canal condition. Metallic posts influenced the diagnostic performance.

										D3) 58.80 D4) 52.90 D5) 61.75 D6) 61.75 D7) 58.80 D8) 58.80 Overall**: A) 0.765 B) 0.6433 C) 0.7761 D) 0.5880	D3) 84.80 D4) 84.80 D5) 87.00 D6) 87.00 D7) 87.00 D8) 78.30 Overall**: A) 0.8889 B) 0.8806 C) 0.8779 D) 0.8482	
Pinto et al. 2021 Brazil	40 single-rooted teeth	UTM	**Complete and incomplete (varied sample)	According to the acquisition parameters (mA, FOV): A) 7 mA, 8x8 cm B) 5 mA, 8x8 cm C) 7 mA, 5x5.5 cm D) 5 mA, 5x5.5 cm According to the specimen position: 1) central 2) peripheral	Orthophos XG (Sirona, Bensheim, Germany)	85 kVp mA: NR FOV: NR Voxel size: 0.16mm	None.	root canal filling + metal post	Dry human skull.	* A1) 0.55 A2) 0.4 B1) 0.575 B2) 0.425 C1) 0.725 C2) 0.625 D1) 0.75 D2) 0.65	* A1) 0.65 A2) 0.6 B1) 0.7 B2) 0.7 C1) 0.775 C2) 0.65 D1) 0.775 D2) 0.65	Positioning the object in the center or closer to the anterior periphery of the FOV while using a small FOV improved the detection of VRF and decreased artifact perception.
Queiroz et al. 2018 Brazil	21 single-rooted teeth	UTM	Incomplete	According to the root canal condition (n=21): A) no filling B) gutta-percha According to the acquisition parameters (FOV and voxel size)(n=21): 1) 4x4-cm FOV, 0.08-mm voxel	Accuitomo 3D (J. Morita, Kyoto, Japan)	80 kVp 6 mA FOV: NR Voxel size: NR	None.	A) no filling B) gutta-percha	Dry human mandible	NR	NR	The Zoom Reconstruction tool allows better accuracy for VRF detection in filled teeth, comparable to the high-resolution protocol.

				2) 10x10-cm FOV, 0.2-mm voxel 3) zoom reconstruction tool, 4x4-cm FOV, 0.08-mm voxel								
Regan Anderson, 2017 United States	60 single-rooted teeth (premolars)	Hammer and pin	Unclear	According to the root canal condition: A) no filling B) gutta-percha	CS 9000 3D (Carestream Dental, Rochester, NY)	68 kVp 2 mA FOV: NR Voxel size: 0.076mm	None.	A) no filling B) gutta-percha	Gypsum stone blocks	A) 0.947 B) 0.853	A) 0.853 B) 0.773	Limited-FOV CBCT is the most sensitive imaging modality for detection of VRFs among obturated and unobturated root samples.
Saati et al. 2019 Iran	70 single-rooted teeth	Hammer and pin	Unclear	According to the CBCT device: A) NewTom 3G B) ProMax 3D C) Cranex 3D According to the imaging mode: 1) original images 2) MATLAB artifact removal software 3) MAR algorithm	A) NewTom 3G (Quantitative Radiology, Verona, Italy) B) Promax 3D (Planmeca, Helsinki, Finland) C) Cranex 3D (SoredexOy, Tuusula, Finland)	A) 90 kVp 10.65 mA FOV: 15x15 cm B) 84 kVp 14 mA FOV: 8x8 cm C) 110 kVp 4 mA FOV: 6x8 cm Voxel size: NR	1) None 2) MATLAB artifact removal software 3) ProMax 3D and Cranex 3D MAR algorithm	Root canal filling (gutta-percha)	Bovine rib sockets	A1) 0.65 A2) 0.77 B1) 0.48 B2) 0.71 B3) 0.57 C1) 0.68 C2) 0.85 C3) 0.82	A1) 0.65 A2) 0.71 B1) 0.51 B2) 0.62 B3) 0.60 C1) 0.68 C2) 0.80 C3) 0.70	The MATLAB artifact removal software can enhance the detection of VRFs on CBCT scans to some extent.
Safi et al. 2015 Iran	80 single-rooted teeth (premolars)	UTM	**Complete and incomplete (varied sample)	According to the CBCT device (n=80): A) NewTom VGI B) Scanora 3D	A) NewTom VG (Quantitative Radiology, Verona, Italy) B) Scanora 3D (Soredex, Tuusula, Finland)	90-110 kVp 12.5 mA FOV: A) 12x8 cm B) 10x7.5 cm Voxel size: 0.2mm	None.	Root canal filling (gutta-percha and sealer) + metal post (NiCr)	Acrylic blocks.	A) 0.638 B) 0.527	A) 0.6706 B) 0.475	The effect of metal artifacts on VRF detection was not significantly different between the two CBCT systems.

Safi et al. 2016 Iran	80 single-rooted teeth (premolars)	UTM	Incomplete	According to the acquisition parameters (FOV and tube current)(n=80): A) 10×7.5 mm FOV, 13 mA B) 13×14.5 mm FOV, 4 mA C) 13×14.5 mm FOV, 13 mA	Scanora 3D (Soredex, Tuusula, Finland)	90 kVp A) FOV: 10×7.5 mm 13 mA B) FOV: 13×14.5 mm 4 mA C) FOV: 13×14.5 mm 13 mA Voxel size: 0.25mm	None.	Root canal filling (gutta-percha and sealer) + metal post (NiCr)	Wax model	A) 0.7775 B) 0.6790 C) 0.7140	A) 0.313 B) 0.667 C) 0.278	A smaller FOV and lower mA should be preferably used for detection of VRFs in teeth with intracanal posts.
Shaker et al. 2019 Egypt	120 single-rooted teeth	Rotation of a large post	Unclear	According to the application of MAR algorithm (n=120): A) original images B) SMAR mode (Scanora 3D)	Scanora 3D (Soredex, Tuusula, Finland)	90 kVp 10 mA FOV: 5x5 cm Voxel size: 0.085mm	SMAR artifact algorithm, Scanora 3D	Root canal filling (gutta-percha + sealer) + metal post	None.	A) 0.65 B) 0.55	A) 0.867 B) 1	In the presence of metallic posts, CBCT with metal artifact reduction algorithm can improve detection of VRF.
Taglihoo et al. 2018 Iran	50 single-rooted teeth	Unclear	Unclear	According to the CBCT view: A) axial B) cross-sectional	NewTom 5G (Quantitative Radiology, Verona, Italy)	NR	None.	no filling	Gypsum stone blocks	A) 0.32 B) 0.2	A) 1 B) 1	The sensitivity, specificity, and accuracy of digital radiography and CBCT were not significantly different.
Takeshita et al. 2014 Brazil	20 teeth	UTM	Unclear	According to the root canal conditions: A) gutta-percha B) gutta-percha + metal post	i-CAT (Imaging Sciences International, Hatfield, PA)	kVp: NR mA: NR FOV; 6X6 cm Voxel size: 0.125mm	None.	A) gutta-percha B) gutta-percha + metal post	Dry human mandible	NR	NR	CBCT was more accurate than conventional periapical radiography in detecting VRF.
Takeshita et al. 2015 Brazil	20 teeth (premolars)	UTM	Unclear	None.	i-CAT (Imaging Sciences International, Hatfield, PA)	120 kVp mA: NR FOV: 6x6 cm Voxel size: 0.125mm	None.	No filling	Dry human mandible	NR	NR	CBCT showed the best results in the diagnosis of VRF.

Taramsari et al. 2013 Iran	78 single-rooted teeth (premolars)	Hammer and pin	**Complete and incomplete (varied sample)	According to the root canal conditions: A) gutta-percha B) gutta-percha + fiber post C) gutta-percha + metal post According to the imaging mode: 1) high-resolution 2) standard	NewTom 5G (Quantitative Radiology, Verona, Italy)	A) 110 kVp 3.07 mA FOV: 15x15 cm Voxel size: 0.125-0.150 mm B) 110 kVp 2.05 mA FOV: 10x10 cm Voxel size: 0.2-0.24 mm	None.	A) gutta-percha B) gutta-percha + fiber post C) gutta-percha + metal post	Macerated bone artificial sockets	A1) 0.8661 A2) 0.6923 B1) 0.6923 B2) 0.4615 C1) 0.6153 C2) 0.6153	A1) 0.2307 A2) 0.3076 B1) 0.5384 B2) 0.3076 C1) 0.6153 C2) 0.50	There were no significant differences between the diagnostic values of the two imaging modes used in the diagnosis of VRF or in the presence of root canal restorations.
Tofangchiha et al. 2017 Iran	80 single-rooted teeth	UTM	Complete	According to the imaging mode: A) original images B) MAR mode	Promax 3D (Planmeca, Helsinki, Finland)	66kVp 8 mA FOV: 8x8 cm Voxel size: NR	Promax 3D MAR mode	Metal post	Acrylic blocks	A) 0.54 B) 0.57	A) 0.61 B) 0.69	The sensitivity and specificity and accuracy of CBCT with or without using the metal artifact reduction algorithms were similar.
Uysal et al. 2020 Turkey	83 single-rooted teeth (premolars)	Hammer and pin	Complete	According to the voxel size: A) 0.125 mm B) 0.2 mm C) 0.25 mm D) 0.3 mm E) 0.4 mm According to the imaging mode: 1) original images 2) MAR	i-CAT (Imaging Sciences International, Hatfield, PA)	120 kV 5 mA FOV: 8x8 cm Voxel sizes: A) 0.125 mm B) 0.2 mm C) 0.25 mm D) 0.3 mm E) 0.4 mm	i-CAT AR mode	Root canal filling (gutta-percha + sealer)	Bovine rib sockets	* A1) 0.9445 A2) 0.9445 B1) 0.917 B2) 0.917 C1) 0.917 C2) 0.917 D1) 0.722 D2) 0.693 E1) 0.583 E2) 0.583	* A1) 0.968 A2) 0.968 B1) 0.915 B2) 0.957 C1) 0.957 C2) 0.957 D1) 0.979 D2) 0.979 E1) 1 E2) 1	High-resolution CBCT images resulted in an increase in sensitivity and specificity for detection of VRFs. The use of MAR did not further improve its diagnostic potential.

Uzun et al. 2015 Turkey	74 single-rooted teeth (mandibular premolars)	Hammer and pin	Unclear	According to the CBCT device, and FOV: A) 3D Accuitomo 170,4x4-cm FOV B) 3D Accuitomo 170, 6x6-cm FOV C) NewTom 3G, 15x15-cm FOV D) NewTom 3G, 22x22-cm FOV	1) Accuitomo 3D (J. Morita, Kyoto, Japan) 2) NewTom 3G (Quantitative Radiology, Verona, Italy)	65 kVp 2 mA FOV: A)4X4cm B)6x6cm C)15x15cm D)22x22cm Voxel sizes: A) 0.08mm B) 0.125mm C) 0.16mm D) 0.25mm	None.	Root canal filling (gutta-percha + sealer)	Dry human mandible	NR	NR	No significant differences were found among observers or voxel sizes, with high Az results reported for all groups.
Valizadeh et al. 2011 Iran	120 single-rooted teeth	UTM	Unclear	None.	New Tom 3G (Quantitative Radiology, Verona, Italy)	110 kVp 1.9 mA FOV: 23x23 cm Voxel size: 0.3mm	None.	Metal post	Acrylic blocks.	* 0.883	* 0.933	CBCT provided favorable results regarding the diagnosis of VRF in teeth with metal posts.
Valizadeh et al. 2015 Iran	**60 single-rooted teeth (premolars)	UTM	**Complete and incomplete (varied sample)	According to the specimen position A) central B) 3 o'clock C) 6 o'clock D) 9 o'clock E) 12 o'clock	New Tom VG (Quantitative Radiology, Verona, Italy)	110 kVp Automatically adjusted mA FOV: 15x15 cm Voxel size: 0.2mm	None.	Root canal filling (gutta-percha + sealer) + metal post	Acrylic blocks.	A) 0.334 B) 0.282 C) 0.375 D) 0.384 E) 0.367	A) 0.651 B) 0.634 C) 0.547 D) 0.534 E) 0.5	The central position is suitable for detection of VRF in teeth with intra-canal posts due to significantly higher sensitivity at this position
Vanderburg, 2010 United States	50 posterior teeth	Hammer and pin	Unclear	None.	Galileos Comfort (Sirona Bensheim, Germany)	85 kVp 42 mA FOV: NR Voxel size: 0.15mm	None.	no filling	Dry human skulls.	0.6	0.49	Periapical radiographs are more accurate than the Sirona Galileos Comfort CBCT scanner for the detection of vertical root fractures.

Varshosaz et al. 2010 Iran	100 single-rooted teeth	UTM	Incomplete	None.	Promax 3D (Planmeca, Helsinki, Finland)	70 kVp 6 mA FOV: 8x8 cm Voxel size: 0.16mm	None.	No filling	Dry human mandible	NR	NR	CBCT was shown to be significantly better than conventional periapical radiography for diagnosis of VRF.
Vieira et al. 2020 Brazil	20 birooted teeth (maxillary first premolars)	Hammer and pin	**Complete and incomplete (varied sample)	According to the conditions (lingual + buccal root canals): A) no filling B) gutta-percha + gutta-percha C) gutta-percha + fiber post D) gutta-percha + metal core E) fiber post + fiber post F) metal core + metal core G) metal post + metal post According to the CBCT device: 1) CS9000 3D 2) OP300	1) CS 9000 3D (Carestream Dental, Rochester, NY) 2) OP300 Maxio (Instrumentarium Dental, Tuusula, Finland)	1) 90 kVp 8 mA FOV: 5x3.75 cm Voxel size: 0.076mm 2) 90 kVp 8 mA FOV: 5x5 cm Voxel size: 0.085mm	None.	A) no filling B) gutta-percha + gutta-percha C) gutta-percha + fiber post D) gutta-percha + metal core E) fiber post + fiber post F) metal core + metal core G) metal post + metal post	Dry human skull	A1) 0.80 A2) 0.95 B1) 0.55 B2) 0.65 C1) 0.80 C2) 0.90 D1) 0.85 D2) 0.85 E1) 0.85 E2) 0.90 F1) 0.80 F2) 0.75 G1) 0.85 G2) 1	A1) 0.95 A2) 1 B1) 0.90 B2) 0.80 C1) 0.95 C2) 0.85 D1) 0.95 D2) 0.60 E1) 0.90 E2) 0.95 F1) 0.95 F2) 0.90 G1) 0.70 G2) 0.30	CS 9000 3D presented better performance than OP300 on VRF detection of endodontically treated teeth.
Wanderley et al. 2017 Brazil	20 single-rooted teeth	UTM	Incomplete	According to the acquisition mode: A) high resolution/standard (512 basis images) B) high resolution/high density (1024 basis images)	Prexion 3D (Yoshida Dental, Tokyo. Japan)	90 kVp 4 mA FOV: 5x5 cm Voxel size: 0.1mm	None.	Root canal filling (gutta-percha + sealer)	Dry human mandible	A) 0.97 B) 0.97	A) 0.83 B) 0.90	Both high-resolution imaging protocols presented high accuracy in the detection of incomplete VRFs of endodontically teeth.

Wanderley et al. 2018 Brazil	30 single-rooted teeth	UTM	**Incomplete	According to the root canal conditions: A) no filling B) gutta-percha C) metal post According to the tooth orientation: 1) perpendicular to the horizontal plane 2) parallel to the horizontal plane	Picasso Trio 3D imaging system (Vatech, Hwaseong, Republic of Korea)	85 kVp 5 mA FOV: 5x5 cm Voxel size: 0.2mm	None.	A) no filling B) gutta-percha C) metal post	Dry human mandible	A1) 0.76 A2) 0.787 B1) 0.56 B2) 0.554 C1) 0.5 C2) 0.554	A1) 0.947 A2) 0.893 B1) 0.693 B2) 0.592 C1) 0.615 C2) 0.5	The orientation of the tooth in relation to the projection plane of the x-rays does not influence the detection of VRF Irrespective of the intracanal material.
Wanderley et al., 2021 Brazil	30 single-rooted teeth	UTM	Incomplete**	According to the root canal conditions: A) no filling B) gutta-percha C) metal post According to the scans assessment: 1) conventional (single scan, teeth positioned perpendicular to the x-rays) 2) combined (two scans: teeth positioned perpendicular and parallel to the x-rays)	Picasso Trio 3D imaging system (Vatech, Hwaseong, Republic of Korea)	85 kVp 5 mA FOV: 5x5 cm Voxel size: 0.2mm	None.	A) no filling B) gutta-percha C) metal post	Dry human mandible	A1) 0.933 A2) 0.955 B1) 0.531 B2) 0.716 C1) 0.466 C2) 0.622	A1) 0.911 A2) 0.909 B1) 0.805 B2) 0.805 C1) 0.604 C2) 0.843	The diagnostic accuracy in teeth with intracanal material was improved when the assessment combines images obtained at 2 orientations.
Yamamoto-Silva et al. 2018 Brazil	30 single-rooted teeth	UTM	*Complete and incomplete (varied sample)	According to the CBCT device, and voxel size: A) Eagle 3D 1) 0.16 mm 2) 0.1 mm B) i-CAT 1) 0.2 mm 2) 0.125 mm	A) Eagle 3D (Dabi Atlante, Brazil) B) i-CAT (Imaging Sciences International, Hatfield, PA)	A) 85 kVp 5 mA FOV: 5x5 cm Voxel size: 1) 0.16 mm 2) 0.1 mm B) 120 kVp 5 mA FOV: 8x8 cm Voxel size: 1) 0.2 mm 2) 0.125 mm	None.	Root canal filling and metal post (NiCr)	Dry human mandible	A1) 0.458 A2) 0.733 B1) 0.357 B2) 0.530	A1) 0.571 A2) 0.700 B1) 0.633 B2) 0.800	Protocols with a smaller voxel size and field of view seemed to favor the detection of VRF in teeth with intracanal metallic posts.

Yamashita et al., 2021 Brazil	60 mandibular premolars	UTM	Unclear	According to the root canal conditions: A) no filling B) root canal filling +fiberglass post C) root canal filling + metal post	i-CAT Next Generation (Imaging Sciences International, Hatfield, PA)	120 kVp 37.07 mA FOV: 8x8 cm Voxel size: 0.125mm	None.	A) no filling B) root canal filling +fiberglass post C) root canal filling + metal post	Dry human mandible	A) 0.85** B) 0.4** C) 0.75**	A) 1.0** B) 0.85** C) 0.1.0**	The presence of metal posts did not influence accuracy; however, the presence of fiberglass post reduced the diagnostic capacity of CBCT.

* Estimated by the reviewers of this systematic review

** Information obtained by email contact with the corresponding author

Appendix 4. QUADAS-2 questions adapted to this systematic review of *in vitro* studies.

Domain 1: Patient selection	
A. Risk of bias	
Describe methods of patient selection:	
• **Was a consecutive or random sample of patients enrolled?**	Yes/No/Unclear
• **Was a case-control design avoided?**	Yes/No/Unclear
• **Did the study avoid inappropriate exclusions?**	Yes/No/Unclear
• **Was the sample size calculated?**	Yes/No/Unclear
• **Were the specimens visually analyzed to detect fractures/cracks before the experiments?**	Yes/No/Unclear
Could the selection of patients have introduced bias?	RISK: LOW/HIGH/UNCLEAR
B. Concerns regarding applicability	
Describe included patients (prior testing, presentation, intended use of index test and setting):	
Is there concern that the included patients do not match the review question?	CONCERN: LOW/HIGH/UNCLEAR
Domain 2: Index test(s) ***(if more than 1 index test was used, please complete for each test)***	
A. Risk of bias	
Describe the index test and how it was conducted and interpreted:	
• **Were the index test results interpreted without knowledge of the results of the reference standard?**	Yes/No/Unclear
• **If a threshold was used, was it pre-specified?**	Yes/No/Unclear
• **Was used any simulation of the conditions *in vivo* (i.e., inserting the specimens in the alveolus of a dry human skull or mandible)**	Yes/No/Unclear
Could the conduct or interpretation of the index test have introduced bias?	RISK: LOW/HIGH/UNCLEAR
B. Concerns regarding applicability	
Is there concern that the index test, its conduct, or interpretation differ from the review question?	CONCERN: LOW/HIGH/UNCLEAR
Domain 3: Reference standard	
A. Risk of bias	
Describe the reference standard and how it was conducted and interpreted:	

• **Is the reference standard likely to correctly classify the target condition?**	Yes/No/Unclear
• **Were the reference standard results interpreted without knowledge of the results of the index test?**	Yes/No/Unclear
• **Was used any auxiliar method to visualize the fracture line (i.e., magnification, application of dyes, transillumination, etc.)**	Yes/No/Unclear
Could the reference standard, its conduct, or its interpretation have introduced bias?	RISK: LOW/HIGH/UNCLEAR
B. Concerns regarding applicability	
Is there concern that the target condition as defined by the reference standard does not match the review question?	CONCERN: LOW/HIGH/UNCLEAR
Domain 4: Flow and timing	
A. Risk of bias	
Describe any patients who did not receive the index test(s) and/or reference standard or who were excluded from the 2x2 table (refer to flow diagram): **Describe the time interval and any interventions between index test(s) and reference standard:**	
• **Was there an appropriate interval between index test(s) and reference standard?**	Yes/No/Unclear
• **Did all patients receive a reference standard?**	Yes/No/Unclear
• **Did patients receive the same reference standard?**	Yes/No/Unclear
• **Were all patients included in the analysis?**	Yes/No/Unclear
• **Was the inter and intraexaminer agreement assessed?**	Yes/No/Unclear
Could the patient flow have introduced bias?	RISK: LOW/HIGH/UNCLEAR

Appendix 5. Excluded articles and reasons for exclusion.

	Author, Year	Reason for exclusion
01	Aristizabal-Elejalde et al. 2020[1]	6
02	Ashmawy et al. 2018[2]	5
03	De Lima Rezende et al. 2016[3]	1
04	de Souza Coutinho-Filho et al. 2012[4]	6
05	Dutra et al. 2017[5]	4
06	Elsaltani et al. 2016[6]	5
07	Gaêta-Araujo et al. 2021[7]	3
08	Gulibire et al. 2020[8]	6
09	Guo et al. 2019a[9]	5
10	Guo et al. 2019b[10]	5
11	González et al. 2022[11]	4
12	Jakobson et al. 2014[12]	5
13	Johari et al. 2016[13]	3
14	Johari et al. 2017[14]	3
15	Karteva et al. 2016[15]	4
16	Kim et al. 2020[16]	6
17	Mansini et al. 2010[17]	4
18	Mizuhashi et al. 2020[18]	6
19	Mora et al. 2007a[19]	3
20	Mora et al. 2007b[20]	3
21	Quintero-Álvarez et al. 2021[21]	6
22	Shah et al. 2018[22]	4
23	Strobel et al. 2017[23]	6
24	Tangari-Meira et al. 2017[24]	4
25	Tiepo et al. 2017[25]	4
26	Wenzel et al. 2009[26]	4
27	Andraws Yalda et al. 2020[27]	4
28	Yuan et al. 2020[28]	4

1. Studies with primary human teeth, or animal teeth (n=1); 2. Studies that included teeth with incomplete root formation (n=0); 3. Studies that did not evaluate CBCT as the index test (n= 5); 4. Studies that did not investigate the diagnostic accuracy of VRF (n= 10); 5. Studies with fracture simulation not consistent with the real aspect of VRF (n= 5); 6. In vivo studies (n= 7); 7. Reviews, letters, case reports and case series (n= 0).

References

1. Aristizabal-Elejalde D, Arriola-Guillen LE, Aliaga-Del Castillo A, Ruiz-Mora GA, Rodriguez-Cardenas YA (2020) Assessment of fractures in endodontically treated teeth restored with and without root canal posts using high-resolution cone beam computed tomography. J Clin Exp Dent 12(6):e547-e54. https://doi.org/:10.4317/jced.56854

2. Ashmawy MS, Yamany I, Abou-Khalaf A, Farid MM, Rady M (2018) Detection of simulated vertical root fractures; which is better multi-detector computed tomography or cone beam computed tomography? The Egyptian Journal of Radiology and Nuclear Medicine 49(1):60-5. https://doi.org/:https://doi.org/10.1016/j.ejrnm.2017.07.003

3. De Lima Rezende MT, Kühl Panzarella F, Fonseca da Cunha M, Batista Souza J, Cintra Junqueira JL, Pedroso Turssi C (2016) Detection of root fractures in glass fiber and metal cast dowel-resto red teeth: Accuracy of Computed Tomography vs Digital Radiography. Rev Odonto Cienc 31(1):6-11. https://doi.org/:10.15448/1980-6523.2016.1.16735

4. de Souza Coutinho-Filho T, Leal da Silva EJN, Gurgel-Filho ED, Martins J, Henriques L, Ferreira C (2012) Deteção de fratura radicular vertical utilizando tomografia computadorizada na presença ou ausência de núcleos metálicos. Revista Portuguesa de Estomatologia, Medicina Dentária e Cirurgia Maxilofacial 53(2):96-8. https://doi.org/:https://doi.org/10.1016/j.rpemd.2011.11.012
5. Dutra KL, Pacheco-Pereira C, Bortoluzzi EA, Flores-Mir C, Lagravere MO, Correa M (2017) Influence of Intracanal Materials in Vertical Root Fracture Pathway Detection with Cone-beam Computed Tomography. J Endod 43(7):1170-5. https://doi.org/:10.1016/j.joen.2017.02.006
6. Elsaltani MH, Farid MM, Eldin Ashmawy MS (2016) Detection of Simulated Vertical Root Fractures: Which Cone-beam Computed Tomographic System Is the Most Accurate? J Endod 42(6):972-7. https://doi.org/:10.1016/j.joen.2016.03.013
7. Gaeta-Araujo H, Nascimento EHL, Oliveira-Santos N, Queiroz PM, Oliveira ML, Freitas DQ, et al. (2021) Effect of digital enhancement on the radiographic assessment of vertical root fractures in the presence of different intracanal materials: an in vitro study. Clin Oral Investig 25(1):195-202. https://doi.org/:10.1007/s00784-020-03353-x
8. Gulibire A, Cao Y, Gao A, Wang C, Wang T, Xie X, et al. (2021) Assessment of true vertical root fracture line in endodontically treated teeth using a new subtraction software - A Micro-CT and CBCT study. Aust Endod J 47(2):290-7. https://doi.org/:10.1111/aej.12476
9. Guo XL, Li G, Yin S, Ma RH, Guo YJ, Bornstein MM (2019) Effect of fracture orientation on detection accuracy of vertical root fractures in non-endodontically treated teeth using cone beam computed tomography. Clin Oral Investig 23(12):4433-9. https://doi.org/:10.1007/s00784-019-02905-0
10. Guo XL, Li G, Zheng JQ, Ma RH, Liu FC, Yuan FS, et al. (2019) Accuracy of detecting vertical root fractures in non-root filled teeth using cone beam computed tomography: effect of voxel size and fracture width. Int Endod J 52(6):887-98. https://doi.org/:10.1111/iej.13076
11. Gonzalez AR, Tosoni GM, Freitas DQ, Oliveira ML (2022) Influence of sharpening filters on the detection of root fractures using low-dose cone-beam computed tomography. Clin Oral Investig 26(7):4797-803. https://doi.org/:10.1007/s00784-022-04444-7
12. Jakobson SJ, Westphalen VP, Silva Neto UX, Fariniuk LF, Schroeder AG, Carneiro E (2014) The influence of metallic posts in the detection of vertical root fractures using different imaging examinations. Dentomaxillofac Radiol 43(1):20130287. https://doi.org/:10.1259/dmfr.20130287
13. Johari M, Esmaeili F, Andalib A, Garjani S, Saberkari H (2016) A Novel Thresholding Based Algorithm for Detection of Vertical Root Fracture in Nonendodontically Treated Premolar Teeth. J Med Signals Sens 6(2):81-90. https://doi.org/:10.4103/2228-7477.181027
14. Johari M, Esmaeili F, Andalib A, Garjani S, Saberkari H (2017) Detection of vertical root fractures in intact and endodontically treated premolar teeth by designing a probabilistic neural network: an ex vivo study. Dentomaxillofac Radiol 46(2):20160107. https://doi.org/:10.1259/dmfr.20160107
15. Karteva E, Manchorova-Veleva N, Stefanova V, Atanasov M, Atanasov A, Pashkouleva D, et al. (2016) Novel methods for the assessment of crack propagation in endodontically treated teeth. Journal of IMAB–Annual Proceeding Scientific Papers 22(3):1308-13. https://doi.org/:10.5272/jimab.2016223.1308

16. Kim JH, Eo SH, Shrestha R, Ihm JJ, Seo DG (2020) Association between longitudinal tooth fractures and visual detection methods in diagnosis. J Dent 101(103466. https://doi.org/:10.1016/j.jdent.2020.103466
17. Mansini R, Akabane CE, Fukunaga D, Baratella T, Turbino ML, Camargo SCC (2010) Utilização da tomografia computadorizada no diagnóstico de fraturas radiculares verticais. RGO: Revista Gaúcha de Odontologia 58(2):185-90
18. Mizuhashi F, Ogura I, Sugawara Y, Oohashi M, Mizuhashi R, Saegusa H (2021) Diagnosis of root fractures using cone-beam computed tomography: difference of vertical and horizontal root fracture. Oral Radiol 37(2):305-10. https://doi.org/:10.1007/s11282-020-00453-y
19. Mora MA, Mol A, Tyndall DA, Rivera EM (2007) Effect of the number of basis images on the detection of longitudinal tooth fractures using local computed tomography. Dentomaxillofac Radiol 36(7):382-6. https://doi.org/:10.1259/dmfr/25073870
20. Mora MA, Mol A, Tyndall DA, Rivera EM (2007) In vitro assessment of local computed tomography for the detection of longitudinal tooth fractures. Oral Surg Oral Med Oral Pathol Oral Radiol Endod 103(6):825-9. https://doi.org/:10.1016/j.tripleo.2006.09.009
21. Quintero-Alvarez M, Bolanos-Alzate LM, Villa-Machado PA, Restrepo-Restrepo FA, Tobon-Arroyave SI (2021) In vivo detection of vertical root fractures in endodontically treated teeth: Accuracy of cone-beam computed tomography and assessment of potential predictor variables. J Clin Exp Dent 13(2):e119-e31. https://doi.org/:10.4317/jced.57471
22. Shah H, Hernandez P, Budin F, Chittajallu D, Vimort JB, Walters R, et al. (2018) Automatic quantification framework to detect cracks in teeth. Proc SPIE Int Soc Opt Eng 10578(https://doi.org/:10.1117/12.2293603
23. Strobel S, Lenhart E, Woelber JP, Fleiner J, Hannig C, Wrbas KT (2017) Comparison of two cone-beam computed tomography systems in the visualization of endodontic structures. Swiss Dent J 127(3):221-9
24. Tangari-Meira R, Vancetto JR, Dovigo LN, Tosoni GM (2017) Influence of Tube Current Settings on Diagnostic Detection of Root Fractures Using Cone-beam Computed Tomography: An In Vitro Study. J Endod 43(10):1701-5. https://doi.org/:10.1016/j.joen.2017.05.008
25. Tiepo M, Magrin G, Kovalik AC, Marmora B, Silva MF, Raitz R (2017) Evaluation of Root Fracture in endodontically treated Teeth using Cone Beam Computed Tomography. J Contemp Dent Pract 18(2):94-9. https://doi.org/:10.5005/jp-journals-10024-1997
26. Wenzel A, Haiter-Neto F, Frydenberg M, Kirkevang LL (2009) Variable-resolution cone-beam computerized tomography with enhancement filtration compared with intraoral photostimulable phosphor radiography in detection of transverse root fractures in an in vitro model. Oral Surg Oral Med Oral Pathol Oral Radiol Endod 108(6):939-45. https://doi.org/:10.1016/j.tripleo.2009.07.041
27. Andraws Yalda F, Clarkson RJ, Davies J, Rout PGJ, Sengupta A, Horner K (2020) Does anthropomorphic model design in ex vivo studies affect diagnostic accuracy for dental root fracture using CBCT? Dentomaxillofac Radiol 49(7):20200093. https://doi.org/:10.1259/dmfr.20200093
28. Yuan M, Gao AT, Wang TM, Liang JH, Aihemati GB, Cao Y, et al. (2020) Using Meglumine Diatrizoate to improve the accuracy of diagnosis of cracked teeth on Cone-beam CT images. Int Endod J 53(5):709-14. https://doi.org/:10.1111/iej.13270

7 CONCLUSÕES

Com base nas investigações executadas, através dos três estudos que compõem esta tese, foi possível concluir que:

- O método desenvolvido é altamente eficaz em induzir FRVs incompletas em dentes humanos extraídos. A sua alta reprodutibilidade permite que futuras investigações aprimorem o diagnóstico por imagem de FRV.
- O filtro BAR do *software* e-vol DX não interfere no diagnóstico de FRV, em dentes vazios, com guta-percha, pino de fibra de vidro, ou pino metálico.
- A presença de pinos metálicos pode diminuir a acurácia diagnóstica de FRV.
- A detecção de FRV em dentes com pinos metálicos pode ser aprimorada utilizando o tamanho de voxel de até 0.125 mm^3.
- As FRV incompletas representam um grande desafio diagnóstico, visto que a sua detecção em imagens de TCFC mostrou-se altamente limitada, independente da presença de materiais intracanais.

REFERÊNCIAS

BECHARA, B. B.; MOORE, W. S.; MCMAHAN, C. A.; NOUJEIM, M. Metal artefact reduction with cone beam CT: an in vitro study. **Dentomaxillofac Radiol**, 41, n. 3, p. 248-253, Mar 2012.

BEZERRA, I. S.; NEVES, F. S.; VASCONCELOS, T. V.; AMBROSANO, G. M.; FREITAS, D. Q. Influence of the artefact reduction algorithm of Picasso Trio CBCT system on the diagnosis of vertical root fractures in teeth with metal posts. **Dentomaxillofac Radiol**, 44, n. 6, p. 20140428, 2015 %J Dentomaxillofac Radiol 2015.

BRADY, E.; MANNOCCI, F.; BROWN, J.; WILSON, R.; PATEL, S. A comparison of cone beam computed tomography and periapical radiography for the detection of vertical root fractures in nonendodontically treated teeth. **Int Endod J**, 47, n. 8, p. 735-746, 2014 %J International Endodontic Journal 2014.

BUENO, M. R.; ESTRELA, C.; AZEVEDO, B. C.; DIOGENES, A. Development of a New Cone-Beam Computed Tomography Software for Endodontic Diagnosis. **Braz Dent J**, 29, n. 6, p. 517-529, Nov-Dec 2018.

CHAN, C. P.; LIN, C. P.; TSENG, S. C.; JENG, J. H. Vertical root fracture in endodontically versus nonendodontically treated teeth: a survey of 315 cases in Chinese patients. **Oral Surg Oral Med Oral Pathol Oral Radiol Endod**, 87, n. 4, p. 504-507, Apr 1999.

CHANG, E.; LAM, E.; SHAH, P.; AZARPAZHOOH, A. Cone-beam Computed Tomography for Detecting Vertical Root Fractures in Endodontically Treated Teeth: A Systematic Review. **J Endod**, 42, n. 2, p. 177-185, Feb 2016.

COHEN, S.; BERMAN, L. H.; BLANCO, L.; BAKLAND, L.; KIM, J. S. A demographic analysis of vertical root fractures. **J Endod**, 32, n. 12, p. 1160-1163, Dec 2006.

DE MARTIN, E. S. D.; CAMPOS, C. N.; PIRES CARVALHO, A. C.; DEVITO, K. L. Diagnosis of Mesiodistal Vertical Root Fractures in Teeth with Metal Posts: Influence of Applying Filters in Cone-beam Computed Tomography Images at Different Resolutions. **J Endod**, 44, n. 3, p. 470-474, Mar 2018.

DE REZENDE BARBOSA, G. L.; SOUSA MELO, S. L.; ALENCAR, P. N.; NASCIMENTO, M. C.; ALMEIDA, S. M. Performance of an artefact reduction algorithm in the diagnosis of in vitro vertical root fracture in four different root filling conditions on CBCT images. **Int Endod J**, 49, n. 5, p. 500-508, 2016 %J International endodontic journal 2016.

ESTRELA, C.; COUTO, G. S.; BUENO, M. R.; BUENO, K. G.; ESTRELA, L. R. A.; PORTO, O. C. L.; DIOGENES, A. Apical Foramen Position in Relation to Proximal Root Surfaces of Human Permanent Teeth Determined by Using a New Cone-beam Computed Tomographic Software. **J Endod**, 44, n. 11, p. 1741-1748, Nov 2018.

FERREIRA, L. M.; VISCONTI, M. A.; NASCIMENTO, H. A.; DALLEMOLLE, R. R.; AMBROSANO, G. M.; FREITAS, D. Q. Influence of CBCT enhancement filters on diagnosis of vertical root fractures: a simulation study in endodontically treated teeth with and without intracanal posts. **Dentomaxillofac Radiol**, 44, n. 5, p. 20140352, 2015.

GAETA-ARAUJO, H.; SILVA DE SOUZA, G. Q.; FREITAS, D. Q.; DE OLIVEIRA-SANTOS, C. Optimization of Tube Current in Cone-beam Computed Tomography for the Detection of Vertical Root Fractures with Different Intracanal Materials. **J Endod**, 43, n. 10, p. 1668-1673, Oct 2017.

HASSAN, B.; METSKA, M. E.; OZOK, A. R.; VAN DER STELT, P.; WESSELINK, P. R. Detection of vertical root fractures in endodontically treated teeth by a cone beam computed tomography scan. **J Endod**, 35, n. 5, p. 719-722, 2009 %J J Endod 2009.

HEKMATIAN, E.; KARBASI KHEIR, M.; FATHOLLAHZADE, H.; SHEIKHI, M. Detection of Vertical Root Fractures Using Cone-Beam Computed Tomography in the Presence and Absence of Gutta-Percha. **ScientificWorldJournal**, 2018, p. 1920946, 2018.

KHASNIS, S. A.; KIDIYOOR, K. H.; PATIL, A. B.; KENGANAL, S. B. Vertical root fractures and their management. **J Conserv Dent**, 17, n. 2, p. 103-110, Mar 2014.

MOULE, A. J.; KAHLER, B. Diagnosis and management of teeth with vertical root fractures. **Aust Dent J**, 44, n. 2, p. 75-87, Jun 1999.

NASCIMENTO, H. A.; NEVES, F. S.; DE-AZEVEDO-VAZ, S. L.; DUQUE, T. M.; AMBROSANO, G. M.; FREITAS, D. Q. Impact of root fillings and posts on the diagnostic ability of three intra-oral digital radiographic systems in detecting vertical root fractures. **Int Endod J**, 48, n. 9, p. 864-871, Sep 2015.

PINTO, M. G. O.; RABELO, K. A.; SOUSA MELO, S. L.; CAMPOS, P. S. F.; OLIVEIRA, L.; BENTO, P. M.; MELO, D. P. Influence of exposure parameters on the detection of simulated root fractures in the presence of various intracanal materials. **Int Endod J**, 50, n. 6, p. 586-594, Jun 2017.

RIVERA, E. M.; WALTON, R. E. Longitudinal tooth cracks andfractures: an update and review. **Endodontic Topics**, 33, n. 1, p. 14-42, 2015.

SCHULZE, R.; HEIL, U.; GROSS, D.; BRUELLMANN, D. D.; DRANISCHNIKOW, E.; SCHWANECKE, U.; SCHOEMER, E. Artefacts in CBCT: a review. **Dentomaxillofac Radiol**, 40, n. 5, p. 265-273, Jul 2011.

VARSHOSAZ, M.; TAVAKOLI, M. A.; MOSTAFAVI, M.; BAGHBAN, A. A. Comparison of conventional radiography with cone beam computed tomography for detection of vertical root fractures: an in vitro study. **J Oral Sci**, 52, n. 4, p. 593-597, 2010 %J Journal of oral science 2010.

WENZEL, A.; HAITER-NETO, F.; FRYDENBERG, M.; KIRKEVANG, L. L. Variable-resolution cone-beam computerized tomography with enhancement filtration compared with

intraoral photostimulable phosphor radiography in detection of transverse root fractures in an in vitro model. **Oral Surg Oral Med Oral Pathol Oral Radiol Endod**, 108, n. 6, p. 939-945, Dec 2009.

ANEXO A – PARECER DO COMITÊ DE ÉTICA EM PESQUISA DO ARTIGO 1

UNIVERSIDADE FEDERAL DE SANTA CATARINA - UFSC

Plataforma Brasil

PARECER CONSUBSTANCIADO DO CEP

DADOS DO PROJETO DE PESQUISA

Título da Pesquisa: Método reprodutível para indução de fraturas radiculares verticais incompletas.
Pesquisador: Eduardo Antunes Bortoluzzi
Área Temática:
Versão: 2
CAAE: 38911120.0.0000.0121
Instituição Proponente: UNIVERSIDADE FEDERAL DE SANTA CATARINA
Patrocinador Principal: Financiamento Próprio

DADOS DO PARECER

Número do Parecer: 4.444.914

Apresentação do Projeto:
Pesquisa qualitativa para analisar taxa de sucesso da obtenção de fraturas radiculares verticais incompletas e as características de cada fratura, conforme método proposto de fratura.
Amostra: 15 dentes permanentes unirradiculares, extraídos de humanos por finalidade terapêutica, de indivíduos adultos (>18anos), recrutados nas clínicas odontológicas da Universidade Federal de Santa Catarina.

Objetivo da Pesquisa:
Segundo pesquisador: "Desenvolver e descrever um método reprodutível para induzir fraturas radiculares verticais completas e incompletas em dentes humanos extraídos."

Avaliação dos Riscos e Benefícios:
Segundo pesquisador:
"Riscos: Não existem riscos diretos relacionados ao estudo. Porém, apesar dos esforços e das providências necessárias tomadas pelos pesquisadores, sempre existe a remota possibilidade de quebra de sigilo, ainda que involuntária e não intencional."
Benefícios: Não haverá benefício direto para o participante. No entanto, ao final da pesquisa, será possível contribuir para a melhora do diagnóstico e planejamento de intervenções de casos complexos da clínica odontológica.

Comentários e Considerações sobre a Pesquisa:
Projeto de pesquisa vinculado à linha de pesquisa “Estudos clínicos e laboratoriais em Endodontia”

Endereço: Universidade Federal de Santa Catarina, Prédio Reitoria II, R: Desembargador Vitor Lima, nº 222, sala 401
Bairro: Trindade **CEP:** 88.040-400
UF: SC **Município:** FLORIANOPOLIS
Telefone: (48)3721-6094 **E-mail:** cep.propesq@contato.ufsc.br

UNIVERSIDADE FEDERAL DE SANTA CATARINA - UFSC

do Programa de Pós-Graduação em Odontologia/UFSC.

Considerações sobre os Termos de apresentação obrigatória:

- Apresenta TCLE
- Apresenta Termo de Cessão
- Folha de rosto eletronicamente assinada pela Coordenadora do Programa de Pós-Graduação em Odontologia, Profa. Dra.Elena Riet Corrêa Rivero em 06/10/2020.
- Carta de anuência, eletronicamente assinada pelo Chefe de Departamento de Odontologia, Prof. Dr. Márcio Correa, em 22/09/2020.

Recomendações:

Nada a recomendar.

Conclusões ou Pendências e Lista de Inadequações:

Os pesquisadores apresentaram nova versão do TCLE, a qual está adequada.

O projeto não apresenta pendências, contudo orientamos corrigir o erro de grafia "Agradecemos", pois acreditamos que o intuito seria escrever "agradecemos".

Considerações Finais a critério do CEP:

Lembramos que a presente aprovação (versão projeto25/11/2020 e TCLE 25/11/2020) refere-se apenas aos aspectos éticos do projeto.

Qualquer alteração nestes documentos deve ser encaminhada para avaliação do CEPSH. Informamos que obrigatoriamente a versão do TCLE a ser utilizada deverá corresponder na íntegra à versão vigente aprovada.

Este parecer foi elaborado baseado nos documentos abaixo relacionados:

Tipo Documento	Arquivo	Postagem	Autor	Situação
Informações Básicas do Projeto	PB_INFORMAÇÕES_BÁSICAS_DO_PROJETO_1626472.pdf	25/11/2020 16:08:54		Aceito
Outros	RESPOSTA_AS_PENDENCIAS.pdf	25/11/2020 16:07:56	Luiz Carlos de Lima Dias Junior	Aceito
Declaração de Instituição e Infraestrutura	DeclaracaoInstituicao.pdf	25/11/2020 16:03:49	Luiz Carlos de Lima Dias Junior	Aceito
Projeto Detalhado / Brochura Investigador	Projeto_detalhado.docx	25/11/2020 16:03:31	Luiz Carlos de Lima Dias Junior	Aceito
Outros	Termodecessao.docx	25/11/2020 16:03:15	Luiz Carlos de Lima Dias Junior	Aceito

Endereço: Universidade Federal de Santa Catarina, Prédio Reitoria II, R: Desembargador Vitor Lima, nº 222, sala 401
Bairro: Trindade **CEP:** 88.040-400
UF: SC **Município:** FLORIANOPOLIS
Telefone: (48)3721-6094 **E-mail:** cep.propesq@contato.ufsc.br

UNIVERSIDADE FEDERAL DE SANTA CATARINA - UFSC

Continuação do Parecer: 4.444.914

TCLE / Termos de Assentimento / Justificativa de Ausência	TCLE.docx	25/11/2020 16:02:35	Luiz Carlos de Lima Dias Junior	Aceito
Folha de Rosto	FolhaDeRosto.pdf	06/10/2020 11:09:45	Luiz Carlos de Lima Dias Junior	Aceito

Situação do Parecer:
Aprovado

Necessita Apreciação da CONEP:
Não

FLORIANOPOLIS, 07 de Dezembro de 2020

Assinado por:
Maria Luiza Bazzo
(Coordenador(a))

Endereço: Universidade Federal de Santa Catarina, Prédio Reitoria II, R: Desembargador Vitor Lima, nº 222, sala 401
Bairro: Trindade **CEP:** 88.040-400
UF: SC **Município:** FLORIANOPOLIS
Telefone: (48)3721-6094 **E-mail:** cep.propesq@contato.ufsc.br

ANEXO B – PARECER DO COMITÊ DE ÉTICA EM PESQUISA DO ARTIGO 2

UNIVERSIDADE FEDERAL DE SANTA CATARINA - UFSC

Plataforma Brasil

PARECER CONSUBSTANCIADO DO CEP

DADOS DO PROJETO DE PESQUISA

Título da Pesquisa: Influência da aplicação de filtro redutor de artefatos e presença de diferentes materiais intracanais sobre a acurácia diagnóstica de trincas e fraturas radiculares verticais.

Pesquisador: Eduardo Antunes Bortoluzzi
Área Temática:
Versão: 2
CAAE: 38912720.2.0000.0121
Instituição Proponente: UNIVERSIDADE FEDERAL DE SANTA CATARINA
Patrocinador Principal: Financiamento Próprio

DADOS DO PARECER

Número do Parecer: 4.444.910

Apresentação do Projeto:
Pesquisa diagnóstica, cuja amostra será constituída de 20 dentes permanentes unirradiculados, extraídos de humanos por finalidade terapêutica. Os participantes, adultos, maiores de 18 anos, serão recrutados nas clínicas odontológicas da Universidade Federal de Santa Catarina.

Objetivo da Pesquisa:
Segundo pesquisadores:
"Avaliar a efetividade do filtro redutor de artefatos BAR do software e-Vol DX sobre a acurácia diagnóstica de trincas e fraturas radiculares verticais, na presença de diferentes materiais intracanais."

Avaliação dos Riscos e Benefícios:
Segundo pesquisadores:
"Riscos: Não existem riscos diretos relacionados ao estudo. Porém, apesar dos esforços e das providências necessárias tomadas pelos pesquisadores, sempre existe a remota possibilidade de quebra de sigilo, ainda que involuntária e não intencional.
Benefícios:Não haverá benefício direto para o participante. No entanto, ao final da pesquisa, será possível contribuir para a melhora do diagnóstico e planejamento de intervenções de casos complexos da clínica odontológica."

Endereço: Universidade Federal de Santa Catarina, Prédio Reitoria II, R: Desembargador Vitor Lima, nº 222, sala 401
Bairro: Trindade **CEP:** 88.040-400
UF: SC **Município:** FLORIANOPOLIS
Telefone: (48)3721-6094 **E-mail:** cep.propesq@contato.ufsc.br

UNIVERSIDADE FEDERAL DE SANTA CATARINA - UFSC

Comentários e Considerações sobre a Pesquisa:

Projeto de pesquisa vinculado à linha de pesquisa “Estudos clínicos e laboratoriais em Endodontia” do Programa de Pós-Graduação em Odontologia/UFSC.

Considerações sobre os Termos de apresentação obrigatória:

- Apresenta TCLE
- Apresenta Termo de Cessão
- Folha de rosto eletronicamente assinada pela Coordenadora do Programa de Pós-Graduação em Odontologia, Profa. Dra.Elena Riet Corrêa Rivero em 06/10/2020.
- Carta de anuência, eletronicamente assinada pelo Chefe de Departamento de Odontologia, Prof. Dr. Márcio Correa, em 22/09/2020.
- Não consta carta de anuência do responsável pelas Clínicas odontológicas da Universidade Federal de Santa Catarina.

Recomendações:

Nada a recomendar.

Conclusões ou Pendências e Lista de Inadequações:

Os pesquisadores apresentaram nova versão do TCLE, a qual está adequada.

Não apresenta pendências e/ou inadequações.

Orientamos remover do documento TCLE o cabeçalho: "TCLE: APÊNDICE 1 –"deixando apenas: Termo de Consentimento Livre e Esclarecido.

Considerações Finais a critério do CEP:

Lembramos que a presente aprovação (versão projeto 25/11/2020 e TCLE 25/11/2020) refere-se apenas aos aspectos éticos do projeto.

Qualquer alteração nestes documentos deve ser encaminhada para avaliação do CEPSH. Informamos que obrigatoriamente a versão do TCLE a ser utilizada deverá corresponder na íntegra à versão vigente aprovada.

Este parecer foi elaborado baseado nos documentos abaixo relacionados:

Tipo Documento	Arquivo	Postagem	Autor	Situação
Informações Básicas do Projeto	PB_INFORMAÇÕES_BÁSICAS_DO_PROJETO_1626476.pdf	25/11/2020 16:22:37		Aceito
Outros	RESPOSTA_AS_PENDENCIAS.pdf	25/11/2020 16:21:15	Luiz Carlos de Lima Dias Junior	Aceito

Endereço: Universidade Federal de Santa Catarina, Prédio Reitoria II, R: Desembargador Vitor Lima, nº 222, sala 401
Bairro: Trindade **CEP:** 88.040-400
UF: SC **Município:** FLORIANOPOLIS
Telefone: (48)3721-6094 **E-mail:** cep.propesq@contato.ufsc.br

UNIVERSIDADE FEDERAL DE SANTA CATARINA - UFSC

Declaração de Instituição e Infraestrutura	DeclaracaoInstituicao.pdf	25/11/2020 16:20:27	Luiz Carlos de Lima Dias Junior	Aceito
Projeto Detalhado / Brochura Investigador	Projeto_detalhado.docx	25/11/2020 16:19:41	Luiz Carlos de Lima Dias Junior	Aceito
Outros	Termodecessao.docx	25/11/2020 16:19:10	Luiz Carlos de Lima Dias Junior	Aceito
TCLE / Termos de Assentimento / Justificativa de Ausência	TCLE.docx	25/11/2020 16:18:26	Luiz Carlos de Lima Dias Junior	Aceito
Folha de Rosto	FolhaDeRosto.pdf	06/10/2020 11:14:56	Luiz Carlos de Lima Dias Junior	Aceito

Situação do Parecer:
Aprovado

Necessita Apreciação da CONEP:
Não

FLORIANOPOLIS, 07 de Dezembro de 2020

Assinado por:
Maria Luiza Bazzo
(Coordenador(a))